GEOLOGICAL SURVEY OF CANADA
OPEN FILE 8535 (revised)

Qualitative petroleum resource assessment of the Labrador margin

J.S. Carey, T. McCartney, M.C. Hanna, C.J. Lister, and L.E. Kung

2020

Canada

GEOLOGICAL SURVEY OF CANADA
OPEN FILE 8535 (revised)

Qualitative petroleum resource assessment of the Labrador margin

J.S. Carey, T. McCartney, M.C. Hanna, C.J. Lister, and L.E. Kung

2020

Permanent link: https://doi.org/10.4095/326017

This publication is available for free download through GEOSCAN (https://geoscan.nrcan.gc.ca/).

Publications in this series have not been edited; they are released as submitted by the author.

TABLE OF CONTENTS

EXECUTIVE SUMMARY

Natural Resources Canada (NRCan) conducted a qualitative petroleum resource assessment for the Labrador continental margin (Figure 1) in order to inform any future decisions related to marine spatial planning including marine conservation. Funding for this study came from the Marine Conservation Targets (MCT) initiative, which provided targeted funding to Environment and Climate Change Canada (represented by the Parks Canada Agency), Fisheries and Oceans Canada (DFO), and Natural Resources Canada (NRCan) as part of the Government of Canada's commitment to conserve 10% of Canada's marine and coastal waters by 2020.

The study area encompasses approximately 425,000 km^2 northeast of Labrador between 53°N and 61°N, and from the shoreline to the 200 nautical mile limit, where water depths can exceed 3000 m (Figure 2). Information compiled, produced and reviewed for this report is included in appendices including the interpretive geologic framework (Appendix A), thermal modeling and petroleum generation (Appendix B), the petroleum system analysis by play (Appendix C), an assessment of the unconventional petroleum potential (Appendix D), mineral potential (Appendix E), list of all reviewed documents (Appendix F), and a glossary of terms (Appendix G).

This qualitative assessment of the conventional petroleum potential of the Labrador Sea builds on previous petroleum potential studies of the Labrador Margin (e.g. Sheppard and Hawkins, 1980), and incorporates new insights gained from recent scientific work (e.g. Jauer and Budkewitsch, 2010; Dickie et al., 2011; Keen et al., 2018a, b) and examination of seismic survey data acquired between 1975 and 2016 (Figure 3). The present study summarizes relative petroleum resource potential of the study area, and provides the scientific foundation for any subsequent quantitative assessment of the potential. The petroleum assessment includes evaluations of petroleum plays in two sedimentary basins: the Hopedale Basin and Saglek Basin (Figure 4), as well as their corresponding deepwater systems. Data coverage and principal geological features and basin architecture are shown in Figures 2, 3 and 4, and discussed in Appendices A and B.

The interpretation of conventional petroleum resource potential, visually represented by a qualitative potential map (Figure 1), indicates the highest potential is located in areas of the continental shelf where early Cretaceous depocentres are found, with moderate to high potential in parts of the continental slope with thick sediments.

A secondary objective of the study was to assess the potential for unconventional hydrocarbons such as gas hydrates, coal-bed methane, shale oil and shale gas (Figure 5). The unconventional energy potential is viewed as moderate based solely on review of the literature with no additional research or analysis.

A tertiary objective of the study was to identify areas with potential mineral resources through literature review (Appendix E) and regional geologic mapping. Mineral resources identified in coastal Labrador include nickel, cobalt, copper and uranium. Figure 6 provides information on mineral occurrences and mines near the study area. Viability of offshore mineral resource extraction would first require a regulatory framework that allows offshore mineral mining in Canada.

1. INTRODUCTION

This report summarizes the qualitative petroleum resource assessment of offshore Labrador, (Figure 1). The assessment studies were undertaken in 2017 and 2018 by a team of geoscientists at the Geological Survey of Canada (GSC). Objectives were to (a) review, analyze and integrate relevant data from previous resource assessments and industry reports, existing scientific literature and available geoscience databases (Appendix F); (b) conduct basin analysis, interpret and map petroleum system elements and regional petroleum plays (Appendices A and B); and (c) provide qualitative summaries of the conventional energy resource potential in the study area (Appendix C).

The study area spans the Labrador Margin from the shoreline to the 200 nautical mile limit where water depths can exceed 3000 m, an area of approximately 425,000 km^2 (Figure 2). The study area extends from 53˚N to 61˚N, which is approximately between the Cartwright Arch and Hudson Strait; this includes all of the Hopedale Basin and the southern (Labrador Margin) part of the Saglek Basin (Figure 4).

The Labrador Margin is a passive margin. Rifting between Labrador and Greenland initiated in the early Cretaceous and the onset of seafloor spreading was in the Maastrichtian (Figure 7; Keen et al., 2018a). The spreading rate decreased during the middle Eocene, and ceased in the early Oligocene (Delescluse et al., 2015). The sedimentary rocks on the shelf are mainly found in two Mesozoic-Cenozoic depocentres: Saglek Basin in the north and Hopedale Basin in the south (Figure 4).

This qualitative assessment was based on integration of the available seismic reflection profiles with lithological, geochemical and biostratigraphic data from twenty-seven petroleum exploration wells on the Labrador continental shelf, three petroleum exploration wells offshore of southeastern Baffin Island, and two scientific deep sea drilling sites in the Labrador Sea. The assessment includes the wells on the continental shelf and the proximal portions of depositional systems that extend into deeper water. Additional information such as heat flow, gravity and magnetic data, and direct indicators of hydrocarbons from seismic and satellite images were also considered.

---

2. GEOLOGIC SETTING

The continental shelf of Labrador is approximately 150 km wide. The Labrador Marginal Trough (Figures 2, 4, 8) extends along the length of Labrador, separating the inner shelf from the outer shelf, and is up to 50 km wide. Phanerozoic sediments have been removed in this trough and the underlying Proterozoic and Archean crystalline rocks reach the seafloor in the trough. South of the Kanairiktok Shear Zone the Grenville and Makkovik province form the crystalline basement (Figure 4). North of the Kanairiktok Shear Zone the crystalline basement consists of rocks belonging to the Nain Province (Wardle et al. 1997; Culshaw et al. 2000). The modern Labrador Shelf, east of the Marginal Trough, is composed of a series of bathymetric banks and saddles. The saddles, some of which have maximum depths greater than 600 m, were the location of Laurentide ice outflow (Margold et al. 2015). It is possible that the overall margin morphology is inherited from a Plio-Pleistocene fluvial landscape (Piper et al. 1990).

The Labrador continental margin formed through crustal extension between Labrador and Greenland beginning in the early Cretaceous. The initial rifting style was "non-volcanic" (Chalmers, 1997; Funck et al., 2007) in that the extension was largely accommodated by faulting and stretching of the crust rather than by emplacement of magma (White and McKenzie, 1989; Reston, 2009). The southern portion of the margin continued to develop in a non-volcanic environment (Chian et al., 1995; Keen et al. 2018a) until the cessation of seafloor spreading in the Labrador Sea in the Oligocene (Delescluse et al., 2015). However, the northern portion of the margin developed into a volcanic rifted margin during the Paleocene (Chalmers, 1997; Keen et al., 2012). The northward transition to a volcanic margin begins seaward of the Snorri well (Figure 2; Keen et al., 2012) and is likely related to volcanism associated with the proposed mantle plume beneath Davis Strait at this time (Keen et al., 2012; Oakey and Chalmers, 2012).

Cenozoic, Mesozoic and limited Paleozoic sediments are found in the sedimentary successions of the Saglek and Hopedale basins. The sedimentary successions of the Hopedale and Saglek basins on the continental shelf are known from wells (Figure 2) and have been described by several authors (e.g. Umpleby, 1979; McWhae et al., 1980; Balkwill et al., 1990; Dickie et al., 2011). The basin fill consists largely of syn-rift terrestrial to shallow marine sediments and shallow to deep marine sediments deposited during and after seafloor spreading (D'Eon-Miller and Associates, 1987; Dickie et al., 2011). Both source and reservoir rocks are identified in this succession and several large gas fields have been discovered, confirming the presence of active petroleum systems. The continental slope in the study area has not been drilled, but recent mapping and hydrocarbon slicks observed from satellite indicate petroleum potential (Wright et al., 2016).

A summary of the different play elements for each interval can be found in Table 1.

3. DATA

Industry evaluation of the petroleum potential of the Labrador Margin began in the late 1960's, with the acquisition of a series of seismic surveys by Tenneco Inc. The period from 1969 to 1984 saw intensive industry activity on the margin with several dozen seismic surveys undertaken. Drilling began with the Leif E-38 well by Tenneco in 1971, followed by twenty-six more wells on the Labrador shelf and three more wells on the shelf of southern Baffin Island over the following twelve years. In addition to data collected by the petroleum industry, the Ocean Drilling Program drilled two wells, site 646 and 647 in the Labrador Sea in 1987.

With the decline of energy prices in the mid-1980's, there was little oil and gas activity in this region for the remainder of the 20th century, but the past fifteen years have seen renewed interest, with a number of modern two-dimensional multichannel reflection seismic surveys collected over the past decade.

3.1 Literature

The Labrador margin has been a subject of both industry and academic interest for fifty years, producing numerous publications that have been reviewed in support of this study. These include the initial well company reports on the biostratigraphy, lithologies, organic matter content and maturation, and fluid analyses that have been submitted to the Canada-Newfoundland and Labrador Offshore Petroleum Board (C-NLOPB). The Geological Survey of Canada has conducted active research on the margin, establishing the biostratigraphic framework, sedimentology and depositional environments (e.g. Gradstein and Williams, 1976, Umpleby, 1979; Bujak-Davies Group, 1987; D'Eon-Miller and Associates, 1987; Balkwill et al., 1990; Williams et al., 1990), as well as the crustal structure and tectonic history of the margin (Srivastava, 1978, 1985; Srivastava and Roest, 1999). Although there has been no new drilling activity in thirty years, the Geological Survey of Canada has continued to study the margin, resampling wells for biostratigraphy and geochemistry, examining and interpreting modern seismic data, and integrating new developments in the understanding of rifted continental margins (e.g. Dickie et al., 2011; Keen et al, 2012; Jauer et al., 2014; Nøhr-Hansen et al., 2016; Keen et al., 2018 a, b). A detailed list of references supporting this study is provided in Appendix F.

3.2 Geophysical Data

2D reflection seismic data provided under the terms of a confidential Memorandum of Understanding with the Canada-Newfoundland and Labrador Offshore Petroleum Board, in combination with 2D reflection seismic data acquired by the Geological Survey of Canada (Atlantic), were used for the seismic interpretation in this project. Over 90,000 line kilometers of data, acquired between 1975 and 2016 were combined into a single IHS™ Kingdom interpretation project (Figure 3). Line spacing ranges from 1 to 20 km on the shelf and between 1 and 60 km in the deep water. Published gravity and magnetic surveys (Funck et al., 2001; Hall et al., 2002) were studied for the general framework of the seismic interpretation project, but were not directly input to the interpretation. Well logs from 24 Labrador Shelf wells were used to generate synthetic seismograms and tie the well information to the seismic data, particularly the D'Eon Miller lithologies and grain sizes published in Wielens & Williams (2009a, b, c). The synthetics were generated using a wavelet extracted from the seismic. To account for the varying bandwidths of the different seismic vintages available, which sometimes impeded horizon interpretation between lines of different vintages, a different synthetic was created for each seismic vintage intersecting a given well location. Stretching and squeezing of the time-depth curve was kept to a minimum, so there are still mis-ties between the formation tops and the seismic horizons. As such, the time-depth (T-D) curves are not robust enough to use for depth conversion of the two-way travel-time horizons, however the formation top depths and the horizon time picks could be used to develop a velocity model on the shelf.

3.3 Geological Data

Industry well data for 27 wells in offshore Labrador and three wells from offshore Baffin Island in Davis Strait were examined for this study, as were data from two Ocean Drilling Program sites in the Labrador Sea (Figure 2). The data considered included wireline logs, petrophysical interpretations of those logs provided by Nalcor Energy, RockEval pyrolysis data, bitumen extract and adsorbed gas data from drill samples, and fluid analyses from well tests.

4. METHODOLOGY

Available geologic and geophysical data were examined for applicability to the resource assessment. New work completed for this study (summarized in Appendices A and B) includes:

i) Mapping of the basement, seafloor, and five major surfaces following the stratigraphic framework of Dickie et al. (2011) using 2D reflection seismic data;

ii) Subdivision and mapping of sand intervals within each major sequence using well information and 2D reflection seismic data;

iii) Structural interpretation and mapping using 2D reflection seismic data;

iv) Depth conversion of interpreted seismic horizons and development of a 3-D model of the margin;

v) Assessment of potential reservoirs from a combination of well log analysis, seismic facies, and conceptual depositional models;

vi) Assessment of potential source rocks using pyrolysis, adsorbed gas and bitumen analysis from wells;

vii) Assessment of source rock maturity using geologic model and heat flow determined from well temperatures, thermal maturity indicators in wells and direct measurements of heat flow;

viii) Assessment of traps using direct hydrocarbon indicators, structural interpretation and facies analysis.

Plays in the study were identified based on the stratigraphic unit (Table 1). Each play was assessed individually, and a chance of geologic success was assigned for each of its petroleum system elements (source, reservoir, trap and seal). Plays were then weighted according to an assigned global scale factor (Lister et al., 2018), which is a subjective estimate of how the play may compare to productive plays in basins worldwide. The qualitative petroleum potential map (Figure 1) represents the sum of the potential for all the identified plays. Note that this resource assessment did not attempt to distinguish between oil and gas potential, however future work could address that distinction.

5. RESULTS AND INTERPRETATION

The petroleum plays are subdivided into six potentially prospective sequences following the stratigraphic nomenclature of Dickie et al. (2011; Figure 7): Paleozoic, Bjarni, Markland, Cartwright, Kenamu and Mokami. Neither the Archaean and Proterozoic basement nor the Saglek sequence are viewed as having any petroleum potential: Archaean and Proterozoic rocks in the area largely consist of igneous rocks and orthogneisses, while the Pliocene-Pleistocene

Saglek sequence is predominantly coarse-grained progradational sands that pose difficulties in sealing hydrocarbon traps..

There are two significant discovery licenses (SDL) in the Paleozoic (the Gudrid H-55 and Hopedale E-33 SDL's). These are attributed to a Bjarni source rock (Powell, 1979; Rashid et al., 1980). Both wells are on basement highs, making hydrocarbon migration from a Bjarni source into an adjacent depocentre viable. Paleozoic source rocks could also exist in the deeper depocentres adjacent to these wells. The sequence consists of erosional remnants, making it difficult to map, and too little is known about the distribution of reservoir lithologies to draw firm conclusions about its potential hydrocarbon resources. The Paleozoic is expected to be absent outside the main Bjarni depocentre trends, as it would have been eroded from uplifting rift shoulders.

Three SDL's lie within the Bjarni sequence, which was the target of most of the petroleum drilling activity on the Labrador margin: Hopedale E-33, Bjarni H-81 and North Bjarni F-06 SDL's. The sequence contains both marginally to moderately mature source rocks in the deeper parts of Bjarni depocentres and coarse-grained, locally developed reservoir rocks. The Bjarni is highly prospective where present and where burial is sufficient to mature the source rock. High potential for Bjarni hydrocarbons exists in Cretaceous depocentres on the continental shelf, especially in the Hopedale Basin (Figure 4).

The Markland Sequence is a predominantly shaley interval deposited during late continental rifting and early seafloor spreading on the margin (Dickie et al., 2011). Reservoir sandstones of the Freydis member are similar to the underlying Bjarni: locally developed and potentially containing hydrocarbons. The shales are relatively poor in organics and do not appear to be good source rocks where encountered in the wells; better source rock is possible farther offshore where the sequence deepens but there is no well control. Seismic interpretation suggests the Markland sequence may thin to zero thickness on the outer shelf and slope, however poor data quality on the slope makes this difficult to confirm. The overall hydrocarbon potential of the Markland interval is relatively poor.

The Cartwright Sequence contains the Gudrid sands and the Cartwright mudstones. The Gudrid sandstone is an extensive, thick sand unit with excellent reservoir properties present on the shelf. The Snorri J-90 discovery encountered hydrocarbons in a Gudrid reservoir (Snorri SDL; Eastcan et al., 1977b). Cartwright mudstones have moderate to high organic matter content, and are marginally mature to immature where encountered. However, beneath the outer shelf and continental slope there are areas where the Cartwright is expected to have achieved thermal maturity and it is likely to be an important source rock for plays in these regions. Cartwright plays based on stratigraphic and structural traps in Gudrid sandstones are an important play type on the shelf.

The Kenamu Sequence is a predominantly shaley interval with thin, laterally extensive shelf sands (Leif Member) known from well data and seismic interpretation. The lower part of the Kenamu is characteristically organic rich and therefore a potential source rock. However, thermal maturity is unlikely except in localized areas on the outermost shelf and thick depocentres on the slope where adequate burial depth occurs. The Leif sand stratigraphic traps are a potentially significant play type on the shelf. There is some potential for both stratigraphic and structural traps in deep water, but reservoir presence may be limited, as the gravity-driven deformation structures on the slope and in the deep water (Figure 8) suggest a mud-dominated system.

The Mokami Sequence records a general sea-level fall. It becomes sandier upwards and is overlain by the predominantly coarse-grained Saglek sequence. Stratigraphic traps in laterally extensive sheet sands or channel sands are expected on the shelf but may have been compromised

by Quaternary glacial movement. Reliable shallow ties between the well logs and the seismic are difficult and prevent mapping of individual sandstone units; however, the lower Mokami sequence is thick on the slope with better potential for reservoir development than the underlying Kenamu. The Mokami Sequence may be an important target for deep-water plays in the C-NLOPB Labrador South call for bids region located between ~54˚30'N and 56˚N and ~52˚30'W and ~55˚30'W (C-NLOPB, 2016a). Following the call for bids, exploration licenses may be awarded (C-NLOPB, 2016b).

A summary of the Labrador Sea petroleum play elements is listed in Table 1. Six plays were assessed, one for each sequence described above. Stratigraphic and structural trap potential was identified for every sequence, often in the same geographic region, therefore the type of trap was accounted for in the assignment of chance of success for the traps rather than by subdividing the plays by trap type. The first step in assigning a global scale factor for each play was to determine whether the entire study area should have the same global scale factor or if it should be subdivided. For the Paleozoic and Bjarni plays, a different global scale factor was needed for shelf regions than for the slope and deep water due to the ages of the crust in these regions. For the Cartwright, Kenamu, and Mokami plays, different global scale factors were assigned based on the sedimentary basins.

The highest petroleum potential overall is on the shelf (Figure 1). This is as much a reflection of the amount of data in the region, as it is of the known discoveries. New seismic data acquired since these wells were drilled gave the opportunity to revisit the structural geology and update the understanding of the trap and reservoir configurations (Appendix A), resulting in high petroleum potential despite the fact that the significant discoveries have never gone to production. Areas of moderate potential, particularly on the slope and in the deep water (Figures 1, 2) would benefit from more data, and it is possible this potential would increase with further exploration.

The petroleum potential of the Paleozoic play (Appendix C) reflects the limited distribution of preserved Paleozoic strata, however a moderately high global scale factor was assigned to the Paleozoic play on the shelf because of the high potential where source and reservoir are present (Table 1), as evidenced by the two significant discoveries in the Paleozoic. (Appendix A). The highest global scale factors, overall, were assigned to the Bjarni play in the Hopedale Basin (with a higher global scale factor assigned to the central part of the Hopedale Basin containing the Bjarni H-81, North Bjarni F-06 and Hopedale E-33 significant discoveries), again a reflection of detailed mapping of the half-grabens these plays are found in (Appendix A). The Markland play is perhaps the least prospective overall, due to the fact that there is very little sandy reservoir identified in the Markland sequence (Appendix C). The limited distribution of the Gudrid sands in the Cartwright Sequence (Appendix A) is the reason a moderate global scale factor was applied to the Cartwright play (Table 1). Although the Leif sands in the overlying Kenamu sequence are more widely distributed, there are fewer structural traps, with the exception of the deep water region identified as a future Call for Bids area by the C-NLOPB, which is why the global scale factor for the Kenamu play is only moderate. Although there is good reservoir potential in the Mokami play, the global scale factor is moderate because of the difficulty identifying potential migration pathways for mature source to reach the reservoirs in the deep water. This play, in particular, is one whose potential could increase if more exploration data was available.

6. CONCLUSIONS

The findings of this report are based on interpretation of existing well data, 2D reflection seismic data and previous reports and publications. Figure 1 presents a summary map of the petroleum potential for the region. The major conclusions are:

1. Potential for conventional hydrocarbons on the shelf is firmly established by discoveries in Hopedale Basin. The most important targets in this area are likely to be Bjarni and Gudrid sands. High to very high potential exists in areas of Bjarni depocentres.
2. There is moderate to high potential for conventional hydrocarbons in regions in deeper water not tested by drilling, but where burial depth is sufficient for source rock maturity.
3. The Labrador Marginal Trough is non-prospective crystalline basement. Prospectivity tends to decline toward the 200-mile limit as sediment thickness decreases and the crust type transitions from continental to oceanic.

7. ACKNOWLEDGEMENTS

FIGURE 1. Qualitative Petroleum Potential of the Labrador Margin as mapped using the GSC method for qualitatively assessing chance of success (Lister et al., 2018)
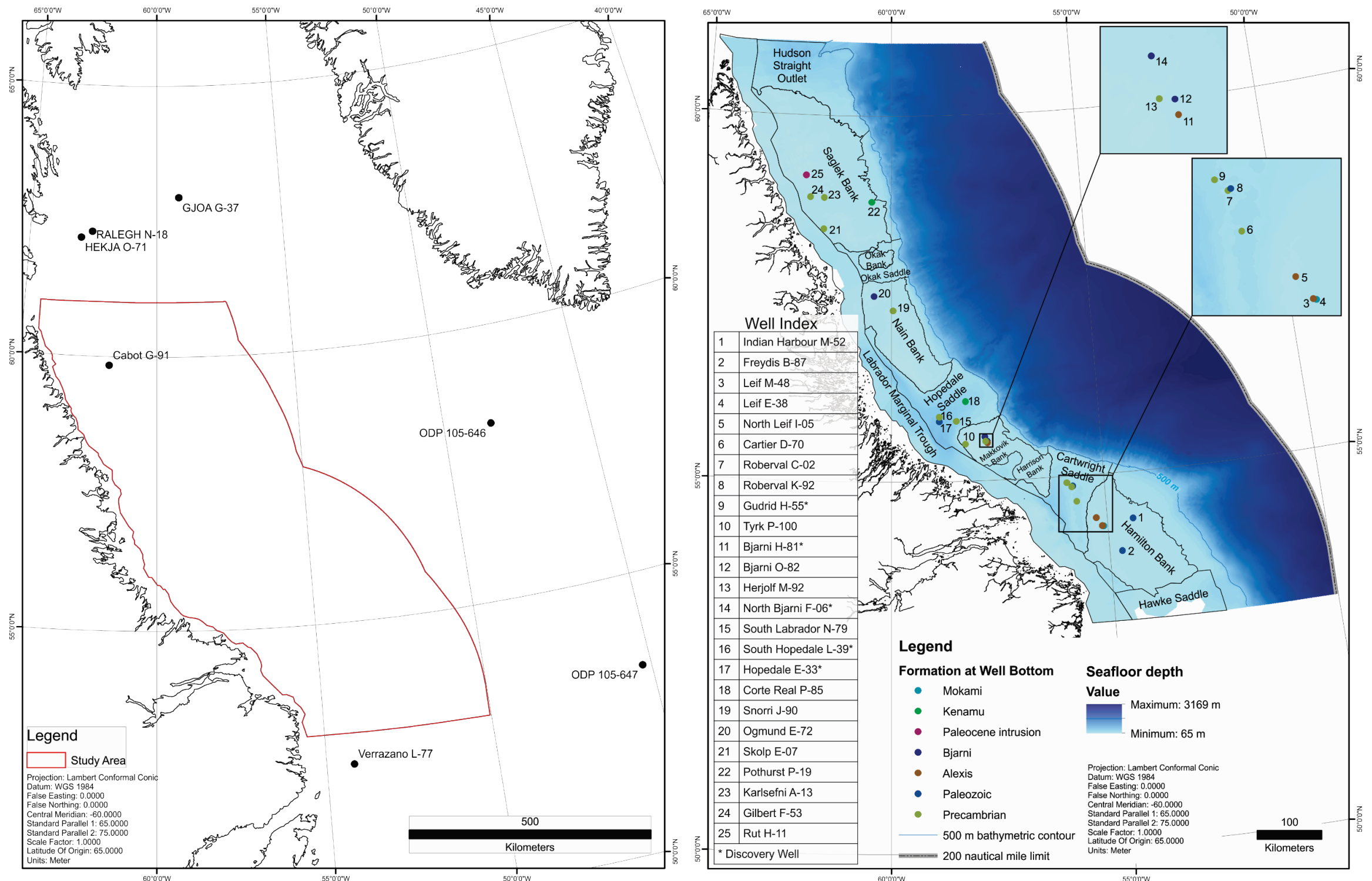
FIGURE 2. Map of Labrador Sea showing well locations. Detailed map of study area shows bathymetric features and well locations with formation at well bottom. Cabot G-91 is in the study area, but was abandoned during drilling due to icebergs, boulders and strong currents, therefore no downhole log data is available for this well. Bathymetric features, 500 m contour and seafloor depth map are based on the depth-converted seafloor horizon interpreted from 2D reflection seismic data. The 500 m bathymetric contour is the approximate position of the shelf break. In the northern half of the margin, the Labrador Marginal Trough is mapped based on the limit of the 2D seismic data. In the southern half of the margin (South of the Okak Saddle), the basement subcrop can be seen on the 2D seismic data and is used to map the basinward edge of the Labrador Marginal Trough.
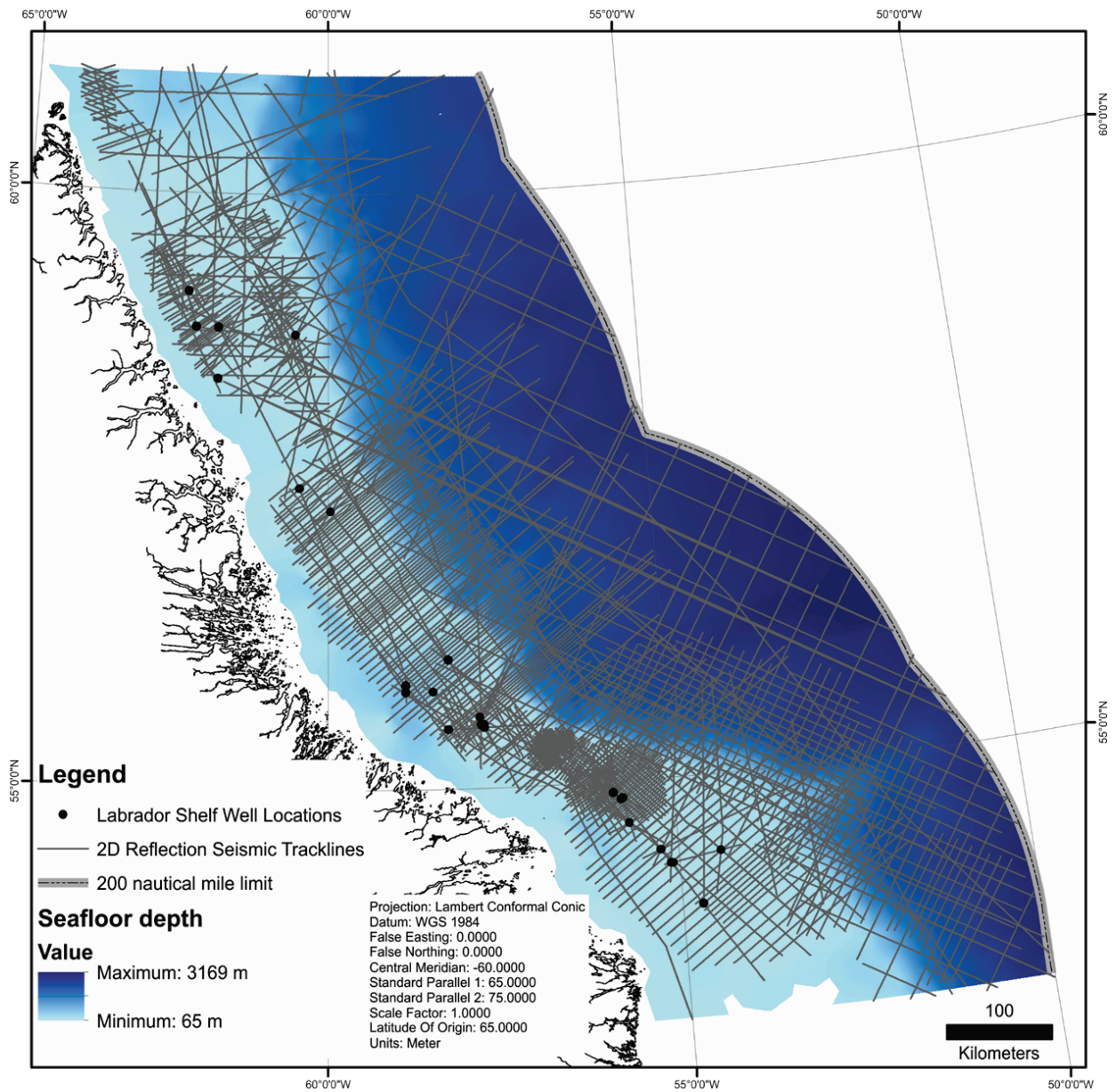
FIGURE 3. Seismic Trackline map. Tracklines show the 2D seismic reflection data available through a confidential Memorandum of Understanding (MOU) with the C-NLOPB. See Figure 2 for well index.
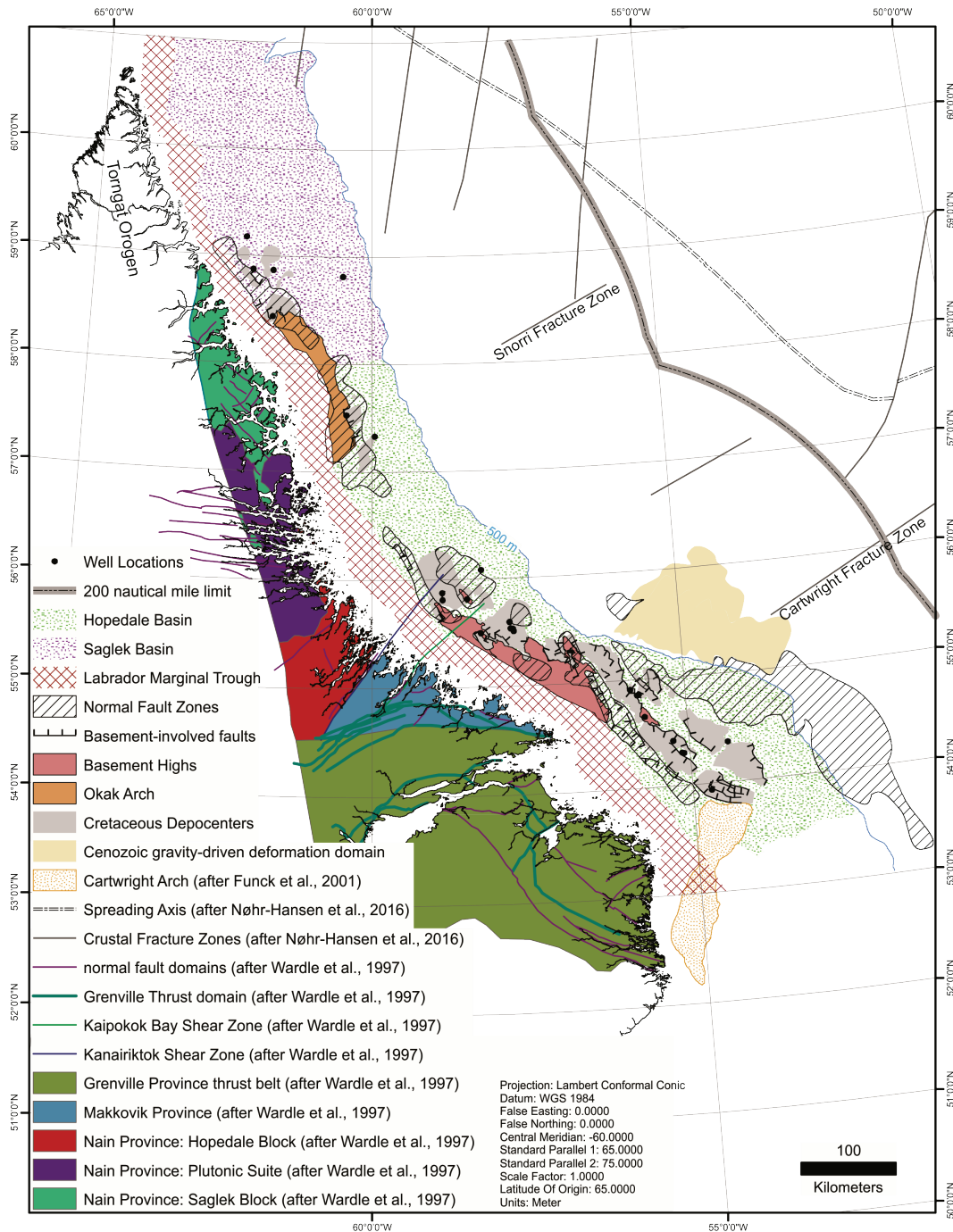
FIGURE 4. Geologic Map of the Labrador Margin. See Figure 2 for well index. Labrador Marginal Trough, normal fault zones, basement-involved faults, Okak Arch, basement highs, Cretaceous depocenters and Cenozoic gravity-driven deformation domain are from the 2D reflection seismic interpretation undertaken for this report. Not all basement-involved faults are shown. Although some Cretaceous depocenters have inward-dipping normal faults on both margins which makes them look like grabens in map-view, their sediment fill pattern is distinctly wedge-shaped, indicating they are actually half-grabens. The boundary between Hopedale and Saglek basins is approximate. Not all crustal fracture zones are shown or named.
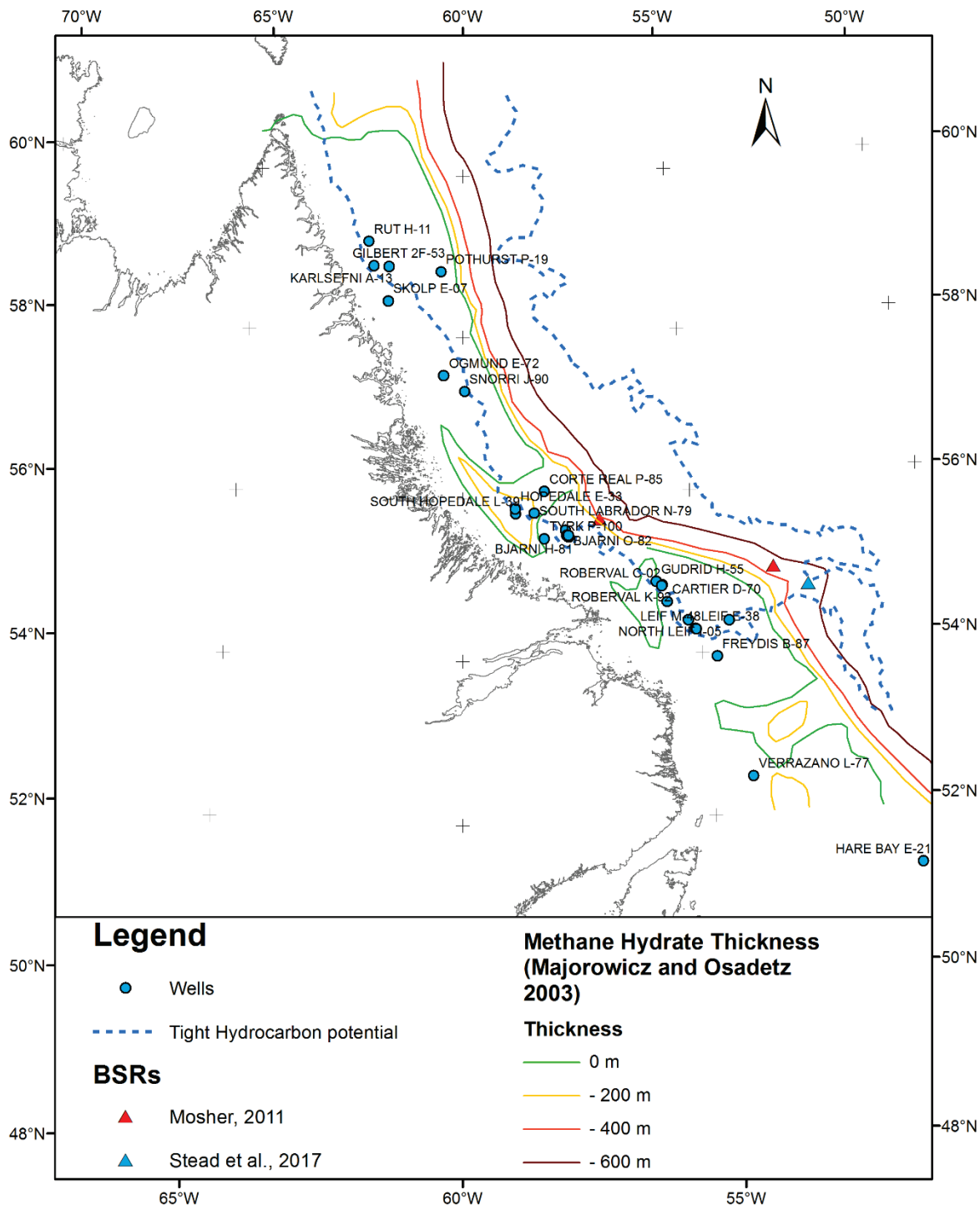
FIGURE 5. Unconventional Resource Potential. BSRs (Bottom Simulating Reflectors) are seismic indications of the presence of gas hydrates in the subsurface. The methane hydrate thickness contours are the calculated thickness of the stability field for Type I hydrates, based on temperature and pressure considerations. The tight hydrocarbon potential shows the region where mudrocks are expected to have reached the oil window (see Appendix B).

13
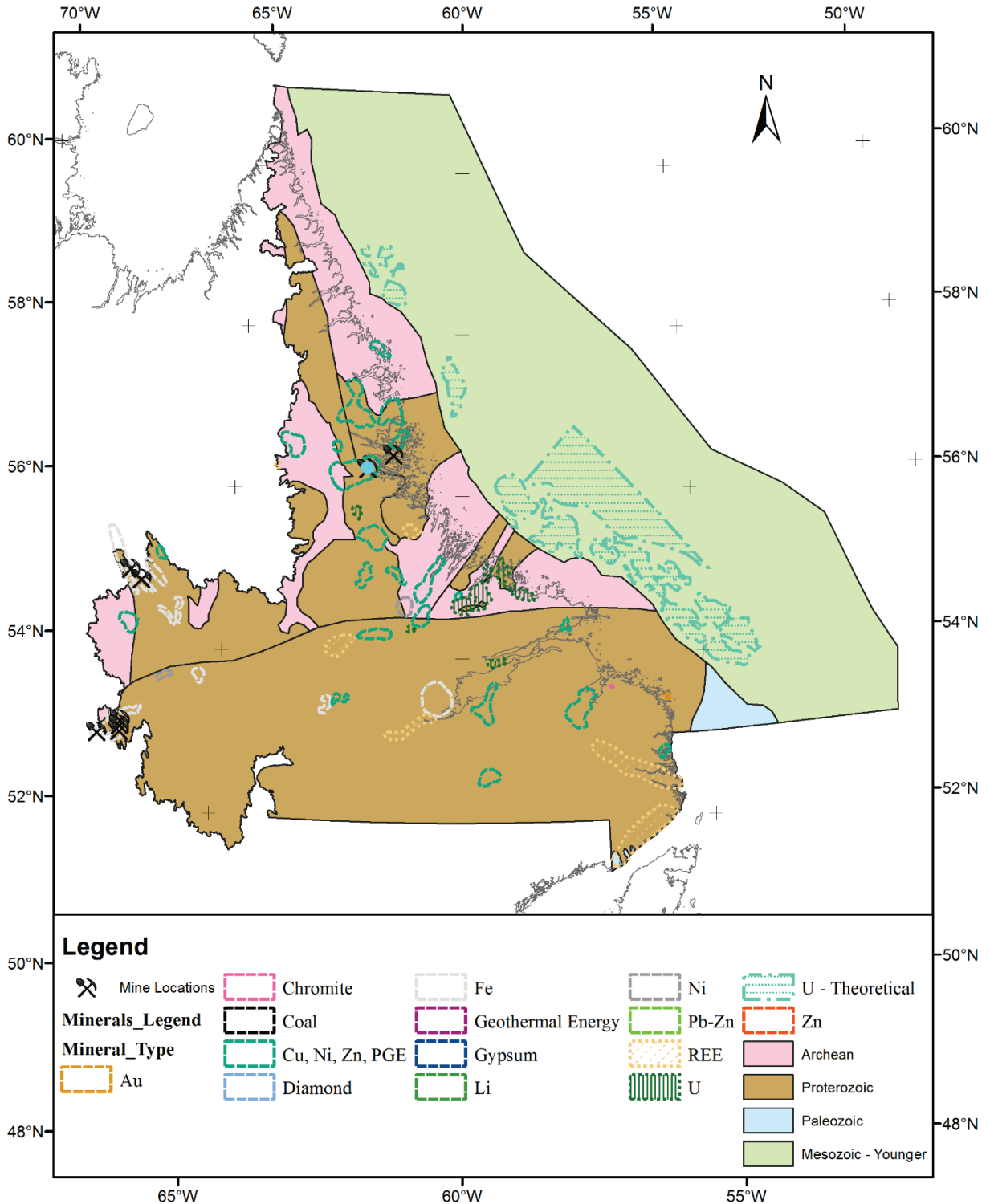
FIGURE 6. Mineral Occurrences and Mineral Resource Potential. See Appendix E.
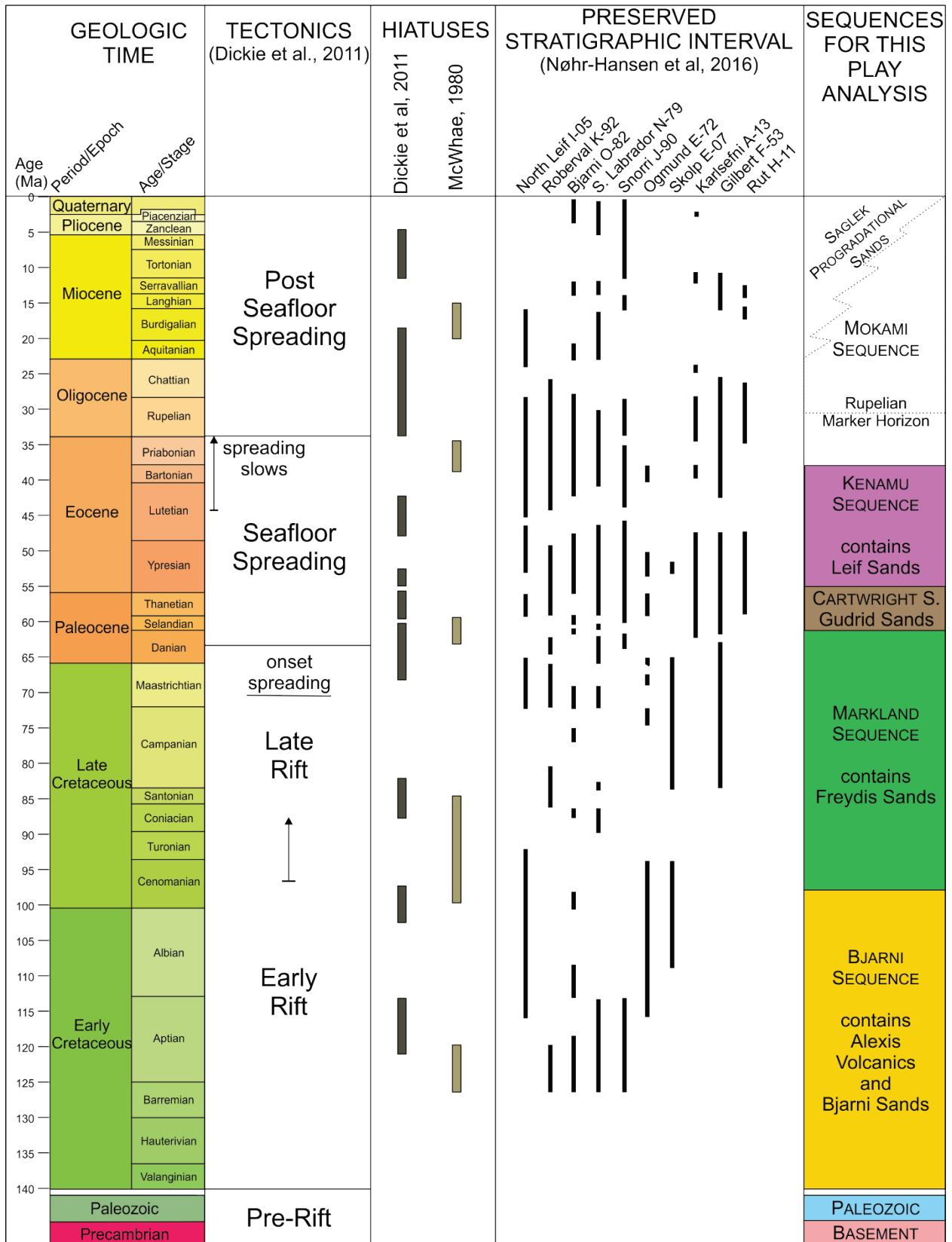
FIGURE 7. Labrador Margin Stratigraphic Column, after Dickie et al, 2011 and Nøhr-Hansen et al, 2016.
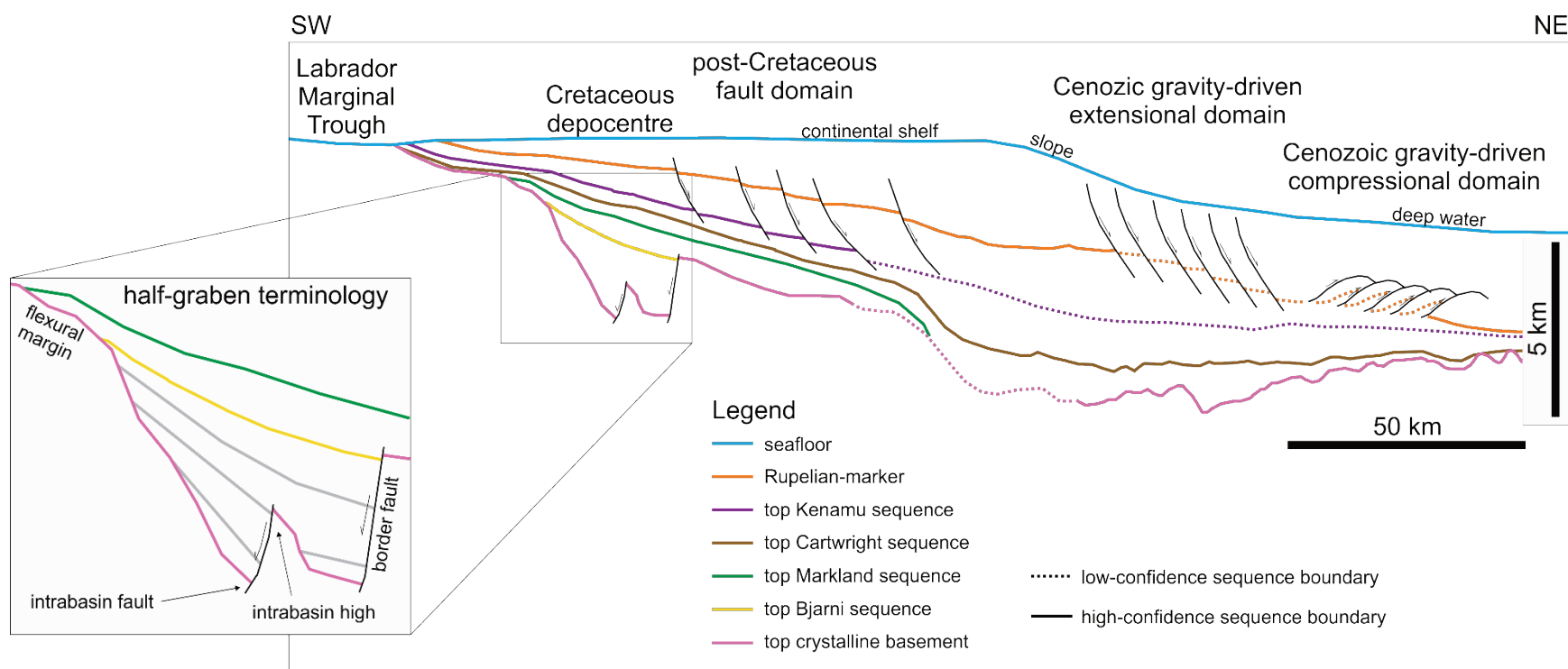
FIGURE 8. Schematic cross-section through the southern Hopedale Basin, showing an example of major features discussed in this report. The inset shows the structural terminology used to describe the Bjarni half-grabens as well as a schematic representation of the wedge-shaped stratal pattern that results from syn-depositional extensional faulting.

TABLE 1. Labrador Sea Petroleum Play Summary, including the global scale factor (GSF) used for each play.

Play	Reservoir	Trap	Source	Seal	Major Risk	GSF region	GSF value
Paleozoic	Paleozoic	Paleozoic	Paleozoic Bjarni	Markland	source or reservoir	Shelf Slope Hyper-extended crust	0.65 0.35 0.2
Bjarni	Bjarni	Bjarni	Bjarni	Markland	reservoir, maturity in shallow half-grabens	Saglek basin Northern Hopedale basin Southern Hopedale basin Slope and deep water	0.35 0.85 0.75 0.2
Markland	Freydis	Markland	Bjarni Markland	Markland (Kenamu at Ogmund well)	migration, reservoir	Entire study area	0.35
Cartwright	Cartwright	Cartwright	Cartwright Markland Bjarni	Kenamu	migration	North region Central region South region	0.6 0.55 0.65
Kenamu	Kenamu	Kenamu	Cartwright Kenamu	Kenamu/Mokami	maturity, trap	North region Central region South region	0.55 0.45 0.65
Mokami	Mokami	Mokami	Cartwright Kenamu	Mokami	maturity, migration	Continental shelf Slope and deep water	0.45 0.55

APPENDIX A. GEOLOGIC FRAMEWORK

The opening of the Labrador Sea can be described in five phases: (i) Pre-rift, (ii) Early rift, (iii) Late Rift, (iv) Seafloor Spreading, and (v) Post Seafloor-spreading (Dickie et al. 2011). Nomenclature describing the Labrador Sea subsurface sediments is complicated. Lithostratigraphic units based on well data were introduced by Umpleby (1979). McWhae et al. (1980) expanded these definitions using seismic stratigraphy so that the "Labrador Shelf stratigraphic nomenclature does not represent true lithostratigraphic units" (Moir, (1989), p 26). Dickie et al. (2011) indicate that all of the formations are unconformity bounded in some places. Previous work and literature in the region gives all sands within a sequence the same name, however well log correlations and preliminary mapping reveal this is not entirely accurate. To avoid adding more confusion to the nomenclature, the six major sequences mapped for this study use the same sequence/formation names as Dickie et al (2011), however they are referred to as sequences because they are unconformity bounded, and because some sequences contain more than one formally-defined formation (Figure 7). The sands within each sequence have been subdivided and mapped based on their temporal and lateral distribution but no new names are assigned.

Phase I. Pre-Rift

1.Precambrian

Coastal Labrador can be subdivided into three structural provinces (Figure 4). From north to south, they are the Archean Nain Province, the Paleoproterozoic Makkovik Province and the Paleoproterozoic-Mesoproterozoic Grenville Province (St-Onge et al. 2009; Wardle et al. 1997). The Nain Province consists of the Saglek and Hopedale Blocks, separated by Mesoproterozoic plutonic suites (St-Onge et al. 2009). The Kanairiktok shear zone separates the Nain and Makkovik Provinces (Culshaw et al. 2000). While the Nain Province is the North American part of the North Atlantic Craton (St-Onge et al. 2009; Funck et al. 2008), the Makkovik Province contains domains amalgamated during assembly of Laurentia (Culshaw et al. 2000). The southern limit of the Makkovik Province is the Grenville Thrust Front (Culshaw et al. 2000; Wardle et al. 1997). The exterior thrust belt of the Grenville Province is found along the Labrador Sea coast, and the interior magmatic belt borders the Straight of Belle Isle (Wardle et al. 1997).

All three structural provinces are assumed to extend offshore to the Labrador Shelf. Eleven offshore wells on the Labrador margin encountered crystalline basement rocks (Figure A-1). From these, six samples were submitted for radiometric dating, all of which returned Proterozoic dates ranging from 1066 +/- 41 Ma (gneiss from Skolp E-07; Total Eastcan Exploration, 1978b) to 1917 +/- 64 Ma (gneiss from Gilbert F-53; Total Eastcan Exploration, 1979). Precambrian rocks do not hold potential as source or reservoir rocks in the study area, so a more detailed treatment of their geologic history is omitted. Further details can be found in the numerous peer-reviewed publications on the Precambrian geology of Labrador, particularly Wardle et al. (1997), Culshaw et al., (2000), Funck et al. (2008), and St-Onge et al. (2009).

2. Paleozoic

 a. Tectonic Setting

 The tectonic setting of the Paleozoic rocks of the region is uncertain. Bell and Howie (1990) inferred a northwest trending anticlinorium, approximately parallel to the present shelf margin, based on the dipmeter data from Roberval K-92, Gudrid H-55, Indian Harbour M-52, and Freydis B-87. However, a continuous Paleozoic section cannot be mapped in the reflection seismic data, nor is a regional dip for the Paleozoic observed; the Paleozoic appears to be present only as erosional remnants preserved through Cretaceous rifting. As a result, dipmeter data may reflect subsequent deformation rather than depositional trends.

 b. Occurrence and distribution

 The presence of Paleozoic rocks in the subsurface of offshore Labrador was first reported from Gudrid H-55, where 140 m of dolostone were encountered, underlain by Precambrian granites and overlain by Cretaceous shales of the Markland sequence (Eastcan Exploration, 1975a). Six other wells in central Labrador have been found with rocks of probable Paleozoic age, varying in thickness from 4 m at Tyrk P-100 to at least 427 m at Indian Harbour M-52 (C-NLOPB, 2019; Figure A-1). The occurrence of Paleozoic rocks in wells from central Labrador led Bell and Howie (1990) to postulate a continuous lower Paleozoic carbonate platform across the southern Labrador Shelf, linking the Anticosti Basin to the relatively thick Paleozoic sections at Indian Harbour M-52 and Freydis B-87. However, Umpleby (1979), noted that the Paleozoic was discontinuous and difficult to map, while McWhae et al. (1980, in their Figure 2b, p.462), describe "sporadic erosional residuals of Paleozoic sediments" rather than a continuous unit, and this study corroborates the latter characterization. The Paleozoic sediments are found at the base of structural lows and half-grabens or on the crests of intrabasin structural highs. Paleozoic strata not tied to wells and not differentiated from the overlying sequence in the seismic are possible at the base of any Cretaceous succession.

 c. Lithology and biostratigraphy

 The lithology of the Paleozoic rocks is variable. Dolostone and limestone are common, but sandstones, siltstones and shales are also present. The age of the Paleozoic deposits is poorly constrained. In many wells, dolomitization has destroyed much of the fossil evidence required for biostratigraphy and there are problems with cavings from overlying formations contaminating drill chip samples. BP Research Center (1977) concluded that the interval below 3504 m at Indian Harbour M-52 was Paleozoic on the basis of the gross assemblage of macrofauna, but could not specify the age more precisely. Cuttings from Tyrk P-100 and South Hopedale L-39 were assigned to the Paleozoic on the basis of their carbonate lithology but without fossil evidence (Total Eastcan, 1979; Robertson Research, 1984). However, Bujak Davies (1987) assigned the carbonates in South Hopedale L-39 to the late Aptian to middle Albian based on palynology. Robertson Research (1975) assigned the interval below 1981m in Freydis B-87 to the Trentonian (Middle Ordovician) and the interval from 1915 to 1981m to the Edenian to Richmondian (Upper Ordovician). Subsequent work continues to support a late

Ordovician age for these rocks (Barss et al., 1979; Riley Geoscience, 2016). A Caradocian (Late Ordovician) Ostracod fauna was found in Hopedale E-33 (Chevron, 1978). More controversially, Carboniferous spores of Visean-Westphalian age were reported from both Gudrid H-55 (Barss et al., 1979) and Roberval K-92 (Total Laboratories, 1980c). Robertson Research (1974) suggested the deposit at Gudrid H-55 might be late Devonian, based on the presence of scolecodonts. Jenkins (1984) questioned whether the palynomorphs in both wells were *in situ*. Bell and Howie (1990) concluded that it was most likely that all the Paleozoic rocks in central Labrador were Ordovician in age, in part based on the absence of any known carbonates of similar age in northeastern North America. Schwartz (2008) found that Strontium isotope ratios suggested deposition occurred in early to middle Ordovician times.

Phase 2. Early Rifting

    a.   Tectonic Setting

    The opening of the Labrador Sea began during the early Cretaceous, with crustal extension accommodated by volcanic deposits and half-graben development (Dickie et al. 2011). The oldest preserved syn-rift half-graben fill is the Bjarni Sequence, which is composed of terrigenous clastic sediments and the Alexis volcanics. Detrital monazite, presumably sourced from uplifting rift shoulders, was carried south to the Scotian Basin by the Sable River as early as the Tithonian (Pe-Piper, et al, 2013). The Bjarni Sequence, including some Alexis volcanics, has also been mapped in depocenters which do not presently resemble half-grabens. Whether they were deposited in half-grabens that have been subsequently deformed is unclear.

    b.   Occurrence and distribution

    The Bjarni sequence is found in syn-rift structural lows, many of which are half-grabens that contain intrabasin faults and structural highs (Figures 8, A-2). In the southern Hopedale basin, the Bjarni sequence is identified in five wells (Freydis B-87, Indian Harbour M-52, Leif M-48, North Leif I-05, and Roberval K-92) associated with six well-defined half-grabens (Indian Harbour M-52 contains Alexis volcanics but is on a structural high between two half-grabens). Gudrid H-55, Roberval C-02 and Cartier D-70, were drilled on basement highs where Upper Cretaceous rocks directly overlie pre-rift sediments (Barss et al., 1979, Williams 2017a, b), however there are half-grabens associated with these structural highs. Leif E-38 is not deep enough to encounter Mesozoic strata. Gudrid H-55 appears to be on a relay ramp between border fault segments of one half-graben while Roberval C-02 and Cartier D-70 are on highs between half-grabens. The South Hopedale half-grabens were likely part of a continental rift valley that could have extended north beneath the modern slope and beyond. The Kanairiktok Shear Zone is the division between the Nain (north) and Makkovik (south) Structural Provinces. On the shelf, the well-defined half-grabens only occur over the Makkovik Province, so it is possible the Kanairiktok Shear Zone was the northern limit of the Cretaceous continental rift valley. Any Bjarni strata beneath the modern shelf edge or beyond would be very thin and deformed as the crust in those regions is extended and hyper-extended.

    On the central Labrador margin, eight wells in the Hopedale Basin encounter the Bjarni sequence. These wells are: Tyrk P-100, Bjarni H-81, Bjarni O-82, Herjolf M-92, North Bjarni F-06, South Hopedale L-39, South Labrador N-79, and Hopedale E-33. Corte Real P-85 did not penetrate deep enough to encounter the Mesozoic, while in the northernmost Hopedale Basin and

in the southern Saglek Basin, the Bjarni sequence is only encountered in Snorri J-90, Ogmund E-72 and Skolp E-07. While current seismic data coverage suggests the Ogmund half-graben is separate from the Snorri depocenter, they may actually be connected. The Bjarni depocenters overlying the Nain Province do not follow rift valley-like trends. In the central Hopedale Basin, the Bjarni depocenter has the largest distributions of mapped Alexis volcanics. In the northern Hopedale and Southern Saglek basins, the Bjarni depocenters may have developed at pre-existing zones of weakness or along re-activated pre-rift faults associated with Okak Arch evolution rather than a continental rift valley.

c. Lithology and Biostratigraphy

The Alexis volcanics are described from cores as weathered basalts with some interbedded siliciclastics (Umpleby 1979; Balkwill et al 1990). K-Ar dates obtained from the Alexis volcanics fall between 139 ± 7 Ma and 122±6 Ma, suggesting volcanism could have begun as early as the latest Tithonian and continued until the mid- to late-Aptian in the Hopedale Basin (Eastcan, 1973b; Total Eastcan, 1977; Total Eastcan 1978). However, the 139 ±7 Ma date comes from an altered sample in Bjarni H-81 and is not considered reliable; an upper Valanginian to mid-Aptian range of volcanism is more likely (Umpleby 1979). Tuffs encountered in Indian Harbour M-52 were dated ~90 Ma but the sample was described as somewhat altered; therefore, the true age is likely older (BP, 1978).

Balkwill et al. (1990) informally divide the Bjarni into upper and lower members. The lower Bjarni consists of feldspathic, lithic, coaly non-marine sandstones with minor conglomerate, whereas the upper member contains sands, siltstones and shales, some of which are carbonaceous and marine in origin. Biostratigraphic analysis of the Bjarni sequence indicates predominantly Aptian to Albian ages (Nøhr-Hansen et al., 2016), though deposition may have begun as early as the Barremian in some locations, or continued into the Cenomanian (Williams, 2007; Riley Geoscience, 2014). The coal-bearing Bjarni successions are mostly Barremian to Aptian in age, while fine-grained Bjarni successions with carbonaceous shale are more often Albian. Marine and non-marine depositional environments may be intercalated at a fine scale. Aptian marine sediments are noted as far north as South Labrador N-79 and coaly non-marine Albian-aged sediments extend as far south as North Leif I-05 (Nøhr-Hansen et al., 2016). The highly radioactive coarse-grained sands (the Bjarni sands south of the Kanairiktok Shear Zone have higher gamma counts than the clay-sized sediments in the same well) in the Hopedale Basin are distinct from those in North Labrador. This fits with the detrital zircon work of Thrane (2014), with local sources from the Hopedale Block of the Nain Province north of the Kanairiktok Shear Zone and sources from the Makkovik Province or Southern Greenland south of the Kanairkitok Shear Zone.

Phase 3. Late Rifting

a. Tectonic Setting

The late rifting phase marks the transition from continental rifting to the onset of seafloor spreading. The timing of the initiation of seafloor spreading on the Labrador margin has been controversial. The oldest unambiguous magnetic anomaly is chron 27 (late Danian), (Chalmers, 1991), but Roest and Srivastava (1989) interpreted anomalies as old as chron 33 (Campanian). Chian et al. (1995) noted a broad band of anomalously high-velocity crust with ambiguous

magnetic signatures and proposed that it consisted of serpentinized mantle peridotite. This implies that by Maastrichtian time the continental crust between Labrador and Greenland had ruptured but a mature sea-floor spreading regime, producing typical oceanic crust, was not established until chron 27. Keen et al. (2018b), using modern seismic, magnetic, and gravity data, concluded that the rupture of the continental crust and exhumation of the mantle began at about chron 31 (Maastrichtian).

      b.   Occurrence and distribution

The shale-dominated Markland sequence is separated from the underlying Bjarni sequence by a major unconformity (Umpleby, 1979; Balkwill et al., 1990; Dickie et al. 2011). The Markland sequence is interpreted to record rapid thermal-sag related subsidence of the margin in the Late Cretaceous (Dickie et al., 2011), however some faults on the shelf have associated growth strata in the Markland sequence and the distribution of the Markland sequence on the shelf is still strongly influenced by the underlying Bjarni depocenters (Figure A-3).

The Markland sequence thins basinward, onlapping the top of the Bjarni sequence in the southernmost part of the Hopedale Basin. Through the rest of the Hopedale Basin, the basinward extent of the top of the Markland sequence cannot be distinguished due to poor seismic quality beneath the modern shelf-edge and slope. Limited seismic data coverage in the Saglek Basin impedes interpretation of the Markland sequence beyond the flexural margin of the Skolp half-graben. Analogous non-volcanic margins are characterized by multi-stage faulting in which later stages of faulting produce local, sediment-starved basins (Reston 2007). The Labrador Margin appears to have been sediment-starved during Markland time, so late-stage faulting may have produced local fault-controlled basins beneath the modern outer shelf and slope.

      c.   Lithology and Biostratigraphy

In some wells on the Labrador Shelf, the oldest Markland sediments are of Campanian to Maastrichtian age while in others the Markland strata are as old as Cenomanian (Barss et al., 1979; Bujak-Davies, 1989; Nøhr-Hansen et al., 2016).The Markland sequence is largely a green to dark grey silty shale (McWhae et al., 1980). However, fine- to coarse-grained quartzose sandstones and poorly-sorted arkosic sandstones of the Freydis Member occur most prominently at Freydis B-87, Ogmund E-72 and Skolp E-07 (Figure A-3). At Freydis B-87, the type section, the sand is medium-grained. These sands are restricted to Bjarni half-grabens and it is unlikely they are related to each other given that they are separated by basement structures and large distances (> 650 km between the Freydis B-87 and Skolp E-067 wells). The sands are typically coarse grained and texturally immature, similar to the Bjarni Formation, suggesting locally derived sediments. Radiometric ages derived from zircons of the Markland Formations indicate Nain crustal sources for the Saglek Basin wells (Thrane, 2014).

Thin intervals (less than 100 m, in some cases only 10 m) of Cenomanian to Santonian aged rocks were reported from several wells on the margin by Barss et al. (1979) and Bujak-Davies (1989). Subsequent work has confirmed these ages for Bjarni O-82 and South Labrador N-79 (Williams, 2007), Herjolf M-92 (Riley Geoscience, 2014), North Leif I-05 (Nøhr-Hansen et al. 2016), Freydis B-87 and South Hopedale L-39 (Riley Geoscience, 2016), and Roberval K-92 (Williams, 2017). The sands in North Bjarni O-82 are mapped as part of the Bjarni sequence, and in chip sample description are indistinguishable from the Bjarni. In view of the microfossil age and outer littoral to open marine environmental association (Williams, 2007), they could reflect

reworking of the Bjarni sands during the subsequent transgression. However, it is also possible that the fossil material has caved from younger overlying sediments in the well.

Phase 4. Seafloor Spreading

      a.   Tectonic Setting

An increased subsidence rate on the southern part of the margin in the Late Cretaceous may be associated with the onset of seafloor spreading (Dickie et al. 2011). A regional unconformity (approximately mid-Paleocene) marks the onset of the Cartwright Sequence. This unconformity is probably related to thermal uplift associated with the North Atlantic Igneous Province and the development of the northern volcanic-dominated margin, which is characterized by Paleocene diabase at the base of Rut H-11 and in wells offshore of Baffin Island as well as seaward dipping reflectors beneath the sedimentary package on the lower slope in Northern Labrador (Chalmers, 1997; Keen et al., 2012 Figure 2).

The end of the Cartwright sequence is marked by an approximately Paleocene-Eocene-aged unconformity and is overlain by the Ypresian-Bartonian Kenamu sequence (McWhae et al., 1980; Dickie et al., 2011). The Kenamu sequence is thick, widespread, and predominantly mudstone, generally recording outer shelf to bathyal conditions (D'Eon-Miller and Associates, 1987), though a sandy Leif Member is present in several wells. The fine-grained nature of the Kenamu sequence and the presence of outer shelf to bathyal faunas suggests that sea level was relatively high with a wide and deep shelf. Kenamu shales, especially in the lower part of the section, are characteristically organic rich (see Appendix C, section 4). Despite the marine depositional environment, both pyrolysis experiments and visual evaluation of the organic matter indicate that most of this material was terrestrial in origin, therefore river systems were providing large quantities of organic material at this time.

The sand bodies of the Leif Member were deposited in the Upper Kenamu when seafloor spreading slowed, and the spreading orientation of the Labrador spreading center changed (Roest and Srivastava, 1989; Delescluse et al., 2015). These sands may have been deposited in response to middle Eocene global sea level fall (Haq and Al-Qahtani, 2005; Miller et al., 2018).

      b. Occurrence and Distribution

The top of the Cartwright sequence is the first sequence boundary that can be easily interpreted from the shelf into deep water on the reflection seismic data, and therefore the first clear indication of a sedimentary system linking the continent with the basin. Furthermore, the Gudrid sandstones are more laterally extensive than the Bjarni and Freydis sands (Figure A-4). They also are typically less radioactive than the older sands, and rounded to sub-rounded, indicating either long transport distances or high-energy environments. The thickest and most widespread Gudrid sandstones are in the southern Hopedale basin, where two widely distributed coarse-grained sand and conglomerate intervals are laterally separated by a fine- to medium-grained Gudrid sand. These sands may be the first signs of drainage from a paleo-Churchill River exiting the remnant Melville Rift in southern Labrador (Figure A-4). Thrane (2014) found that the Cartwright Formation at Ralegh N-18 off Baffin Island contained zircons with a much wider range of ages, including signatures from the Grenville Province and Appalachian Orogen, suggesting the presence of a northward flowing fluvial system that transported sediments over hundreds of kilometres. Thrane (2014) did not find zircons from far-travelled sources in the

Cartwright samples from Cartier D-70. However, the Cartier D-70 well is on a significant structural high and a fluvial system from the south may not have breached it so that only local sediments are preserved there. In Central Labrador a coarse-grained sand at Tyrk P-100 and a medium-grained sand with interbedded muds at Herjolf M-92 have been mapped as laterally equivalent but separated by mudstone. In North Labrador, a continuous sand can be mapped between Snorri J-90 and Ogmund E-72. This sand is coarse-grained at Ogmund E-72 and fine-grained at Snorri J-90. A coarse-grained Gudrid sand is also found at Skolp E-07.

   The Leif sands in the Kenamu sequence are thinner and finer-grained than the underlying Gudrid sands (Figure A-5), but mapping indicates they are more laterally extensive, and could even be considered sheet sands. As with the sands in all sequences on the Labrador Margin, the Leif sands are not all at the same stratigraphic level and stacked sand bodies separated by mudstone intervals have been identified in the wells and mapped on the shelf. The Leif sands are found throughout the Kenamu sequence, but cycles of coarsening upward sands are more likely in the upper part of the Kenamu.

       c.   Lithology and biostratigraphy

   Deposition of Gudrid sands and intertonguing Cartwright shales began during the Selandian (McWhae et al., 1980; Dickie et al., 2011). The depositional environment of the Gudrid sands is controversial. Some workers describe it as a deep-sea fan deposit created by turbidites (McWhae et al., 1980; D'Eon-Miller and Associates, 1987) based on the presence of deep-water foraminifera. However, Dafoe et al. (2015) reported wave ripples and shallow water trace fossils such as *Macaronichnus*, indicating a nearshore environment for these sands. Dickie et al. (2011, p 1669) described the "shingled" seismic character of the Gudrid sands, suggestive of a forced regression, although this facies could also represent clinoforms or even chaotic reflections caused by coarse-grained sediments. Dafoe (pers. comm., 2017) suggested that the deep water foraminifera were derived from caved material from the overlying Kenamu sequence.

Phase 5. Post Seafloor-Spreading

       a.   Tectonic Setting

The Labrador Sea spreading center slowed in the mid-late Eocene and spreading ceased in the early Oligocene (Srivastava and Roest, 1989; Delescluse et al., 2015). Global climatic cooling during the late Paleogene and Neogene led to continental glaciation and global sea level fall (Haq and Al-Qahtani, 2005; Zachos et al., 2001). On the Greenland margin, Neogene uplift (Chalmers, 2000; Japsen et al, 2006) amplified the sea-level fall, resulting in widespread erosion. Whether synchronous uplift occurred on the Labrador Shelf is unclear (Dickie et al., 2011). During the Pleistocene, the continental shelf was deeply scoured by glaciation with ice grounded to depths of up to 400-600m below sea level (Josenhans et al., 1986). Sediment delivery to the continental slope was enhanced by the grounded ice margin, resulting in significant slope progradation, slumping and mass wasting, and increased turbidite activity (Myers and Piper, 1988; Wang and Hesse, 1996). Most of the strata on the continental slope and in the deep water are late Eocene and younger. This young thick sediment package is the result of Neogene progradation caused by long-term sea level fall, cooling climate and glaciation.

b. Occurrence and Distribution

Late Paleogene and Neogene sea-level fall is reflected by a broadly progradational regime on the Labrador Margin (Dickie et al., 2011). The Mokami and Saglek sequences were deposited on the shelf prior to glaciation (McWhae et al., 1980). While the Saglek sequence was originally described as unconformably overlying the Mokami sequence (McWhae et al., 1980), Dickie et al. (2011) show a more complex relationship between the two. There is a highly diachronous boundary between the two sequences and evidence for multiple progradational Saglek sand packages spanning the Miocene to Pliocene. The top of the Mokami sequence can be considered the base of the deepest progradational sand; however, the diachronous nature of the progradation makes mapping this as a continuous surface across the entire margin complicated. A mid-Mokami seismic marker, tied to the mid-Rupelian interval at Roberval K-92, is the youngest continuous horizon interpreted for this project (Figure A-6). Heavy glacial scouring in the Saglek Basin reaches this horizon in places, but a second mid-Mokami marker, in the Rupelian zone at Skolp E-07, can also be mapped. The vertical separation between these two marker horizons is unknown.

c. Lithology and biostratigraphy

McWhae et al. (1980) described the Mokami sequence as consisting of poorly consolidated muds with thinner beds of silt, sand and limestone. Balkwill et al. (1990) informally divided the Mokami into an upper and lower member. The lower Mokami is mudstone dominated and thickest in the central parts of Saglek and Hopedale Basin. It tends to become sandier upward and northward (Balkwill et al., 1990). McMillan (1973) and Duk-Rodkin and Hughes (1994) attributed the thick sedimentary package seaward of Hudson Strait to a large river system outflow in this area that drained the Hudson Bay region. This drainage system could have provided the sand supply to account for the higher sand contents in this region, in addition to sediments derived from the Torngat Mountains at the northern tip of Labrador. The paleoenvironment of the Mokami Formation is predominantly marginal marine to neritic, especially in the upper part (D'Eon-Miller and Associates, 1987; Nøhr-Hansen et al., 2016). The Saglek Formation is a clastic wedge of gravels and coarse sands and is generally thicker in Saglek Basin than in Hopedale Basin. Balkwill et al. (1990) suggest that it probably formed as a system of coalescing fan deltas sourced in the Torngat Mountains.
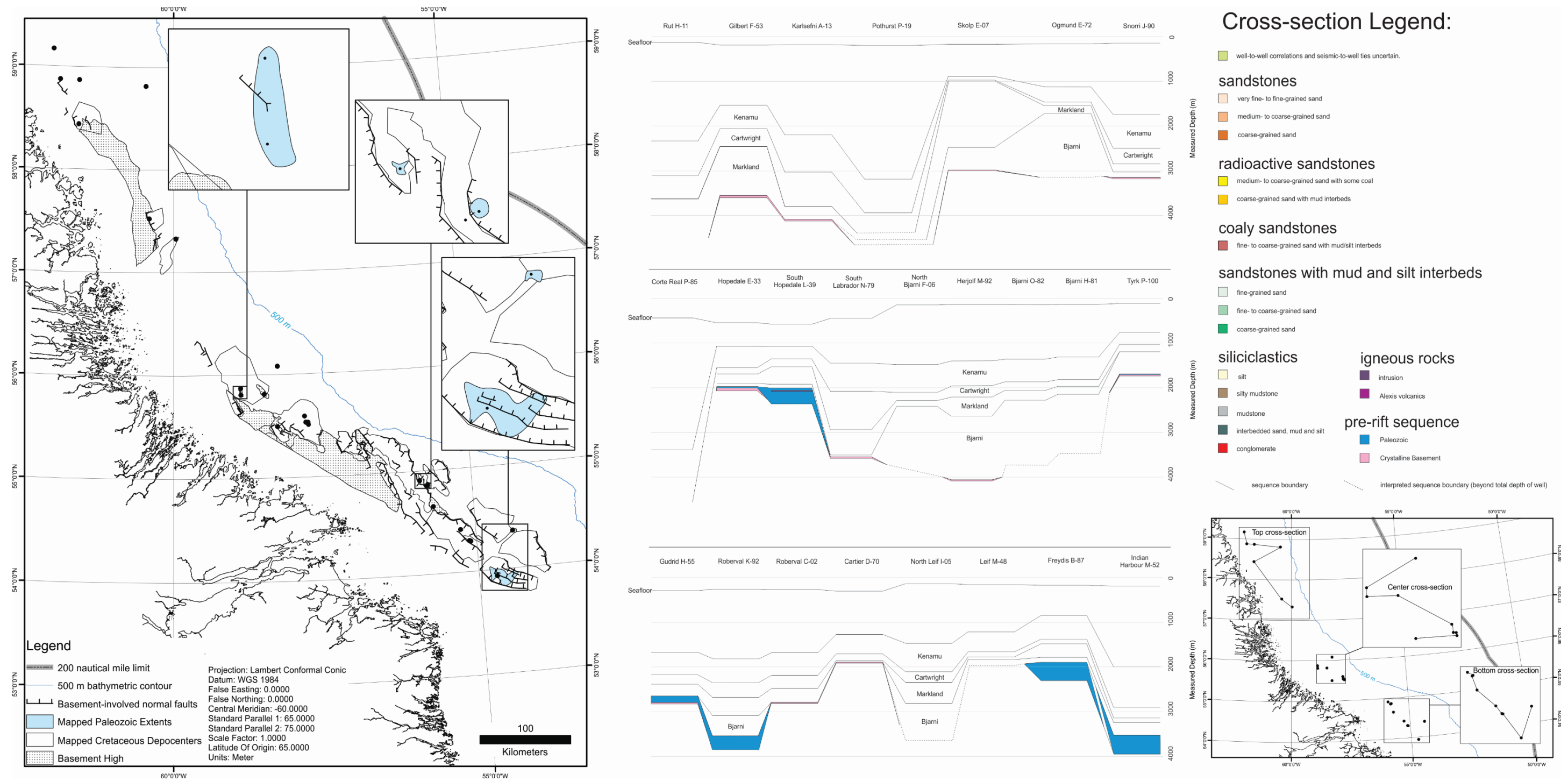
FIGURE A--1. Paleozoic distribution and pre-rift cross-sections. Basement highs, mapped from the depth-converted basement horizon grid mapped in 2D reflection seismic data, and the mapped extents of the Paleozoic strata and overlying Cretaceous depocenters are included on the map. The cross-sections show where Paleozoic and Precambrian rocks are intersected by wells. Each cross-section has north on the left and south on the right. See Figure 2 for well index. The Paleozoic section identified in the Tyrk P-100 well is too thin to map in the seismic.
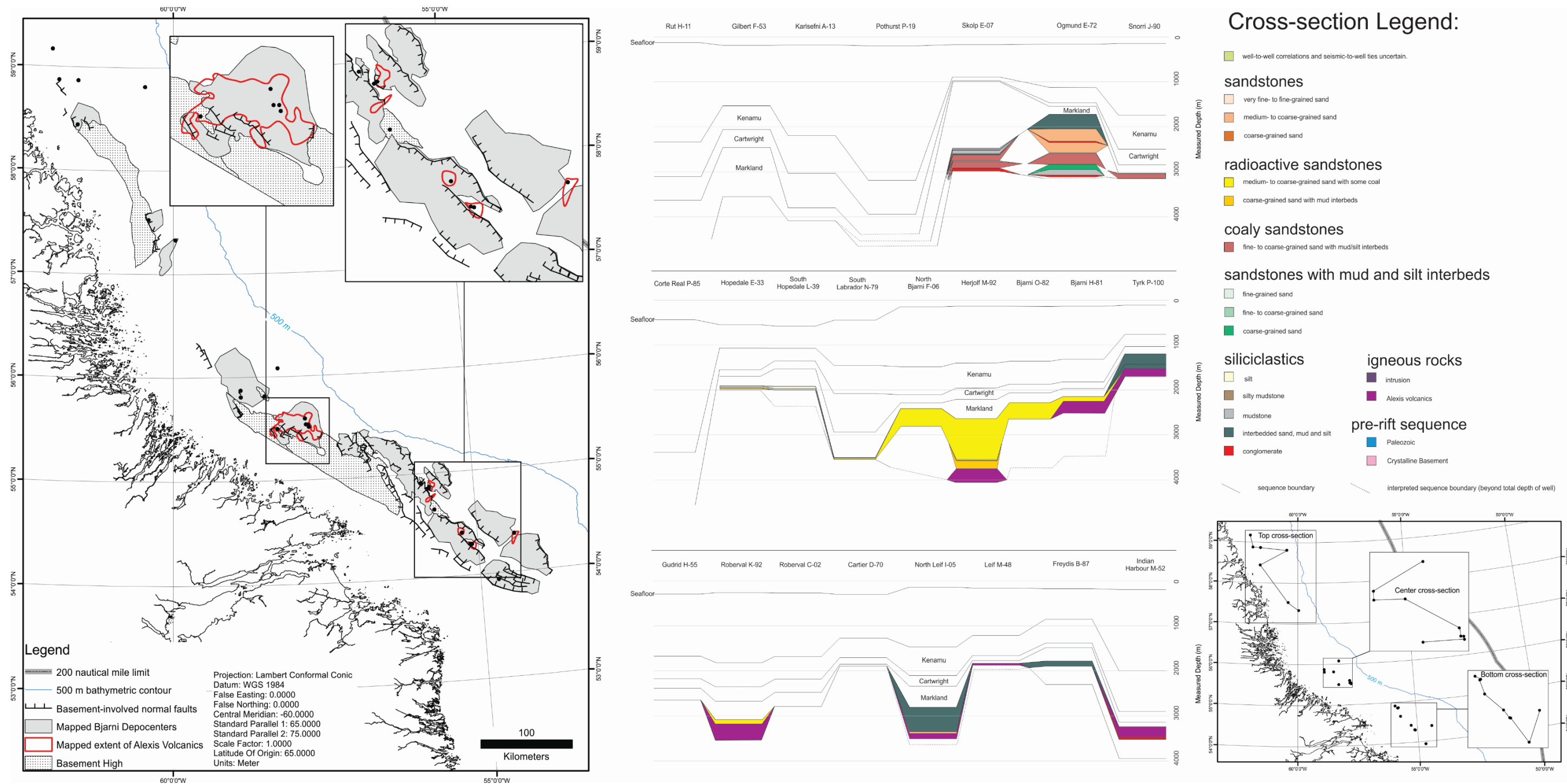
FIGURE A--2. Bjarni distribution and cross-sections. Basement highs, Bjarni depocenters and Alexis Volcanic extents have all been mapped from the seismic interpretation. Each cross-section has north on the left and south on the right. Sand facies shown here were identified from the D'Eon Miller grain sizes shown in the Wielens and Williams (2009a, 2009b, 2009c) cross-sections and were used to map the extent of the sands (where not prevented by poor seismic resolution at the Bjarni stratigraphic level). Although some Bjarni depocenters have inward-dipping normal faults on both margins, the sediment fill is distinctly wedge-shaped, indicating the depocenter is a half-graben rather than a graben. See Figure 2 for well index.
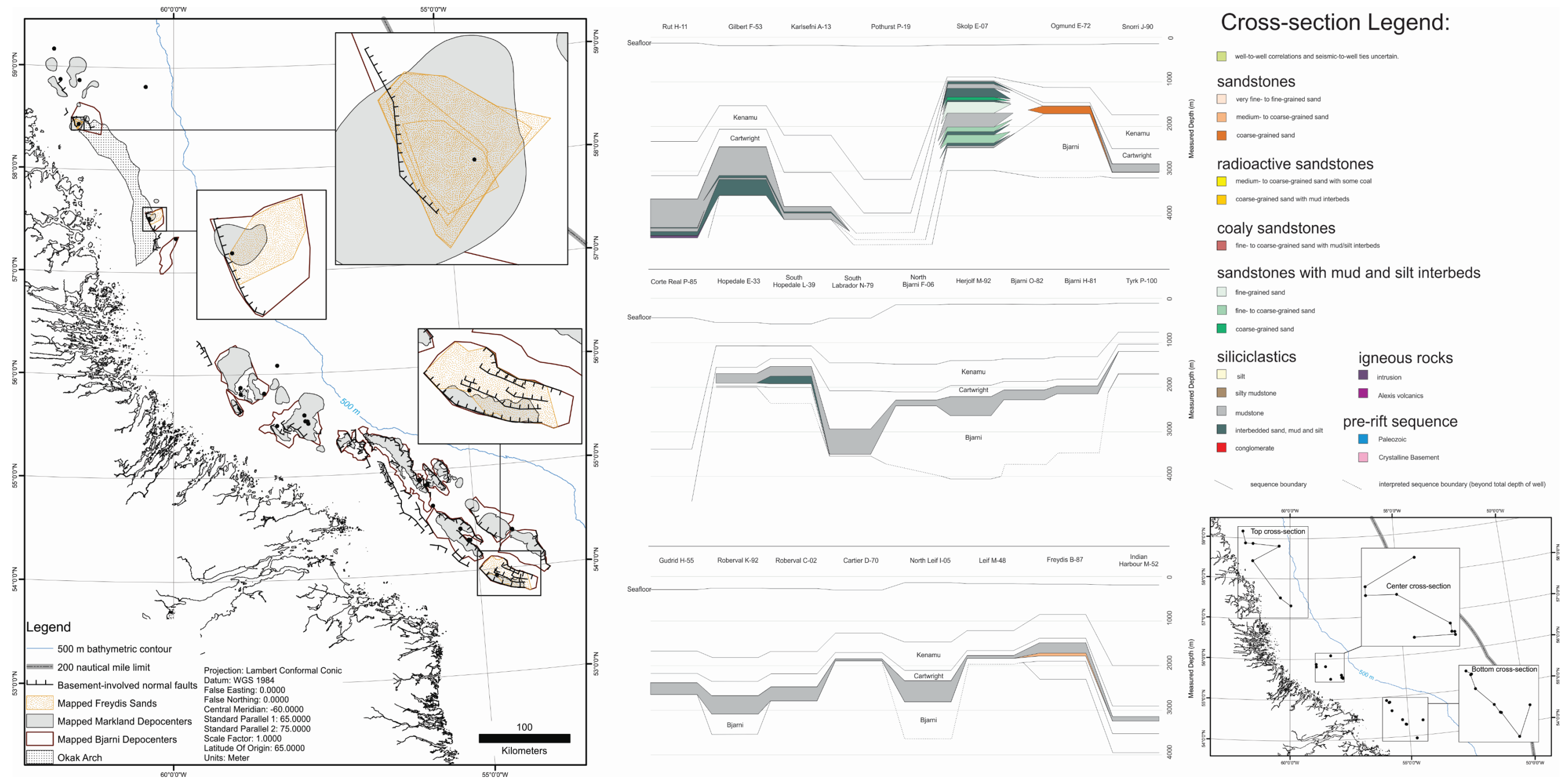
FIGURE A--3. Markland distribution and cross-sections. Basement highs, Bjarni depocenters, Markland depocenters and Freydis sand extents have been mapped from the seismic interpretation. Each cross-section has north on the left and south on the right. Sand facies shown here were identified from the D'Eon Miller grain sizes shown in the Wielens and Williams (2009a, 2009b, 2009c) cross-sections and were used to map the extent of the sands. The Markland depocenters were defined as regions where total thickness of the combined Markland, Bjarni and Paleozoic intervals was greater than 1200 m. The Markland depocenters within Bjarni depocenters reflect the thickest portion of the Bjarni depocenters adjacent to border-faults, however some new depocenters not near any wells were identified through this process – the age of these strata cannot be differentiated. See Figure 2 for well index.
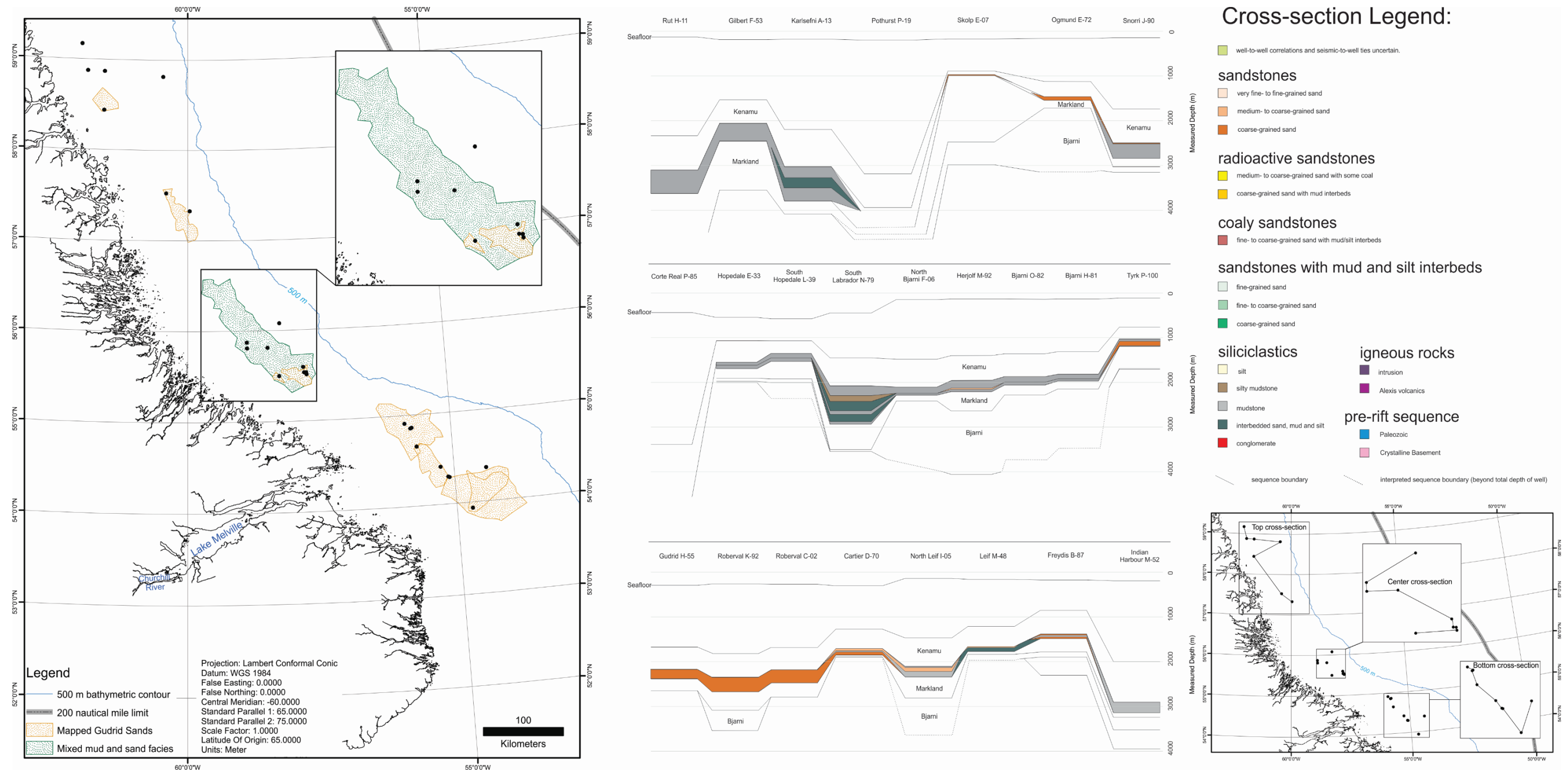
FIGURE A--4. Cartwright distribution and cross-sections. Sand facies shown here were identified from the D'Eon Miller grain sizes shown in the Wielens and Williams (2009a, 2009b, 2009c) cross-sections and were used to map the extent of the sands. Each cross-section has north on the left and south on the right. See Figure 2 for well index. Modern Lake Melville is in the ancient Lake Melville Rift System.
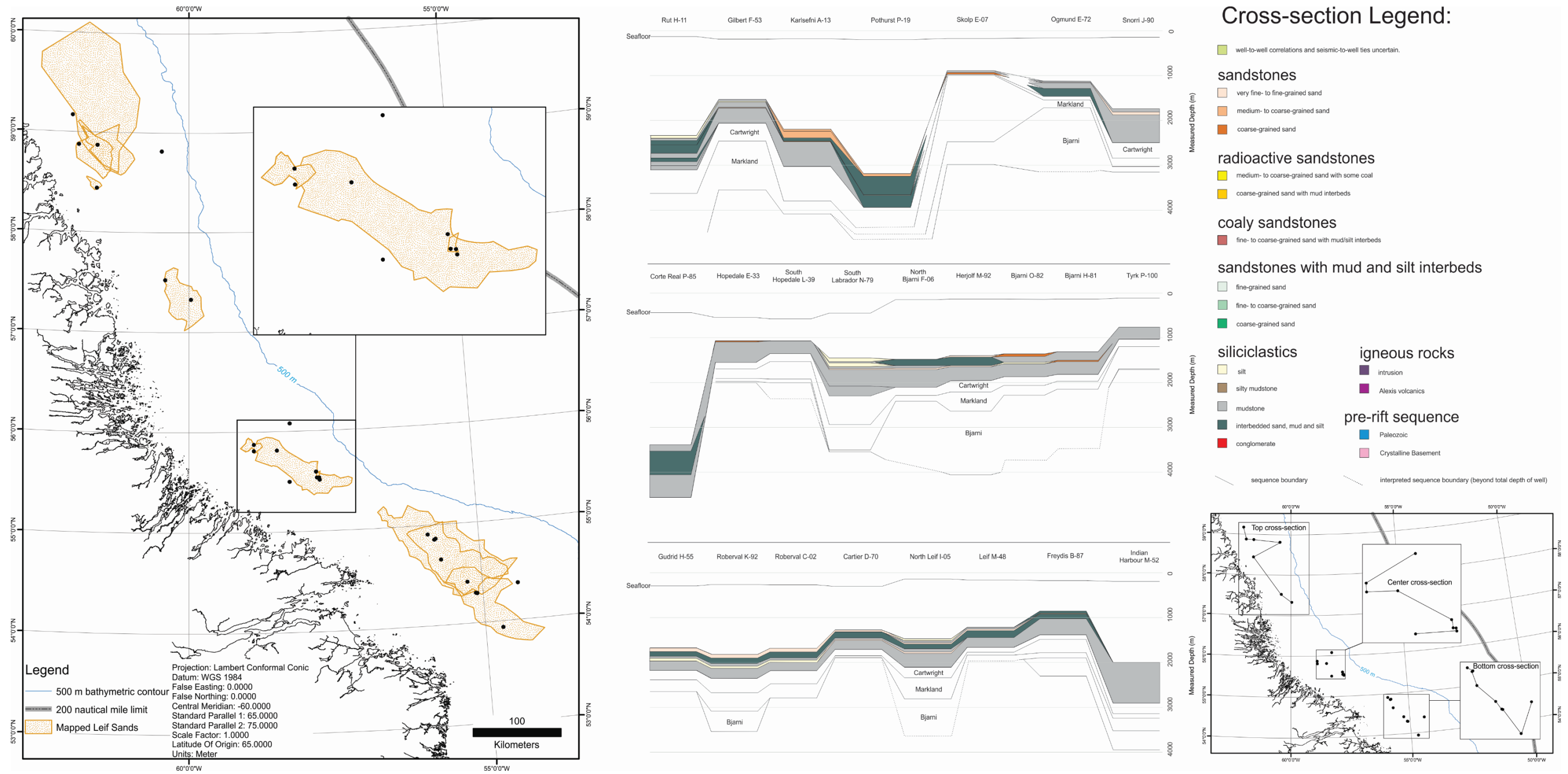
FIGURE A--5. Kenamu distribution and cross-sections. Sand facies shown here were identified from the D'Eon Miller grain sizes shown in the Wielens and Williams (2009a, 2009b, 2009c) cross-sections and were used to map the extent of the sands. Each cross-section has north on the left and south on the right. See Figure 2 for well index.
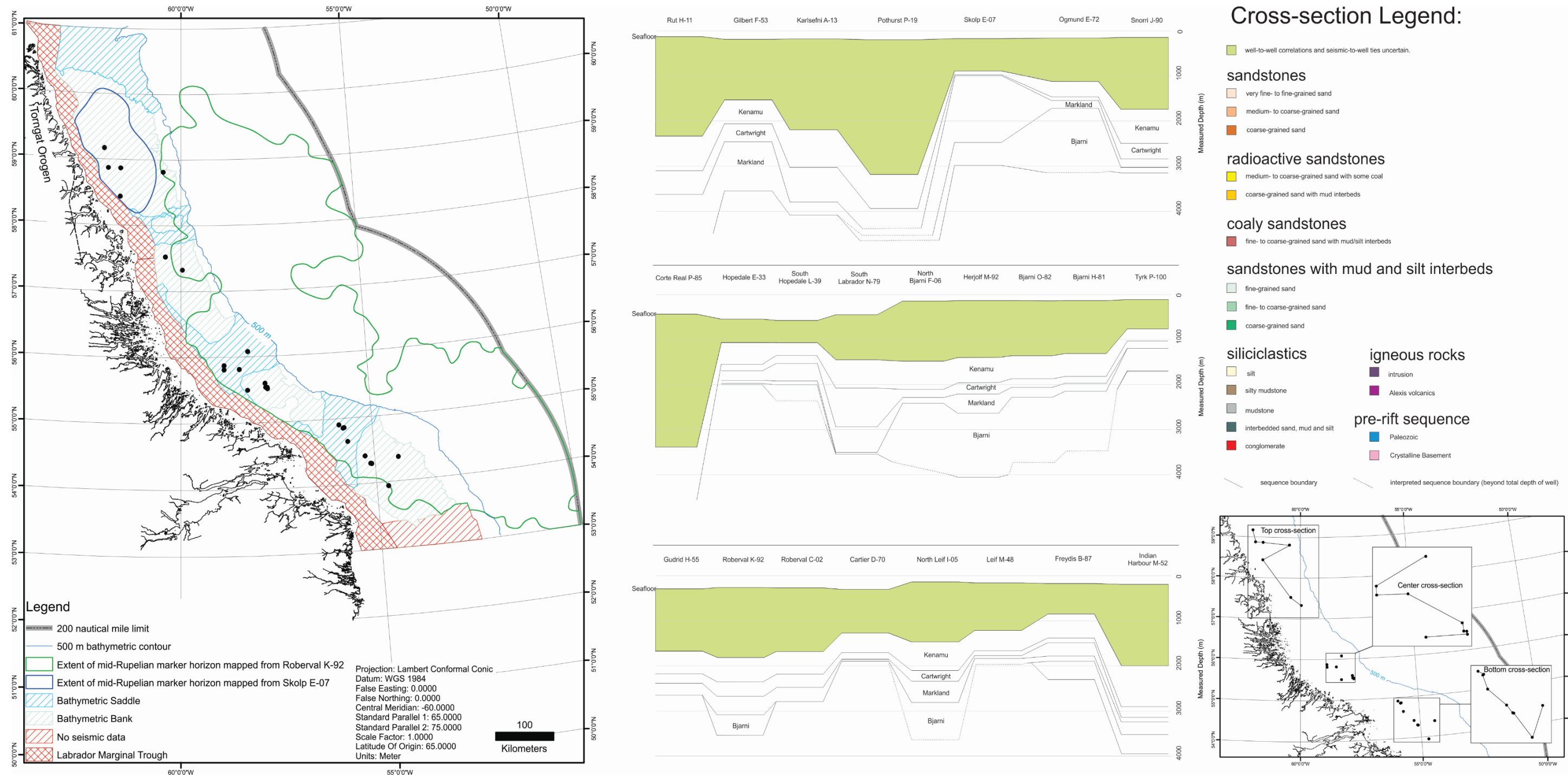
FIGURE A--6. Mokami distribution and cross-sections. Well-to-well correlations and seismic-to-well correlations are not robust enough to map lithologies within the Mokami sequence, therefore two mid-Mokami marker horizons, tied to the Rupelian zones in Roberval K-92 and Skolp E-07, were mapped to provide an Oligocene surface for thermal modeling. The vertical separation between these two marker horizons is unknown, as they are laterally separated by a scoured interval. Well-to-well correlations to determine sand facies was not possible, and seismic-to-well ties above the top of the Kenamu Sequence are unreliable. See Figure 2 for well index.

APPENDIX B. PETROLEUM SYSTEMS MODELING

In order to assess the hydrocarbon potential of the Labrador Margin, it was necessary to assess the degree of maturation of the known and potential source rocks. Regional maps of thermal maturity for the Atlantic margin of Canada by Dehler and Keen (1993) estimate vitrinite reflectance at the base of the rifted Mesozoic section and the depths to key levels of maturity (Ro of 0.7 and 1.2). Due to the limited seismic coverage beyond the shelf edge and a coarse (5 km x 5 km) model grid, modeling the thermal maturity of the potential source rocks on the Labrador Margin was required. Inputs to the model were an assessment of spatial and stratigraphic trends in organic matter content and type, estimates of the thermal history based on modern heat flow, sedimentation rates and rifting history, and indicators of thermal maturation of the organic matter from the wells. The resulting Trinity^{TM} model of the margin was used to estimate the degree of thermal maturation of each of the potential source rocks in support of the chance of success mapping for source rock.

1. Data Sources

Considerable work has been done on source rock analysis on the Labrador Margin, both during the time of active drilling and subsequently. Results of source rock characterization using pyrolysis experiments (RockEval 6) were reported by Bojesen-Kofoed (2002), Petro Canada (1980a, 1980d, 1981a, 1981b, 1982a; 1983b; 1984a, 1984b), Robertson Research (1982, 1983), and Total-C.F.P. (1979a,1979b, 1980a, 1980b). Additional RockEval work has been done by the Geological Survey of Canada-Calgary (Snowdon, pers. comm. to Graham Williams, 1984; Fowler et al., 2019)

More than 2000 RockEval results providing total organic matter content (TOC), and the main pyrolysis parameters and their derivatives (S1, S2, S3, Hydrogen Index (HI), Oxygen Index (OI), and productivity index) are available for 17 wells on the Labrador Margin. Sampling strategies and densities varied, but 10 m sample intervals were common for all the potential source rock intervals. For some wells, full RockEval results were not available, but total organic matter was reported in the well history reports (Eastcan Exploration, 1973b; 1975a; 1976a,b). These provide both source rock richness and indications of the dominant sources of organic matter for these rocks, as well as whether they can be expected to be oil or gas prone. Descriptions of organic matter by visual examination were also reported for a number of wells (Avery 1976a, 1976b, 1987, 2005a, 2005b, 2005c, 2005d, 2005e, 2008, 2009; Geochem Laboratories 1977, 1978a, 1978b, 1978c, 1978d; Petro-Canada, 1980d, 1981d, 1982a, 1983b, 1984a, 1984b; Total C.F.P. 1979a, 1979b, 1980a, 1980b).

Formation temperature estimates derived from downhole measurements were reported in the original well history reports from the companies. These were reviewed by Nantais (1984), Reiter and Jessop (1985), and Moir et al. (1989), who estimated gradients for the wells.

Constraints on the thermal history of the margin are derived from measurements of the maturity of the organic matter and hydrocarbons present. Vitrinite reflectance measurements (Ro) were available for 17 wells on the Labrador Margin (Avery, 1976a, 1976b, 1987; Avery and Hacquebard, 1976, 1980; Bujak-Davies, 1987, 1989; Geochem Laboratories 1977, 1978a, 1978b, 1978c, 1978d; Petro-Canada, 1980d, 1981d, 1982a, 1983b, 1984a, 1984b; Total-C.F.P., 1979a, 1979b, 1980a, 1980b)

Thermal alteration indices (TAI) on palynomorphs were reported by Barss (1977), BASIN (2019), Bujak-Davies (1987, 1989), Chevron (1978), Geochem Laboratories (1977, 1978a), Petro-Canada (1980a, 1980d, 1981b, 1982a, 1983b, 1983c, 1984b), Robertson Research (1974, 1975), Total-C.F.P. (1979a, 1979b, 1980b), and Williams (1976). While vitrinite reflectance data were the primary data used to match the thermal model, TAI provided a useful check to validate the Ro values and ensure that they were not based on reworked or caved material.

An additional source of data on the nature and maturity of organic matter in potential and effective Labrador petroleum systems was analysis of hydrocarbons. These analyses include anlaysis of fluids from well tests for several wells (BASIN, 2019; Chevron, 1978; Eastcan Exploration, 1975a, 1975b; 1977b; Otis Engineering, 1981; Petro Canada, 1982a; Total C.F.P., 1980a) bitumen extracts from samples (Geochem Laboratories 1977, 1978a, 1978b, 1978c; Petro-Canada 1980d, 1981d, 1982a, 1983b, 1984a, 1984b; Rashid and Leonard, 1975) and characterization of adsorbed gases in samples (INRS-Petrole, 1983).

2. 1-D Modeling

The first phase of the petroleum systems modeling was the development of 1-D models for each well using Genesis^{TM}. For five of the wells, calculated crust and lithospheric stretching factors (β and δ) derived from Hamdani and Mareschal (1993) were used. For the other wells, these parameters were estimated from their geographic position and through comparison to the maps of Welford and Hall (2013, Figure 8). Some additional constraints (the rifting period, initial lithospheric and crustal thickness and densities, and asthenosphere temperature were derived from Dehler and Keen (1993). Figure B-1 depicts the lithospheric thickness (a) and resultant heat flow model (b) for the Bjarni O-82 well.

The sedimentary column at each well was created using a combination of lithologies from the Can Strat well log, geophysical log analysis and the best available age constraints from biostratigraphy (see Table B-1). A secondary "rifting" event was introduced for the wells in Saglek Basin to slightly increase their heat flow during the Paleocene, as a way of modeling the mid-Paleocene volcanic event (Figure B-1, c and d).

Subdivisions of the major sequences were created using the hiatuses shown in Dickie et al. (Figure 6) and the boundaries chosen where there were notable lithological changes from sample descriptions and logs that closely corresponded to the biostratigraphic stage boundaries. These subdivisions are listed in Table B-2. Note that these surfaces attempt to accurately model the age of the sediments in the well and do NOT always correspond to the well tops used for seismic correlation or traditional formation names based in part on lithology. For example, the Saglek Formation as defined by its lithology and seismic character can be as old as early Miocene. Thus, although formation names have been used in the stratigraphic columns for these wells, they will differ in detail from the lithostratigraphic units.

The Paleozoic was excluded from the thermal model because there was insufficient information about its preserved distribution away from the wells, and its depositional distribution is uncertain.

Table B-1 Biostratigraphic Age Sources

Well	Source
Bjarni H-81	Williams et al. (1990)
Bjarni O-82	Nøhr-Hansen et al. (2016)
Cartier D-70	Williams et al. (1990)
Corte Real P-85	Williams (2017a)
Freydis B-87	Williams et al. (1990), Riley Geoscience (2016)
Gilbert F-53	Nøhr-Hansen et al. (2016)
Gudrid H-55	Williams et al. (1990)
Herjolf M-92	Williams et al. (1990), Riley Geoscience (2014)
Hopedale E-33	Bujak-Davies (1987), Riley Geoscience (2016)
Indian Harbour M-52	Williams et al. (1990)
Karlsefni A-13	Fensome (2015)
Leif E-38	Williams et al. (1990)
Leif M-48	Williams et al. (1990)
North Bjarni F-06	Bujak-Davies (1987), Riley Geoscience (2014)
North Leif I-05	Nøhr-Hansen et al. (2016)
Ogmund E-72	Nøhr-Hansen et al. (2016)
Pothurst P-100	Williams (2017a)
Roberval C-02	Williams (2017b)
Roberval K-92	Williams (2017b)
Rut H-11	Fensome (2015)
Skolp E-07	Nøhr-Hansen et al. (2016)
Snorri J-90	Nøhr-Hansen et al. (2016)
South Hopedale	Bujak-Davies (1987), Riley Geoscience (2016)
South Labrador L-39	Nøhr-Hansen et al. (2016)
Tyrk P-100	Bujak-Davies (1987)

The percentage of sand, silt, gravel, limestone, dolostone, marlstone, igneous rock and coal were calculated within each interval using a thickness-weighted averaging of data downloaded from BASIN (2019). These data were obtained by the Geological Survey of Canada from digital files created from sample logs by Canadian Stratigraphic Services, Ltd. Missing intervals were modeled as hiatuses, with the exception of the Pleistocene. For the Pleistocene, an imaginary paleo-shelf surface was created from the shoreline to the shelf edge with a water depth of 0 at the shoreline and 100m at the shelf-edge. The thickness between the modern sea bottom and that imaginary surface was added as a depositional interval ending at 2 Ma, and then removed during erosion between 2 Ma and the present. The purpose of this was to simulate the material removed by Pleistocene erosion that created an irregular shelf surface. If the well did not penetrate to the basement, its depth was estimated from seismic grids and the unpenetrated formations given typical lithologies based on the average statistics of the unit. All volcanics in the Bjarni interval

were assigned to the Alexis interval. The volcanics in the Rut H-11 well were assigned to the lower Cartwright interval based on a radiometric age of 59.1+/-6.5 Ma (Petro-Canada, 1983c).

Table B-2 Stratigraphic Intervals used in 1-D Model

Unit	Age	Age in Ma (top)
Upper Saglek	Pliocene or younger	3
Lower Saglek	Tortonian – Messinian	5
Upper Mokami	Langhian – Serravalian	10
Middle Mokami	Aquitainian – Burdigalian	18
Lower Mokami	Oligocene	28
Basal Mokami	Priabonian	32
Upper Kenamu	Bartonian	36
Middle Kenamu	Lutetian	40
Lower Kenamu	Ypresian	44
Basal Kenamu	Basal Ypresian	52
Upper Cartwright	Thanetian	55
Lower Cartwright	Selandian	58
Upper Markland	Maastrichtian – Danian	62
Middle Markland	Campanian	70
Lower Markland	Cenomanian - Santonian	85
Upper Bjarni	Albian	100
Lower Bjarni	Barremian to Aptian	115
Alexis Volcanics		130

Some scenarios incorporating the effects of adding and removing sedimentary material were tested. As many wells had a long hiatus between the Albian and the Campanian, scenarios where as much as 2 km of additional Bjarni-like sediment was added during the Cenomanian, then removed prior to the Campanian (Figure B-2) were tested. While this produced a prominent spike in burial temperatures for the deposits in Cretaceous time (Figure B-2b), the duration of that increased temperature was too short to significantly change the degree of maturity of organic matter (compare Figures B-3a and B-3b). Another scenario tested the removal of up to 1 km of Kenamu-time material on the inner shelf during the early Oligocene, with similar results. It was concluded that modeling non-depositional periods as hiatuses without significant erosion and deposition was adequate for the purpose of this study, so the simpler burial and thermal history shown in Figure B-1a was used for further modeling.

The thermal history was modeled using the rift model of genesis and assuming a transient heat flow boundary at the base of the sedimentary column. This was calculated from the measured temperature gradient using a constant surface temperature of 2.5C. In most cases, this resulted in a good match to both the modern temperature gradient (Figure B-4) and the predicted maturity profile (Figure B-3a). In a few wells, the initial temperature gradient was increased by about

35

10% to get a better match to the thermal maturity data, but in no case was it allowed to increase beyond 3.3C/km.

In order to control the thermal behavior of the model beyond well control, seven imaginary wells were created in deep water. Four of the wells (Fake 1, 2, 4 and 6) were interpreted as being on hyperextended continental crust, for which the crustal thickness and stretching coefficients were estimated using the maps of Welford and Hall (2013). Three of the wells were on transitional oceanic crust (Fake 3, 5 and 7) and were assigned thermal properties based on the Trinity defaults for the upper mantle.

3. 3-D Modeling

After the 1-D Genesis™ models were created for each, a 3-D model of the margin was created in Trinity™. The Genesis™ well models were loaded into a project, along with a series of depth-converted surfaces from the seismic interpretation. These were resampled to an 800 m x 800 m grid size in order to reduce the number of grid cells because of software limitations. The first surface loaded into the model was the seafloor, and the second was the basement. The final depth-converted basement horizon did not cover the complete study area because, although the basement was mapped everywhere, some surfaces required for the interval velocities were not mapped throughout the region. In order to extend the model, a second basement surface based on a single interval velocity was used and warped to gently merge with the basement surface made from the more detailed velocity model using the smart merge routine in Trinity. The seafloor and basement were used as master surfaces; all other surfaces were truncated if they were estimated to be shallower than the seafloor or deeper than the basement. An age of 140 Ma was assigned to the base of the sedimentary succession.

The top Bjarni depth-converted surface was loaded and truncated against the basement where it crossed. In places where it did not intersect the surface was smoothly extended to merge with the basement within 3km of where the surface was mapped, so that the Bjarni and basement are coincident (i.e. Bjarni thickness = 0 where the Bjarni is not mapped). The age of the top Bjarni surface was assigned as 100 Ma.

Other than the seafloor and basement, the surfaces that were mapped over the largest areas were the unconformity at the top of the Kenamu sequence (approximately mid-Eocene) and the unconformity at the top of the Cartwright sequence (approximately Paleocene-Eocene). In areas where these surfaces were not mapped, they were extrapolated as a proportion of the interval between the basement and the seafloor. Figure B-5 and B6 illustrate how the input seismic grids were extended to create the 3-D model. The approach used creates some artifacts in areas beyond the seismic interpretation limits, but is adequate for the purposes of this study.

Two other surfaces were incorporated into the model. In the deep water, beyond the mapped limit of the top of the Markland Sequence, the surface was extrapolated as a small proportion of the top Cartwright to basement interval in deep water and smoothly thinned to zero where Keen et al. (2018) infer the edge of continental crust.

The Genesis™ models for the wells were used to model the heat flow within Trinity. A relationship between sediment thickness and temperature gradient was determined from the well data (as is typical, temperature gradients were generally higher where the basement was shallow). This relationship was used to estimate temperature gradients in areas of thicker sediment on the outer shelf and slope. The values at the individual wells were used to model

local variation and smoothed to create two temperature scalar maps, one at present and a second at 55 Ma during the mid-Paleocene volcanic event (Figure B-7).

The maturity levels were modeled by using the temperature history to predict the vitrinite reflectance ratio (Ro) using the ARCO kinetics model in Trinity^{TM}. Examination of the temperature gradients and Ro values generally showed good agreement when compared with both the Genesis^{TM} models and data (e.g. Figure B-8).

4. Source Rock Maturity Maps

To assist with assessing the chance of finding mature source rock for plays on the Labrador margin, the maturity level of five potential source rocks at five horizons within the model was estimated. The deepest of these was one-tenth of the total Bjarni thickness above the base of the Bjarni. This horizon was chosen to test the maturity of the basal Bjarni section, which is often coal rich (see Appendix A Figure A-2, cross-sections). Coals were observed in the lower part of the Bjarni in Herjolf M-92, Bjarni H-81, Bjarni O-82, Snorri J-90, and Ogmund E-72 wells. The second horizon was the top of the Bjarni. The upper part of the Bjarni Sequence in many wells included carbonaceous deltaic shales (see Appendix A Figure A-2, cross-sections). A third horizon was one quarter of the Markland thickness above the base of the Markland. This horizon was selected to test the maturity of a hypothetical Cenomanian-Turonian shale formed in anoxic conditions during an oceanic anoxia event (OAE2). Rock of this age are poorly represented on the margin in wells, but it is observed in many other regions of the Atlantic (Schlanger et al., 1987; Sinninghe and Koster, 1998; Sinninghe et al., 2008). A fourth horizon tested is the middle of the Cartwright Formation, to test the maturity of the Cartwright Shale which is often organic rich (see Appendix A Figure A-2, cross-sections). The final and shallowest horizon is one fifth of the way above the base of the Kenamu Sequence. Although organic rich shales commonly make up more than half of the Kenamu Sequence, a position close to the base was selected to allow a significant section of potential source rock beneath it, as insufficient burial depth was expected to be a significant risk.

Figure B-9 shows the predicted maturity for source rocks within the lower Bjarni section. The deeper parts of the Bjarni depocenters in central and southern Hopedale basin are well into the oil window. The significant discoveries in the Bjarni at Hopedale E-33, the Bjarni and North Bjarni wells, and the Gudrid H-55 well can be explained by hydrocarbon migration from these deeper parts of the basin where the source rocks are more mature. Wells that were not located within depocenters predicted to contain mature Bjarni source rock (e.g. Freydis B-87, Tyrk P-100, Skolp E-07 and Ogmund E-72) did not find significant quantities of gas. The Snorri J-90 well did find gas in the Gudrid, but not in the Bjarni, though it has been interpreted as derived from a Bjarni source (Powell, 1979). There is an area of about 55 km^2 with a predicted Ro of 0.8 to 0.9 just southwest of Snorri that is a possible source for this gas. Initial estimates of gas expulsion appear insufficient which may be an indication that the model is under predicting maturity here, but it is also possible the gas has a different source. This may be an indication the model is too conservative, but elsewhere the model appears to have adequately predicted where hydrocarbon production is sufficient.

Figure B-10 shows the predicted maturity for source rocks at the top of the Bjarni section. Areas of mature source rock are significantly less extensive, particularly outside of southern Hopedale Basin. There are limited areas of potentially mature source rock along the seaward margins of the depocenters.

Figure B-11 shows the predicted maturity for a hypothetical source rock in the Markland associated with OAE2. This shows widespread regions of mature to locally super mature source rock on the outer shelf and upper slope, particularly in Saglek Basin and southern Hopedale Basin.

Figure B-12 shows the predicted maturity for source rocks in the middle of the Cartwright section. The greatest likelihood of mature source rock is on the outer shelf and slope in Saglek Basin and southern Hopedale Basin, but areas along the shelf edge and upper slope may have reached the oil window throughout the study area. Maturity levels on the outer shelf seaward of Snorri J-90 are similar to the most mature part of the Bjarni in the mapped Snorri depocentre and constitute a possible alternate source for gas in that well. With the possible exception of Snorri J-90, no hydrocarbon discoveries in Labrador are based on a Cartwright source. However, the Hekja O-71 discovery off Baffin Island (north of this study area) may be from the Cartwright (Jauer & Wielens, 2014), and Paleocene oil seeps are known from western Greenland (Bojesen-Kofoed et al., 1999).

Figure B-13 shows the predicted maturity for source rocks in the lower Kenamu section. The model indicates that source rocks in the Kenamu Sequence will only have entered the oil window in the areas where sediment thicknesses are greatest. Maturation of the Kenamu likely began no earlier than the middle Oligocene, even in the deepest areas.

5. Model Limitations

The maps in Figure B-9 to B13 are not to be taken as robust predictions. Our knowledge of the thermal history and timing of deformation are limited, and a large number of simplifying assumptions were made to facilitate modeling. Firstly, the structural complexity of the margin is greatly reduced by gridding across faults and the relatively coarse (800m x 800m) resolution. Large-scale faulting likely had a significant impact on the burial history in some areas. Another important source of error in the structural model is the time to depth conversion beyond well-control, particularly in deep water. However, since we only used the model to predict regional patterns in source rock maturity, these details are much less significant than they would be if we were using it to predict migration patterns and hydrocarbon resources.

There are significant uncertainties in the age model that defines the burial history. The seismic surfaces are treated in the model as instantaneous time surfaces, rather than time-transgressive hiatuses. The biostratigraphic control in the post-Kenamu section is poor, and there is no direct age control on the surfaces beyond the well control on the shelf. In addition, the burial history is oversimplified. In addition to the regional sequence-bounding unconformities, there are local unconformities within each sequence and some removal of sediment must have occurred, but only the last (Pleistocene) period of erosion is accounted for in the model. As such, the model can be considered conservative. The compaction model in the 3-D model is simplistic, and does not take into account differences of lithology. The effect on the thermal model of this simplification is not large (compare the Genesis and Trinity models in Figure B-8a), but should be noted.

There is limited data on the thermal history of the margin, and the crustal properties likely vary in ways that affect the degree of thermal maturity. Prior to the Pleistocene, the bottom water temperature may have been significantly warmer than today and there are likely variations in the thickness and properties of the crust and lithosphere that the model does not represent.

The vitrinite reflectance ratios predicted by the model are in general agreement with the well data, and the predicted levels of maturity are consistent with the known hydrocarbon occurrences on the margin. As this is true, the model is an adequate tool for a qualitative assessment of the regional patterns in maturity of potential source rocks.
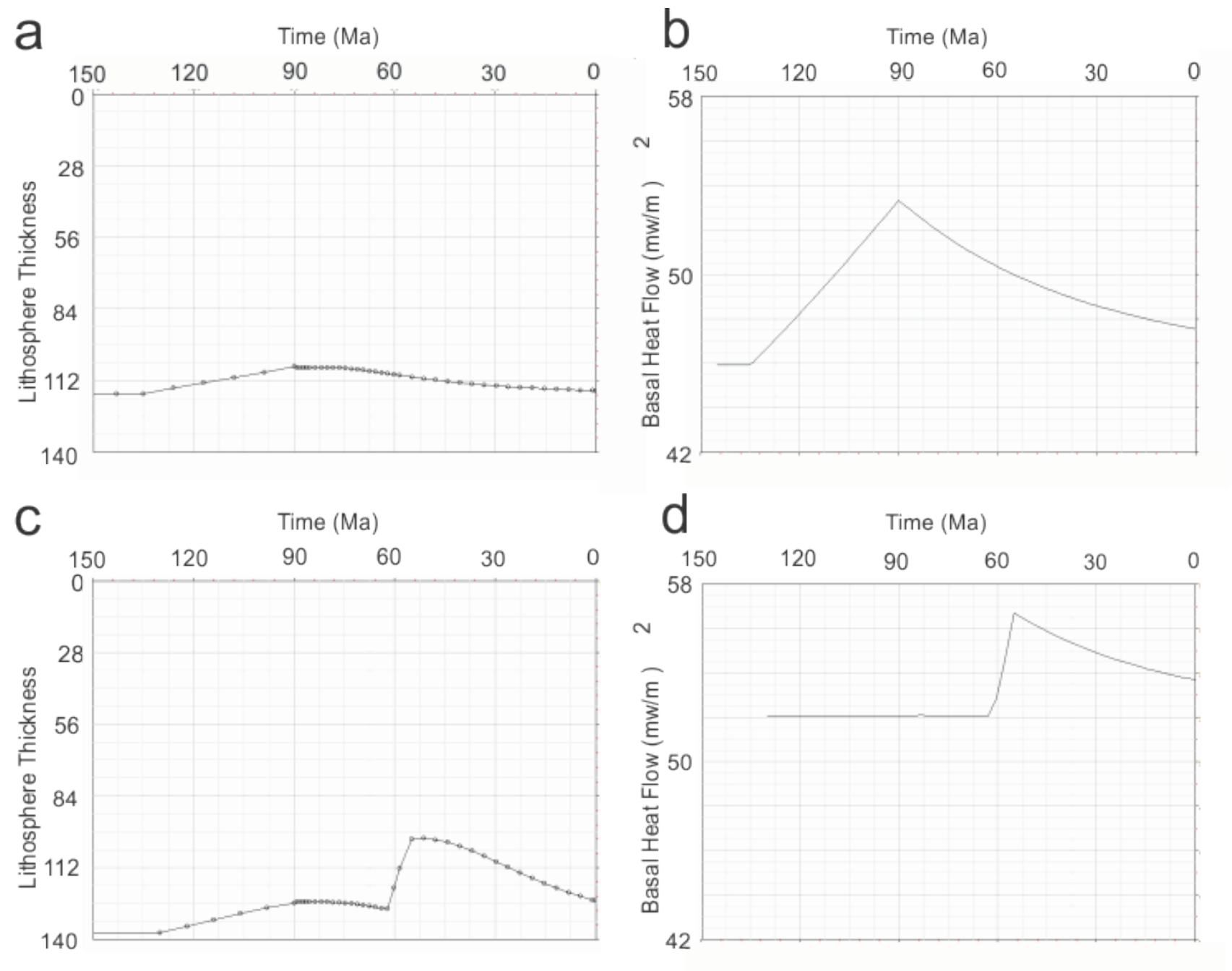
FIGURE B-1. Lithospheric thicknesses and basal (base of sediment) heat flow models for two wells. The models for Bjarni O-82 in Hopedale Basin are depicted in a and b. The models for Skolp E-07 from Saglek Basin are depicted in c and d. Bjarni O-82 was modeled as a single rifting event with a crustal stretching parameter of 1.37. For Skolp E-07, the stretching parameter was 1.35, and the effect of the inferred heating event associated with Paleocene volcanism is modeled as a second rifting event.
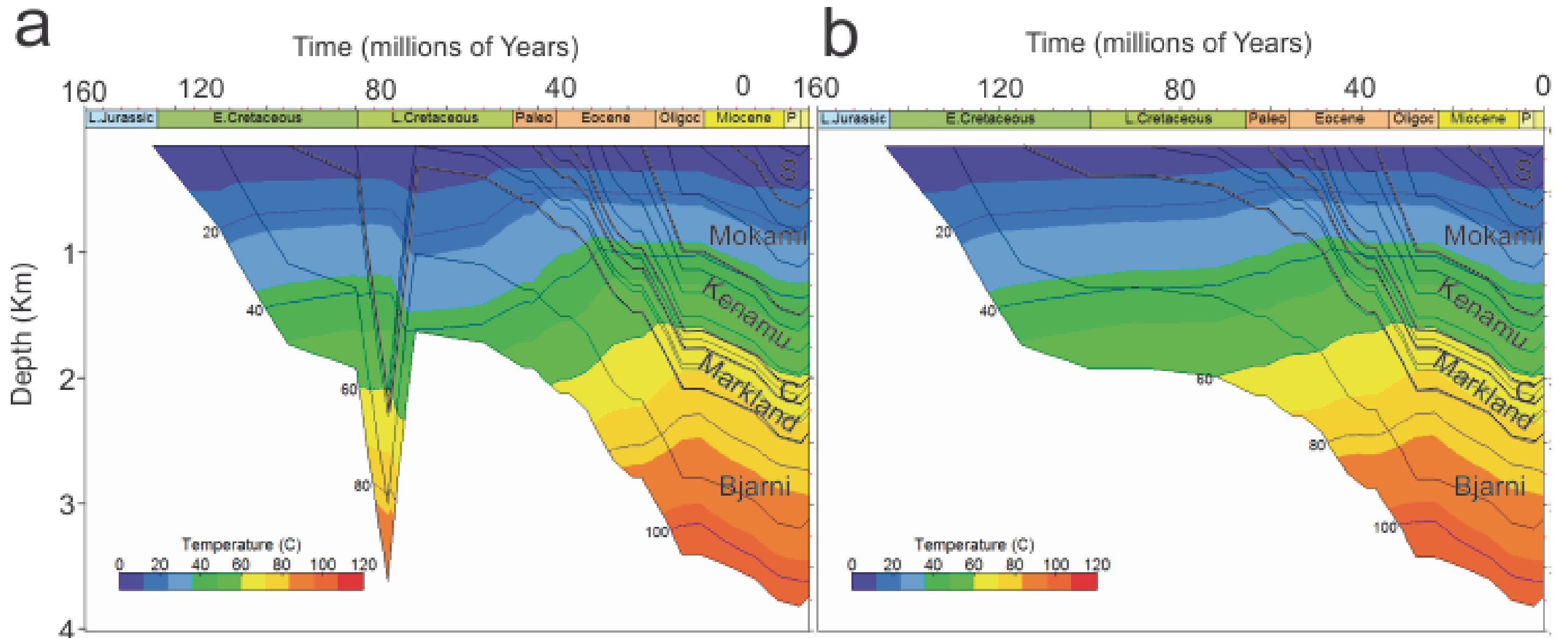
FIGURE B-2. Burial and temperature history scenarios for Bjarni O-82 with (a) and without (b) significant post-Bjarni erosion. Heavy black lines separate the sequences. "C" and "S" refer to the Cartwright and Saglek sequences respectively.
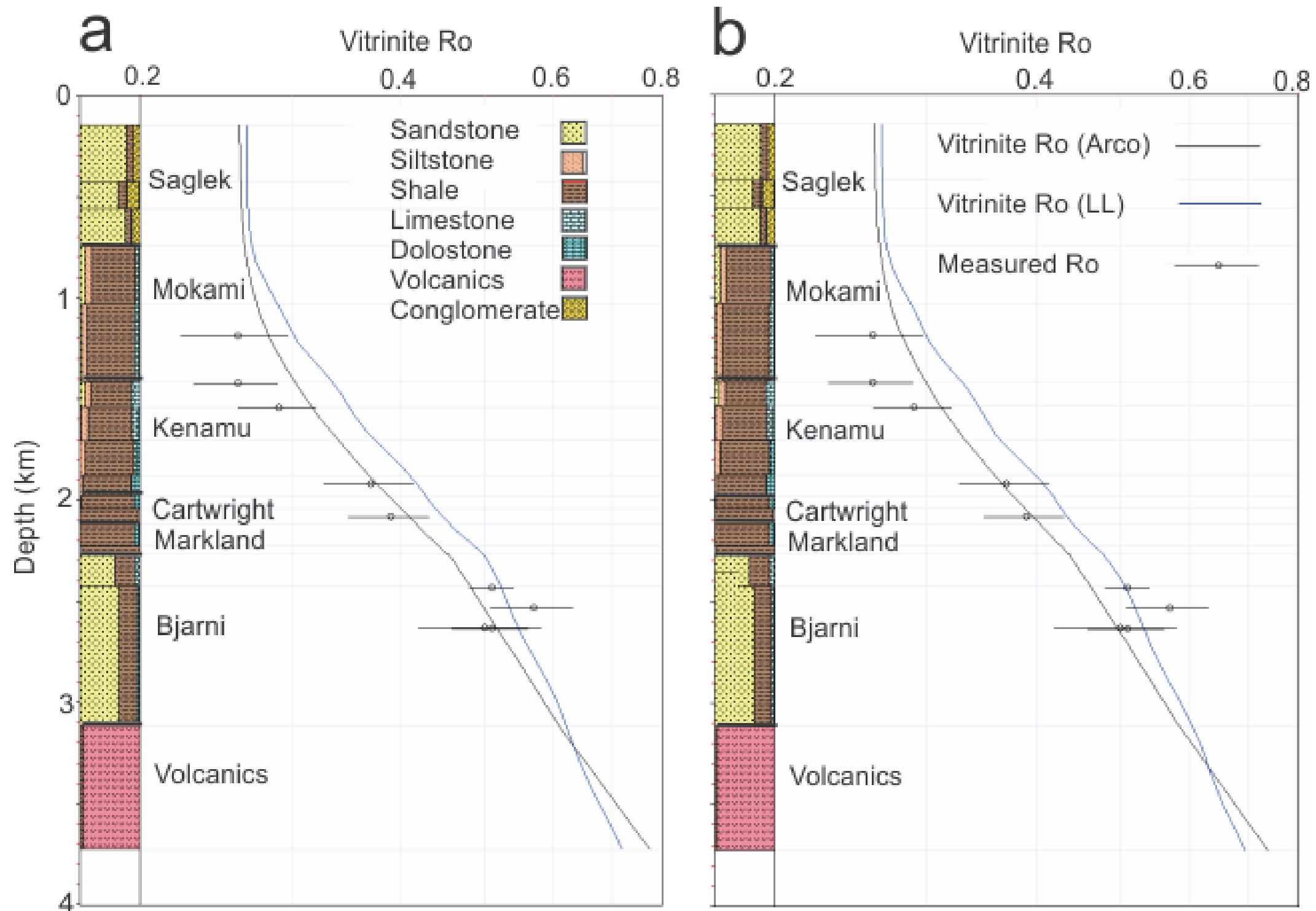
FIGURE B-3. Vitrinite vs Depth plot for Bjarni O-82, a) with 2000m of post-Bjarni erosion between 93 and 87Ma and b) without any post-Bjarni erosion. Vitrinite values with error bars from Total-CFP (1980a) against model curves. Line on measured Vitrinite reflectance values indicates standard deviation.
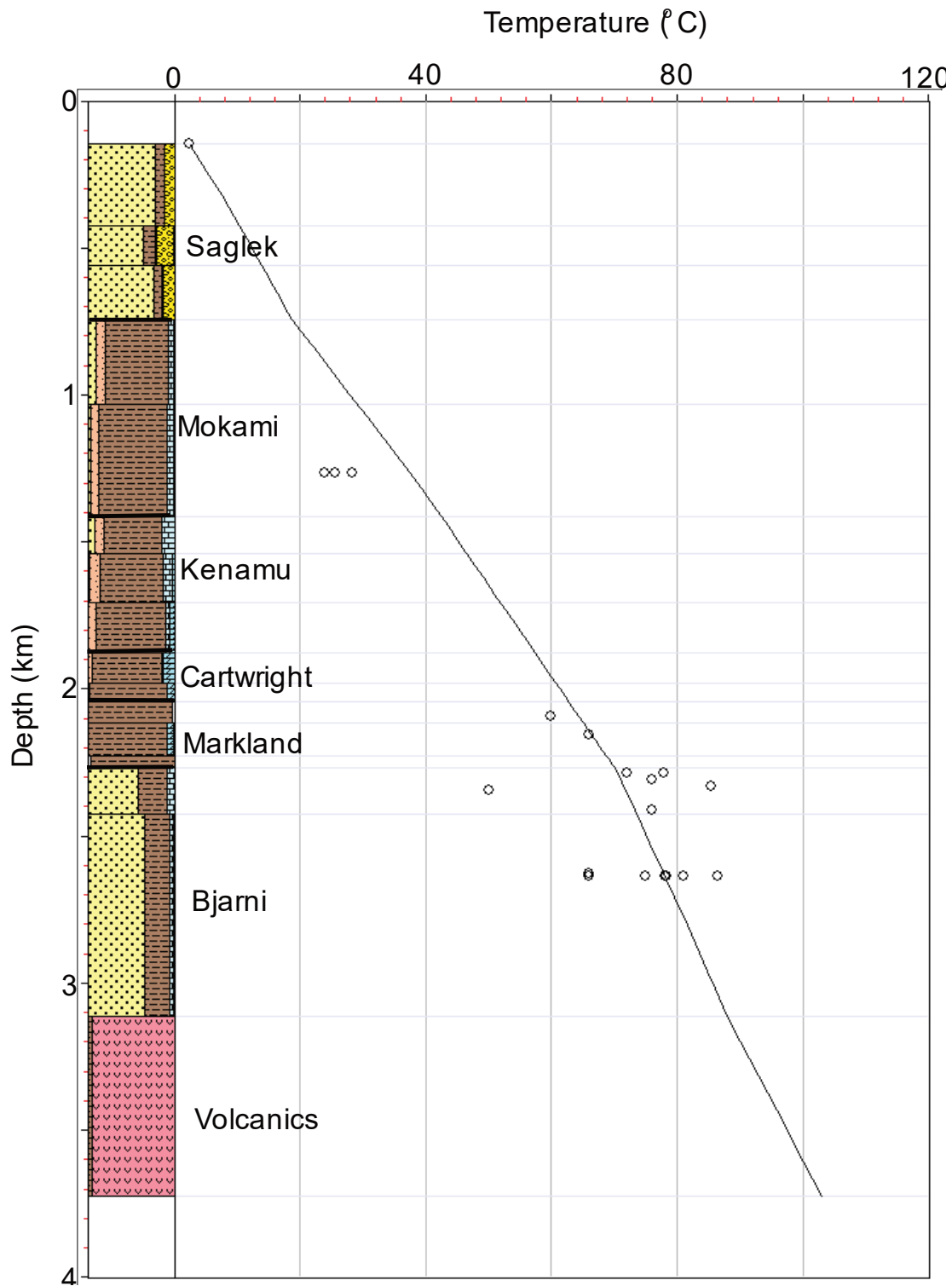
FIGURE B-4. Temperature depth profile for Bjarni O-82. Temperature data shown from Total-C.F.P. (1980a), Petro-Canada (1981a) and Moir et al. (1989) shown against thermal model. Lithology legend is the same as in Figure B-3.
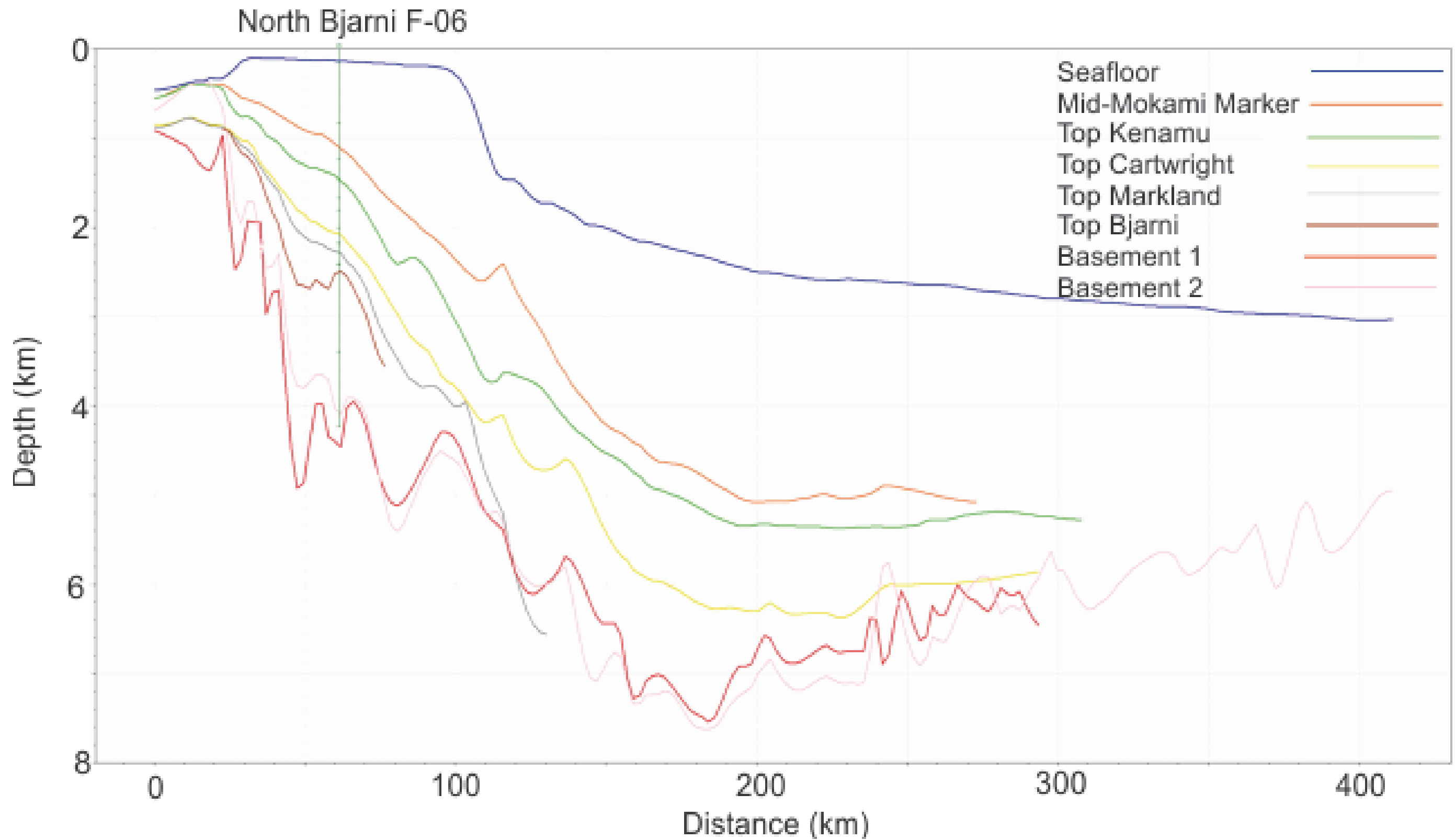
FIGURE B-5. Dip-section through North Bjarni well showing depth-converted seismic grids. Note that due to extrapolation away from seismic lines, some grid surfaces may cross. Note two different basement depth conversions in red and pink, with pink horizon used for control in deep water. See Figures B-7 for location of section.
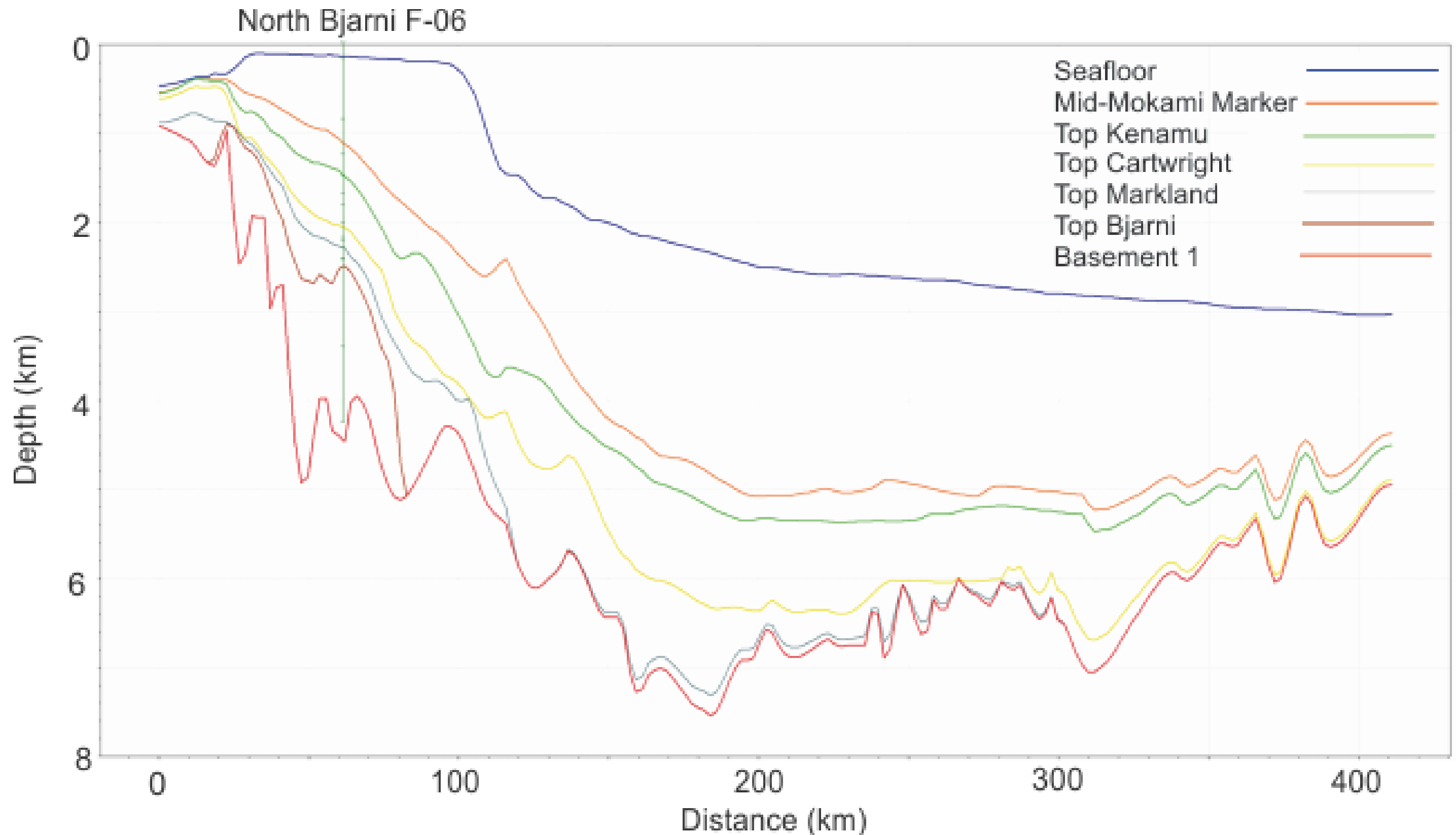
FIGURE B-6. Dip-section through model cross-section surfaces, illustrating how they were extended beyond seismic mapping. See FIGURE B-7 for location of section.
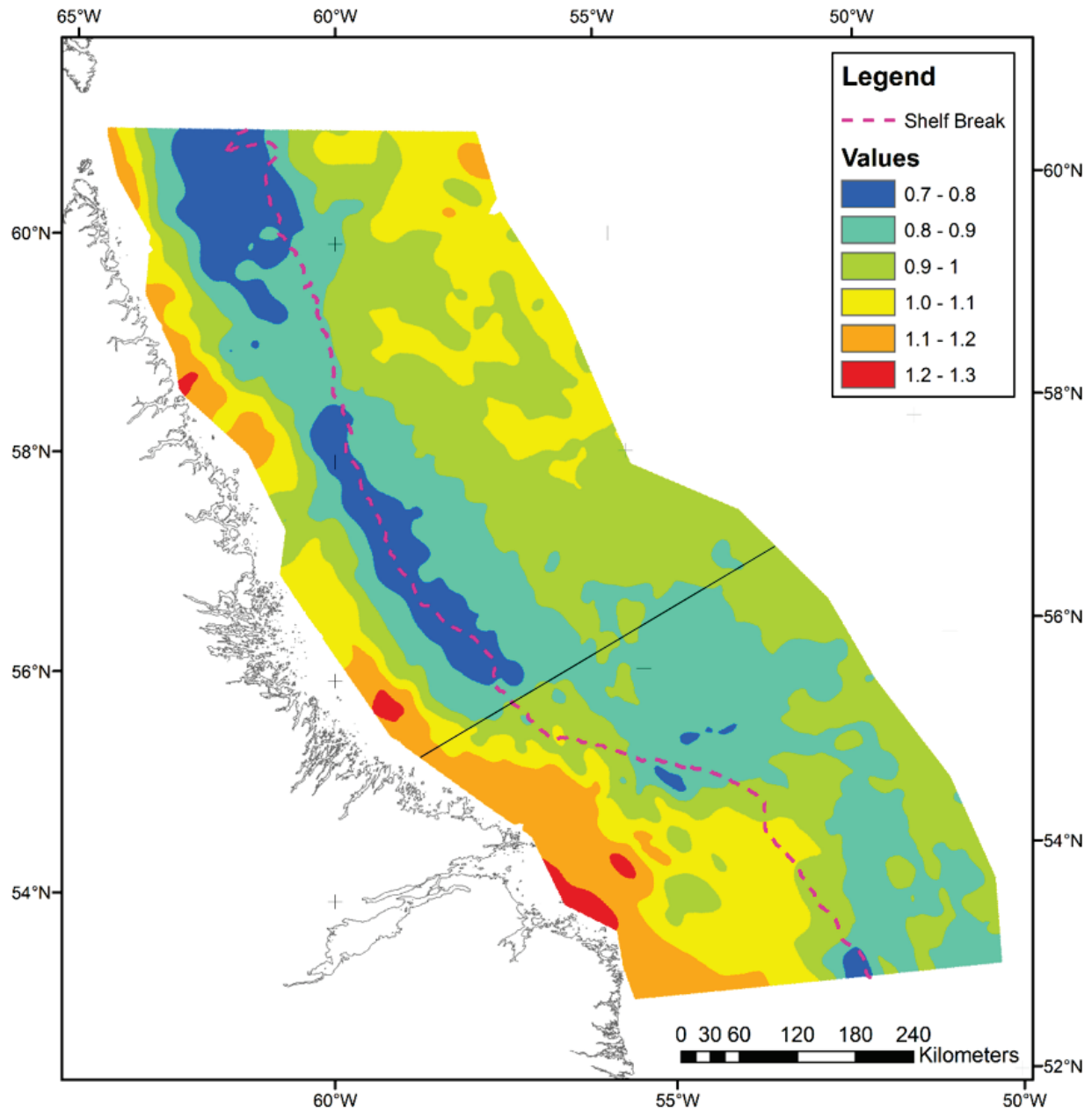
FIGURE B-7. Temperature scalar map for the Labrador margin at present. The temperature scalar map controls the heat flow in the Trinity[TM] model through a coefficient such that 1 is the heat flow at a reference point. Larger values indicate higher heat flow, smaller values indicate lower heat flow. Location of cross-section line for Figures B-5 and B-6 is shown.
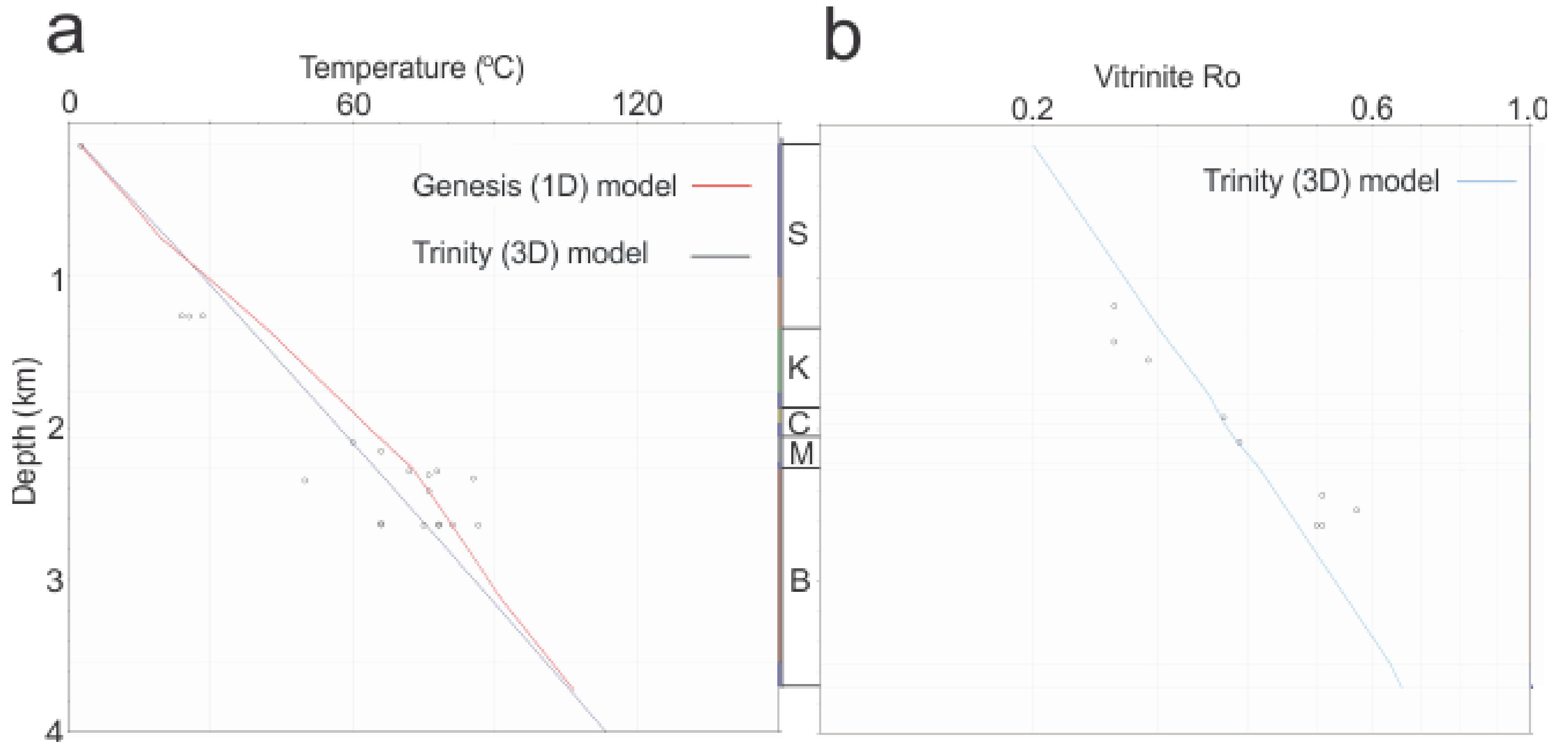
FIGURE B-8. Comparison of 3-D model temperature and vitrinite reflectance to data from Bjarni O-82. Similar comparisons were made for all wells with vitrinite data; this well is chosen as an example.
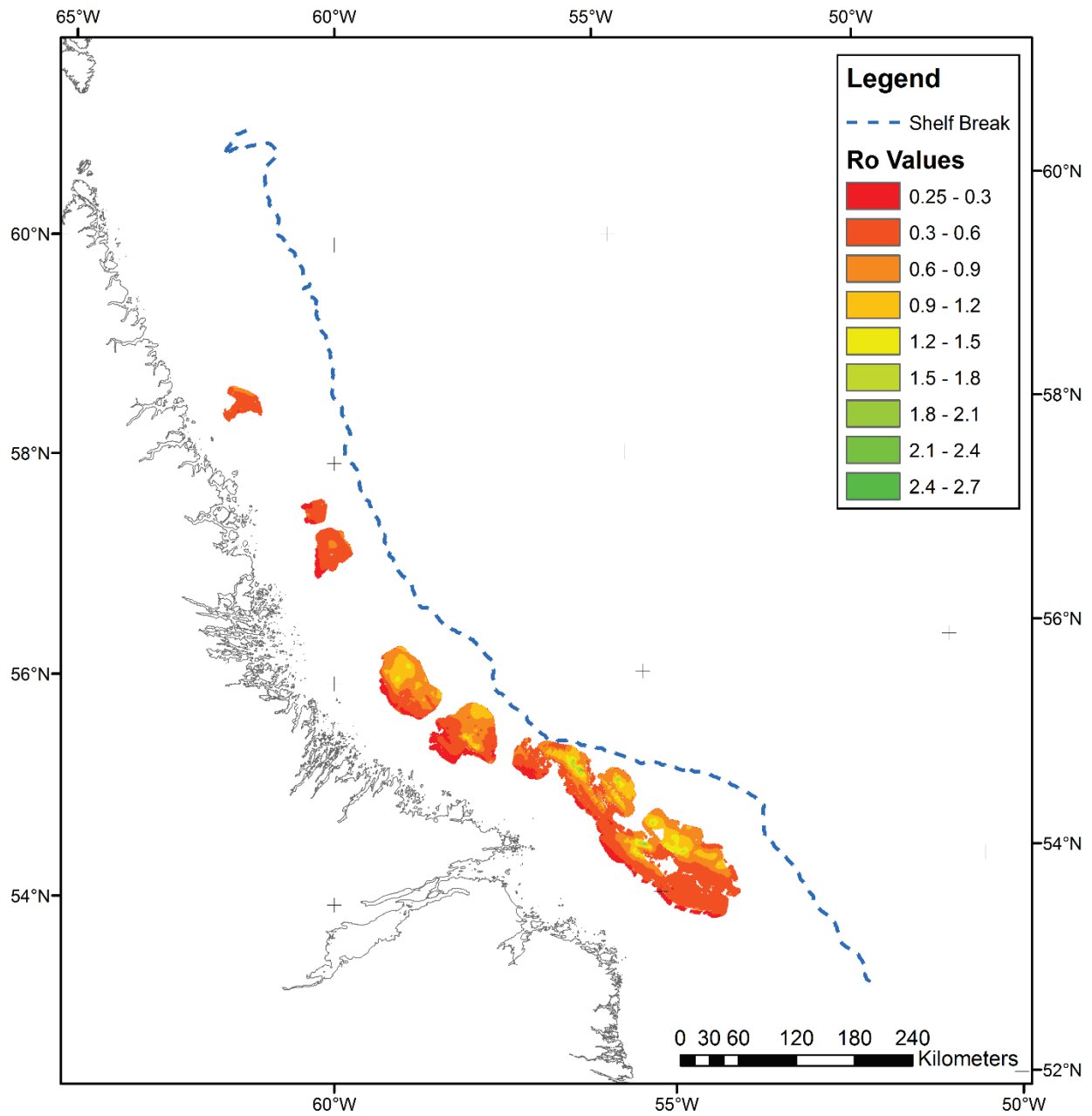
FIGURE B-9. Predicted Ro for a Lower Bjarni Source Rock. Blank areas are where the Bjarni is not mapped.
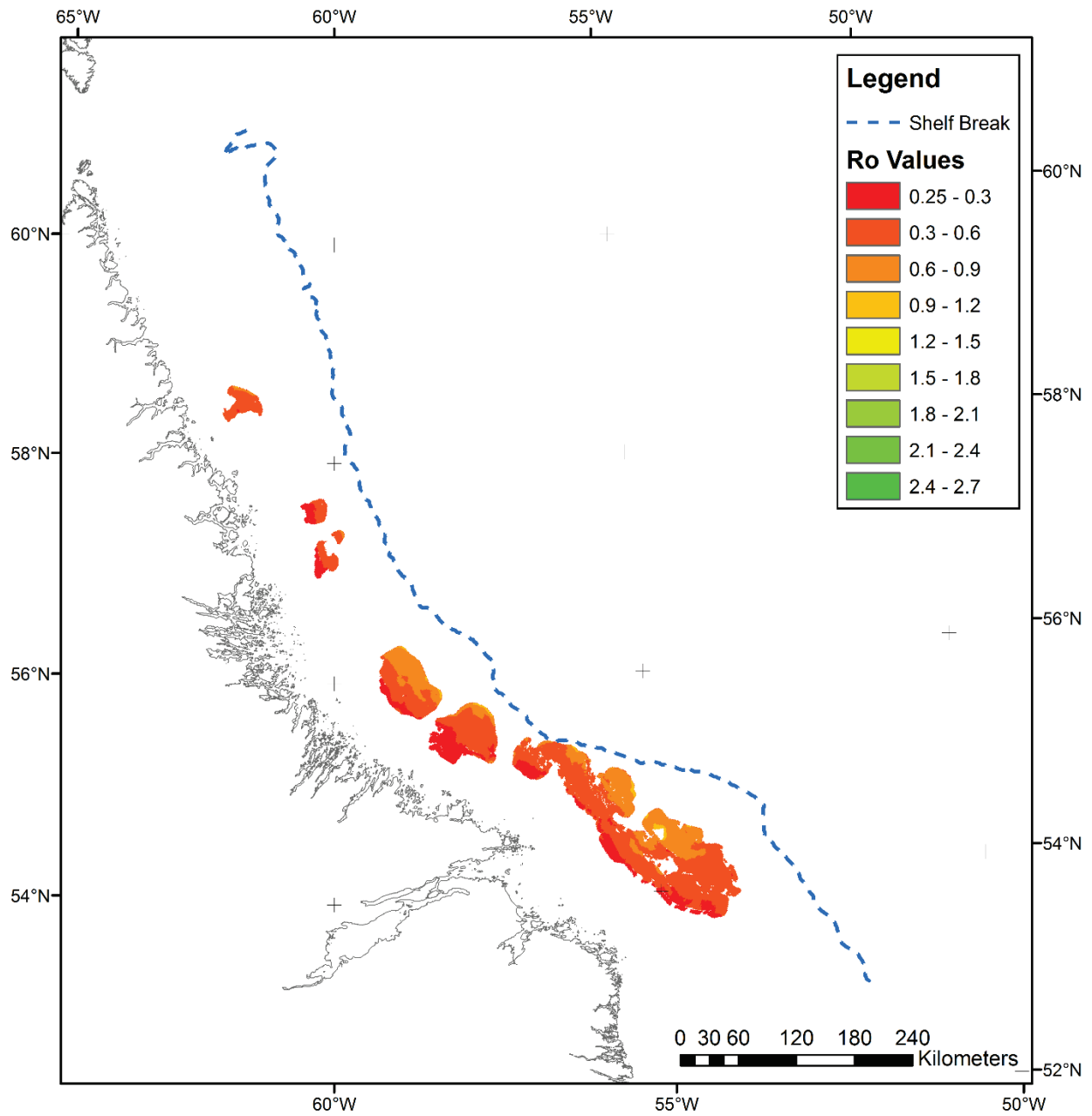
FIGURE B-10. Predicted Ro for an Upper Bjarni Source Rock. Blank areas are where Bjarni is not mapped.
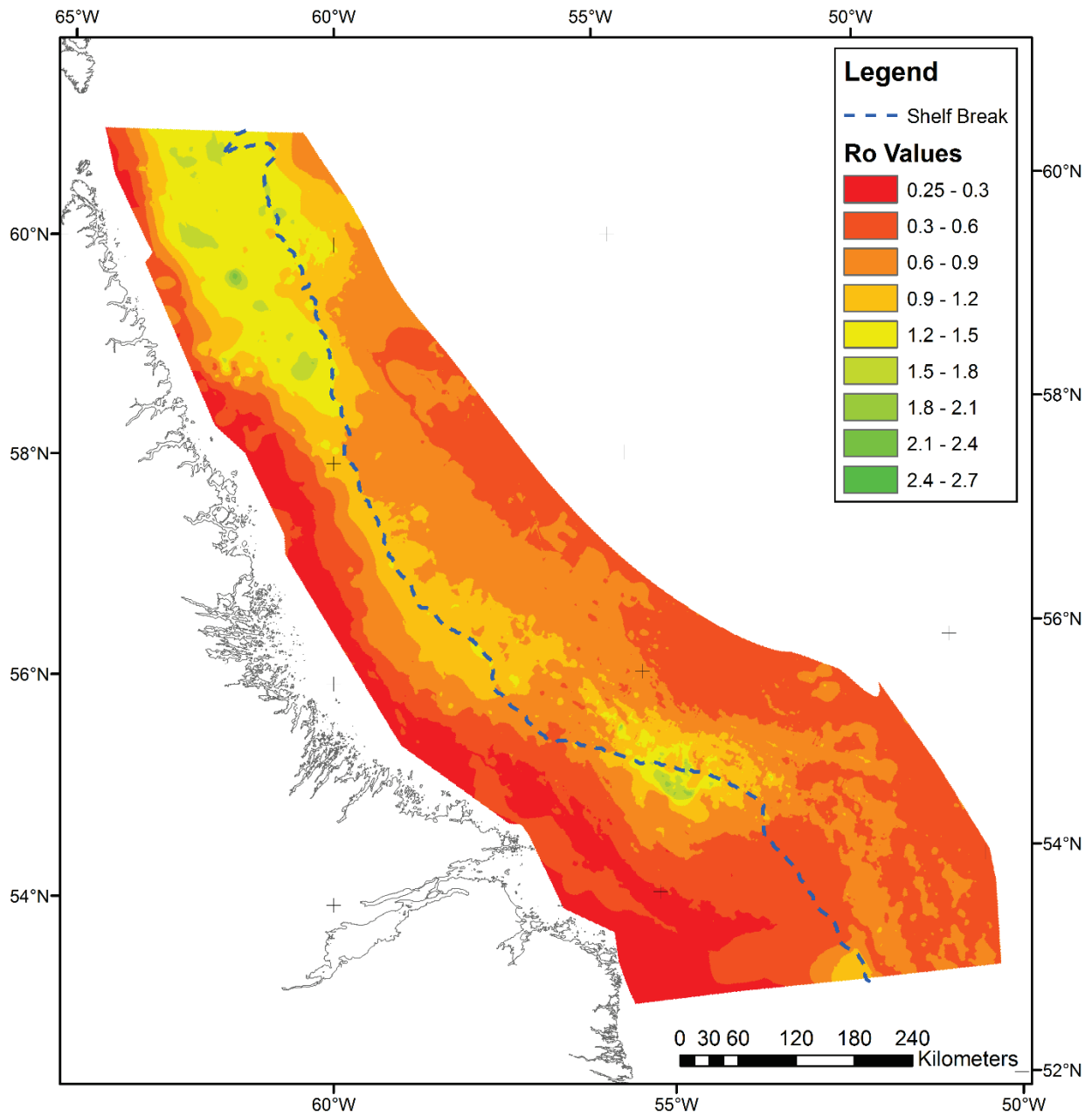
FIGURE B-11. Predicted Ro for a Lower Markland Source Rock. Limited by approximate edge of continental crust. This map was also used for risking source rock for possible Bjarni in areas where the Bjarni was not mapped.
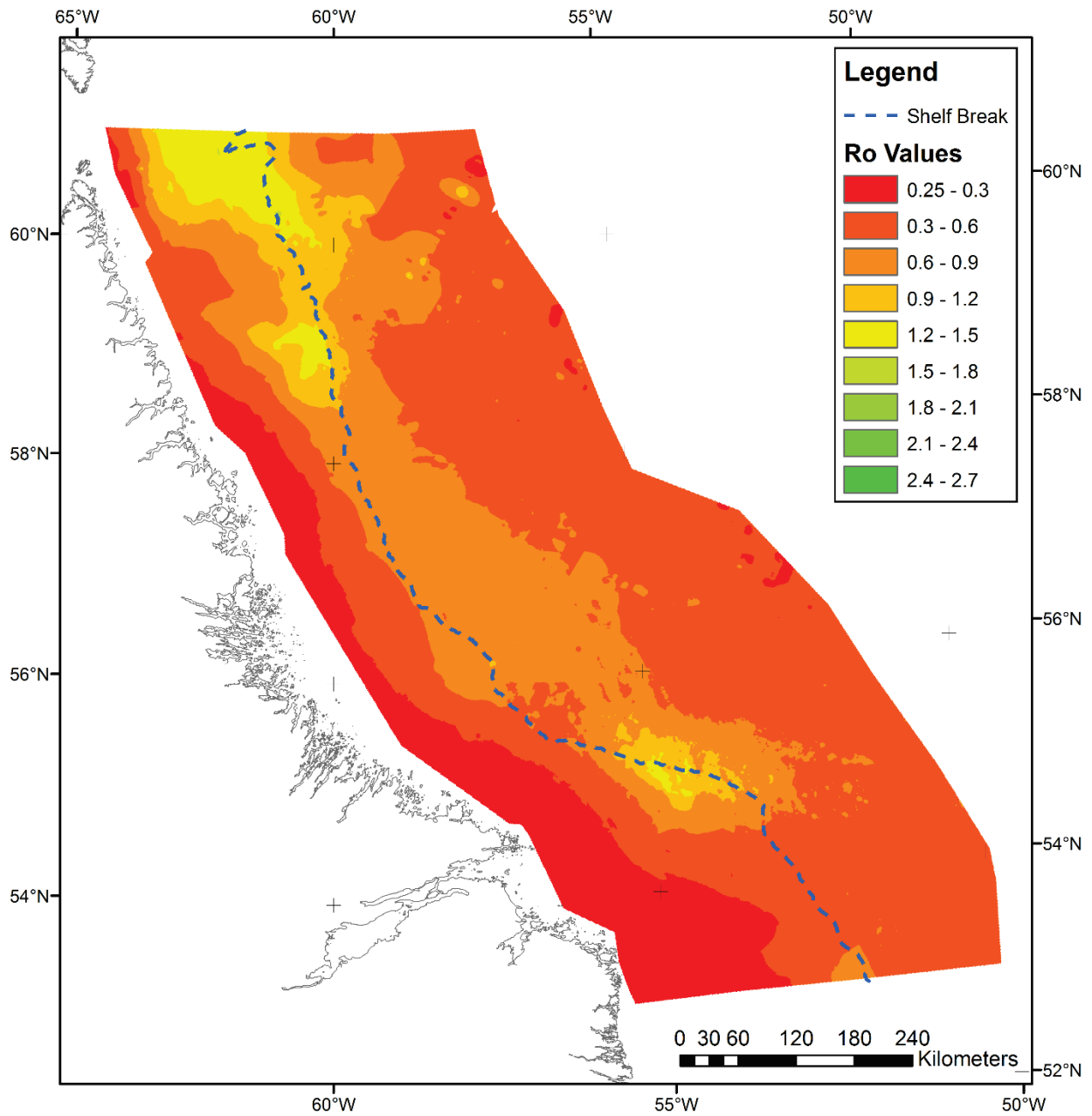
FIGURE B-12. Predicted Ro for a middle Cartwright Source Rock. Note that a lack of seismic control in the area with high Ro values along the northern edge of the study area makes that prediction suspect. The burial depth of the Cartwright in this area is uncertain.
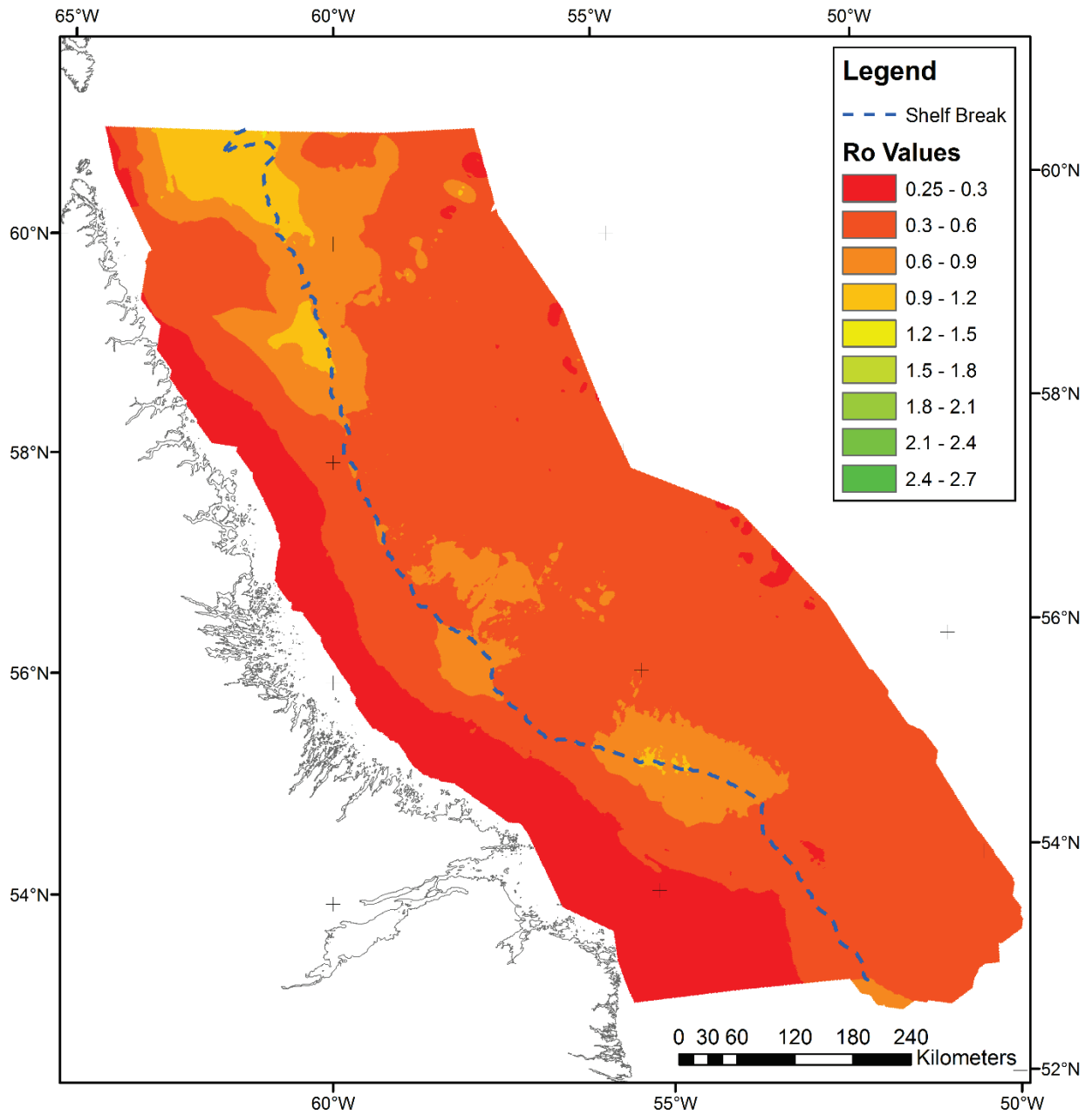
FIGURE B-13. Predicted Ro for a lower Kenamu Source Rock. Note that a lack of seismic control in the area showing as mature along the northern edge of the study area makes that prediction suspect.

APPENDIX C. PETROLEUM SYSTEM ANALYSIS

1. Paleozoic Section

A. Source Rock

No organic-rich shales have been reported from the Paleozoic interval in Labrador. RockEval data for the interval are limited, but no organic carbon contents greater than 1.5% have been reported, and most samples have less than 1%. Analysis of the hydrocarbons at Gudrid H-55 and Hopedale E-33 suggests that they are likely sourced from Bjarni rather than Paleozoic source rocks (Powell, 1979; Rashid et al., 1980). However, INRS Petrole (1983) attributed adsorbed gases in chip samples from Indian Harbour M-52 to a super mature source, unlikely to be the Bjarni given the implied thermal maturity. While these could be derived from the limited organic material within the host rock, rich Paleozoic source rock somewhere on the margin is plausible, given the limited sampling to date and the abundance of source rock of similar age in surrounding basins.

The source rock for known hydrocarbon occurrences in the Humber Zone of western Newfoundland is the late Cambrian Green Point Formation (Williams et al., 1998). There is no evidence for late Cambrian rocks on the Labrador shelf. However, there are middle Ordovician black, organic rich shales in the Humber Zone such as the Black Cove and Cape Cormorant Formations (Williams et al., 1998), which could have equivalents in Labrador. On the St. Lawrence Platform, regionally extensive upper Ordovician oil-prone source rocks such as the Macasty Shale on Anticosti Island and the Utica Shale in the St. Lawrence Lowlands (Dietrich et al., 2011) occur. Organic-rich black shales of upper Ordovician age are also known from southeastern Baffin Island (Zhang et al., 2014). In northwest Scotland, Parnell et al. (2018) found hydrocarbon fluid inclusions that they attributed to an Ordovician source rock in the Laurentian margin succession there.

Early thermal maturity work suggested that the Paleozoic rocks throughout Labrador lay within the oil window. Vitrinite reflectance values ranged from 0.67 to 0.75 at Gudrid H-55 (Robertson Research, 1974), from 0.65 to 0.81 at Freydis B-87 (Robertson Research, 1975, from 0.62 to 0.95 at Roberval K-92 (Total, C.F.P. 1979a; Bujak Davies, 1987), and from 0.50 to 0.83 at South Hopedale L-39 (Robertson Research, 1983; Bujak Davies, 1987). The degree of thermal alteration observed in palynomorphs appeared consistent with these results. Thermal alteration indices within the range of 2.5-3.5 were reported for the Paleozoic interval at Gudrid H-55 (Williams, 1976), at Hopedale E-33 (Chevron, 1978), and from Roberval K-92 (Total C.F.P., 1979a; Bujak Davies, 1987).

Work that is more recent suggests that the Paleozoic strata have undergone greater heating than previously thought. Avery (2009) reported vitrinite reflectance ratios of 1.14 to 1.27 from Roberval K-92, significantly higher than previously reported. It is possible that the low values of thermal alteration and vitrinite reflectance previously reported resulted from examining younger material introduced into the drill chip samples through caving.

In summary, while known hydrocarbon occurrences in the Paleozoic are apparently based on Bjarni source rocks, a Paleozoic source rock could be present in some areas. If such a source rock exists, it should be mature to super mature. The chance of success mapping for Paleozoic source rocks reflects the uncertainty of source rock presence, however if present it is very likely to be mature.

B. Reservoir Rock

The productive reservoir rock at the Gudrid H-55 well is a pervasive, fabric-destructive crystalline dolostone. Cores of Gudrid H-55 and similar dolostones from Roberval K-92 were analyzed for porosity and permeability (Eastcan Exploration, 1975a; Core Laboratories, 1979; Figure C-1) All samples had grain densities of $2810 - 2830$ kg/m^3, indicating the dolostone may be composed of nearly pure dolomite. The data follow a log-normal porosity-permeability trend (Figure C-1), suggesting a dominance of intracrystalline porosity rather than fracture or vuggy porosity. While the permeabilities indicate that the rock will flow at quite low porosities (1 millidarcy permeability at 3% porosity, possibly due to microfracturing), the bulk of the flow would likely come from the dolostones with porosities of 8-15% and permeabilities ranging from 10-200 millidarcies (mD).

Examination of the well log data from Gudrid H-55 indicates that of the 140 m Paleozoic section, 53m consists of very clean dolostone with porosity exceeding 8%, with an average porosity of 10.5%, based on the density log and a matrix density of 2830 kg/m^3. Porosity is generally better toward the top of the section. The Roberval K-92 well was also predominantly dolostone, though it contains more argillaceous material and is less porous. More than 100 m of dolostone with fair to good porosity averaging ~8% were encountered. Thick successions of dolostone were also encountered at Indian Harbour M-52 (about a third of the section), but there were more interbedded clastics and argillaceous limestones than at other wells, and the porosity of the dolostones was generally poor.

In Hopedale E-33 and South Hopedale L-39, both dolostone and limestone are present in the Paleozoic succession. The average density porosity in Hopedale E-33 was about 9% on a limestone scale, though the drill chip descriptions note some possible dead oil, suggesting that some of its pores may be clogged with bitumen. Nevertheless, it flowed gas and condensate at 553,000 m^3/day and 80 m^3/day respectively (Chevron, 1978). Porous streaks were also reported in South Hopedale L-39, particularly in a dolostone unit near the base (Canterra, 1983), but the rock appears wet. Most of the carbonate material in Freydis B-87 was also limestone, but showed very little porosity. The Freydis B-87 Paleozoic succession was much richer in siliciclastics than any of the other wells; minor sandstones, and some siltstones and shales are present (Eastcan Exploration, 1976b).

In summary, four of the seven wells had moderate to good reservoir quality in dolostone (Gudrid H-55, Roberval K-92) or limestone (Hopedale E-33, South Hopedale L-39). Two of the wells flowed gas (Hopedale E-33, Gudrid H-55), and two appeared to be wet (Roberval K-92, South Hopedale L-39). Because of the poor age constraints and small number of samples, it is uncertain whether the distribution of dolostone and clastics is controlled by geographic trends, different ages of rock, or is coincidental. The best reservoir rock is likely dolostone similar to that in Gudrid H-55 and Roberval K-92, but limestone or sandstone reservoirs where diagenesis (and fracturing?) is favorable are possible targets. Reservoir chance of success for Paleozoic plays reflects the difficulty in identifying Paleozoic rocks from the seismic data alone, which in turn complicates quantifying reservoir potential.

C. Seal

Where the Alexis volcanics overly the Paleozoic sediments, as at the Indian Harbour M-52 and Roberval K-92 wells, the volcanics may form a seal for the Paleozoic reservoirs. At the

South Hopedale L-39 well, fine-grained Bjarni strata may form a seal for the underlying Paleozoic reservoir. Fine-grained clastics and low permeability carbonates within the Paleozoic succession could also provide seals locally, but these would not be resolvable on seismic. However, a much more widespread seal, and therefore the seal used in the chance of success play mapping undertaken for this project, is in the Markland Sequence, which consists of fine-grained sediments over most of the Labrador shelf.

D. Trap

The most likely traps for Paleozoic plays are structural traps created by the Cretaceous syn-depositional faults that formed the Cretaceous depocenters (Figures 4, 8). Limited stratigraphic traps within the Paleozoic plays are possible; however, these cannot be easily identified in the reflection seismic data. In some areas, Alexis volcanics overlie the Paleozoic section, obscuring the seismic data imaging, and rendering clear trap definition difficult. The Roberval K-92 is an example of Alexis volcanics overlying the Paleozoic strata. The Roberval K-92 well did not contain hydrocarbons in the Paleozoic section, which could be due to the overlying volcanics over cooking potential source rock and/or heating and destroying the Paleozoic reservoir itself. However, the Gudrid H-55 and Hopedale E-33 wells did encounter hydrocarbons (gas and natural gas liquids or NGL's) in the Paleozoic. Figure C-2 is the Total Combined Chance of Success (TCCOS) map created for the Paleozoic plays.

2. Bjarni Sequence

A. Source Rock

The Bjarni sequence is considered the probable source rock for all the significant discoveries in the Hopedale Basin (Powell, 1979). Two different types of source rock have been commonly encountered. The first consists of coal beds, typically within sandy to interbedded clastic sections, which are especially common in the older Barremian to Aptian age sediments near the base of the succession. While individual coal layers are thin (< 3 m), they are numerous and very organic rich. Sixteen samples from the interval between 2750 - 2985m in Skolp E-07 yielded an average total organic matter content (TOC) of 23% (Bojesen-Koefoed, 2002). Hydrogen indices (HI) in this material are generally fairly low. Samples from Ogmund E-72 primarily lie between 40 and 90 HI, but at Skolp E-07 values are close to 200 HI (Bojesen-Koefoed, 2002). Pepper and Corvi (1995) regarded a hydrogen index of 200 HI as the minimum for oil expulsion from source rocks, therefore these are good potential source rocks for gas and may be locally fair source rocks for oil.

The other kind of source rock seen in the Bjarni section are carbonaceous shales, typically associated with finer-grained successions. These are more common in the Albian strata. Herjolf M-92 has source rocks interbedded with sands throughout the thick (>1000 m) section. Of ninety-five Bjarni samples from Herjolf M-92, fifty-four had TOC's above 2%, averaging 4.2%. Hydrogen indices were largely in the range of 100 - 200 HI. A few samples were richer in TOC and had higher hydrogen indices, including a sample from 3380 m that yielded an HI of 335 and 10.85% organic matter. The North Leif I-05 well has a nearly continuous succession of organic rich shales from 2910 - 3390 m, with an average TOC of 3.8% and an average hydrogen index of 207 (Petro-Canada, 1982a). These hydrogen indices are suggestive of deltaic source rocks that

may produce both gas and oil, though lacustrine or mixed lacustrine deltaic sources are also possible.

In summary, potential hydrocarbon source rocks are a common constituent of the Bjarni sequence. All eight wells with thick (>120 m) Bjarni sections had significant thicknesses of section with greater than 2% TOC. The North Bjarni F-06 Bjarni section is predominantly coarse-grained. The others had significant occurrences of rich source rocks with either Type III (terrestrial) kerogen or a mixture of Type II (marine) and Type III (terrestrial) kerogen. Thus, gas prone source rocks are common in the Bjarni, and some oil prone source rocks are present.

Vitrinite-reflectance ratios reported from the Bjarni sequence in wells range from a low of 0.19 reported from Tyrk P-100 (Total-C.F.P., 1980b) to up to 0.84 in North Leif I-05. All wells with sufficient data show similar depth to vitrinite reflectance trends (Figure C-3), which can be used to estimate hydrocarbon maturation, though the reaction kinetics vary depending on the nature of the organic matter (Pepper and Corvi, 1995). Hydrocarbon generation can begin at vitrinite reflectance values of as low as 0.5 (Tissot and Welte, 1984), but sufficient buildup of hydrocarbons to force oil expulsion generally requires greater maturation. Values of .85 vitrinite reflectance are capable of generating significant oil volumes in humic coals (Petersen, 2006). As visual observations of organic matter in the Bjarni sequence generally describe predominantly woody and herbaceous plant material (Geochem Laboratories, 1977), it is reasonable to use humic coal as a reference point. Comparison with the vitrinite reflectance values from the wells suggests that oil generation should have begun from Bjarni source rocks at a (current) depth of ~2500 m, but significant expulsion might require depths greater than 3500 m. This implies that where penetrated, the Bjarni ranges from immature to moderately mature for oil. These findings are consistent with the observations of INRS-Petrole (1983), which placed the Bjarni within the "upper condensate" and oil window zones for the Roberval K-92, Skolp E-07 and Herjolf M-92 wells. However, they noted the actual hydrocarbons present were predominantly wet gas, which they attributed to the gas-prone source rocks. Hence, at least some of the gas observed in the Bjarni sequence can be attributed to generation in adjacent source rocks, though some likely migrated in from more deeply buried, thermally mature source rocks.

The oil show in North Leif I-05 was from thin sands interbedded with source rocks rich in humic material with a vitrinite reflectance ratio of 0.79 to 0.84 (Petro-Canada, 1982a). Given the relatively high TOC's and hydrogen indices observed in the adjacent shales, the oil may have been locally generated, rather than migrated from a distant source rock. While there has not been live oil encountered elsewhere in the Bjarni, the characteristics of the source rock at North Leif are not unique. Both Herjolf M-92 and Tyrk P-100 have thick successions with similar organic matter contents and hydrogen indices. However, a DST of Herjolf M-92 produced water, suggesting that any hydrocarbons expelled had migrated away, while the Bjarni sequence in Tyrk P-100 is immature (Total-C.F.P., 1980b).

Chance of success mapping for mature source rock in areas with mapped Bjarni depocenters was based on three factors: whether there were wells confirming hydrocarbons within the depocenter, whether wells in the depocenter contained source rock, and the thermal maturity predicted through modeling (see Appendix B). For undrilled depocenters, the burial depth was considered the most important factor, as most Bjarni successions contained at least some source rock.

56

B. Reservoir Rock

Bjarni reservoir rocks include unconsolidated sands, conglomerates, and sandstones. The reservoir rocks are typically arkosic to feldspathic litharenite (Umpleby, 1979; Balkwill et al, 1990). Full-diameter cores were taken from the Bjarni sequence in four wells (Ogmund E-72, North Bjarni F-06, North Leif I-05, and Roberval K-92). Plotting the porosity and permeability from these cores, along with a few sidewall cores, indicates a general log-linear trend between permeability and porosity (Figure C-4). The rocks with higher permeabilities at lower porosities tend to be coarser-grained, while the rocks with lower permeabilities at higher porosities are typically argillaceous. Although the degree of induration is the dominant control on reservoir quality, the grain size effect is highly significant. For instance, fine argillaceous sandstones with 15% porosity had permeabilities of less than 1mD, while coarse or pebbly sandstones without shale breaks at the same 15% porosity had permeabilities of ~100mD (Figure C-4).

Another important control on reservoir quality is porosity, which is largely a function of diagenesis. Schwartz (2008) identified six major authigenic minerals, including oxides, carbonates and authigenic clay minerals. Some matrix clays are also present in poorly sorted Bjarni sediments (Umpleby, 1979). Petro-Canada (1981e) attributed intervals with good porosity in the Bjarni at Ogmund E-72 to secondary dissolution of early-formed calcite cements and feldspar grains. However, they also noted chlorite rims around grains, which can impede the development of calcite cements and preserve primary porosity (Hillier, 1994; Okwese et al., 2012). Schwartz (2008) found that while chlorite was found in thin sections from Roberval K-92 and Herjolf M-92, it was more abundant at Ogmund E-62. This might indicate that mineral suites sourced from the Nain Province, such as those found at Ogmund E-62, favoured preservation of higher porosities than those sourced from the Makkovik and Grenville Provinces (i.e. at Roberval K-92 and Herjolf M-92). Depositional environment and sedimentation have also been found to be important predictors of early chlorite cementation (Okwese et al., 2012). Schwartz (2008) interpreted iron oxide cementation derived from biotite degradation as an early diagenetic product.

A simple petrophysical analysis of the wells was performed, using a density-neutron cross-plot method assuming a grain density of 2650 kg/m^3 and a shale porosity of 0. Because some of the Bjarni sands contain significant amounts of potassium-feldspar, V-shale was estimated through neutron-density separation as well as the gamma ray log and the minimum value was used. V-shale values were calibrated by comparing the proportion of siltstones and shales in the sample log to smoothed log curves averaged over 3m intervals (the approximate sampling interval). Sand and shale values were calculated for each formation independently for each well. There are drawbacks to this simple approach. In particular, carbonates and basalts rocks will be incorrectly interpreted as low-porosity sandstones, but these are minor components in the section and unlikely to be significant reservoirs. Another difficulty is posed by coaly intervals. Intervals with very low densities (<2070 kg/m^3) were interpreted as coal and excluded, but some intervals with mixed coal and siliciclastic sediments or abundant coal clasts in sandstone will have significantly overestimated porosities. The data were not normalized, but some effort was made to exclude dubious density readings using the density correction. This simple petrophysical model would not be suitable for simulation of reservoir performance of North Bjarni F-06, but it should be adequate for characterization of the relative abundance of coarse-grained clastics and the broad trends in porosity within the Bjarni sequence.

The relative abundance of coarse-grained clastics in the Bjarni section is highly variable (Figure A-2). The wells in central Hopedale Basin are over 60% sand (Bjarni H-81, Bjarni O-82, North Bjarni F-06, Herjolf M-92) while fine-grained sediments predominate at South Labrador N-79, North Leif I-05, South Hopedale L-39, and Tyrk P-100. As noted in the discussion of permeability and porosity above, permeability is likely to be quite sensitive to interstitial clays and cements. Petro-Canada (1981b) found that their net pay calculations were very sensitive to the shale volume cut-off at North Bjarni F-06. The most conservative pay cut-offs (10% shale, 40% water saturation, and 10% porosity) yielded 48 m of net pay with an average porosity of 18.6%, and a net:gross of only 17%. A more liberal calculation with a shale volume cut-off of 20%, and a water saturation cut-off of 60% yielded 177 m of net pay, a porosity of 17.6% and a net:gross of 62% for the same well. Thus, while gross reservoir is likely to be abundant (and chance of success mapping reflects this), the effective reservoir may be quite variable.

Plotting the data from all the wells suggests a significant decrease in porosity with depth within the Bjarni sequence (Figure C-5). By removing all intervals with estimated shale contents greater than 25%, the impact of lithology was limited, allowing an assessment of the effect of depth on cementation. Tightly cemented rocks represent an uncommon facies; most sandstones had porosities greater than 10%. The caveat is that porosity-depth comparisons between depocenters are limited by the fact that very few wells have Bjarni reservoir in the same depth intervals. The data suggest that the typical porosities in sandstones decline from 16-25% at 2 km to 10-16% at a depth of 3.5 km. Schwartz (2008) noted decreased porosity in Bjarni sandstones at depths greater than 3 km due to an increase in quartz overgrowths and pyrite.

Chance of success mapping of Bjarni reservoir was undertaken for each depocenter as there was insufficient data to support detailed subdivision of the individual depocenters. Subdivision of the reservoir units within each depocenter is not deemed necessary because the distribution of reservoir sands is restricted to the mapped depocenters. The chance of success was assessed primarily on whether there were wells with porous sands in the depocenter. Depocenters lacking well data were assigned chances of success greater than 50% because of the overall sand-rich character of the Bjarni sequence known from wells. More deeply buried depocenters were assigned a slightly reduced chance of reservoir success because of the observed decreased porosity with depth.

C. Seal

The fine-grained strata of the overlying Markland sequence are the most important seals for Bjarni plays, due to their thickness and widespread distribution (Figure A-3). Mudstones within the Bjarni sequence could also provide local seals, although that detail is beyond the seismic data resolution.

D. Trap

The primary trap for Bjarni plays are the structural traps associated with syn-rift half-grabens where the Bjarni is preserved on the shelf (Figure A-2). The half-graben border faults and intra-basin faults are likely to be good traps (Figure 8). Stratigraphic traps are possible downdip of the wells within the half-graben depocentres for the Bjarni sequence. There may be additional Bjarni traps from the slope section and into the deeper water; that trap potential was included in the

COS assessment however, challenging seismic data resolution in the slope makes trap definition difficult. The TCCOS map for the Bjarni sequence plays is shown in Figure C-6.

3. Markland Sequence

A. *Source Rock*

Despite its predominantly dark grey color (Balkwill et al., 1990), the Markland shale is the least organic-rich of the major shale intervals in the Labrador Margin. Markland shales in the Hopedale Basin average 1-1.5% TOC, and rarely exceed 2%, with the highest values typically occurring near the top of the section. The well recording the largest number of organic-rich samples is Herjolf M-92, where the TOC reaches 3% in several samples between 2400 to 2614m (BASIN, 2019), but the average for the interval is still only 1.5%. Hydrogen indices are typically very low (<75), though the organic rich interval in Herjolf M-92 has values of 100-150 HI.

There is one anomalously high value from 2165m in Danian (lower Paleocene)-Maastrichtian (upper Cretaceous) sediments from the Bjarni O-82 well (BASIN, 2019). The very high TOC (36%) and low hydrogen index (100) are suggestive of a coal, but sample descriptions mention only carbonaceous flakes. The formation density log drops to 2100 kg/m^3 from 2162.7 - 2163m, but there is no corresponding increase in neutron porosity or sonic velocity. It may be a thin coal seam or even a large coal clast.

Two wells from the Saglek Basin record slightly higher organic matter contents than are typical of Hopedale Basin wells. The very thick Markland section at Skolp E-07 averages 1.8% TOC over 99 samples, with a maximum of 3.33% (Bojesen-Kofoed, 2002). With nearly a third of the samples exceeding 2% TOC, this indicates over 400 m of moderately organic rich shale with an average TOC of 2.2%. Organic rich shales were also found near the base of Karlsefni A-13, averaging 2.2% (BASIN, 2019) with a maximum of 3.5% at 3941m. Hydrogen indices at both wells were below 100.

The hydrogen indices from the Markland shales are low for a marine shale, and suggest a predominance of terrestrial-derived organic matter. This may reflect deposition in well-oxygenated waters where preservation of organic matter was only possible when rapidly buried. For example, organic matter from terrestrial plant material in flood events was preferentially preserved in the modern prodelta deposits of the Po River (Miserocchi et al., 2007) , and on the west African margin, terrestrial organic material is predominant in Quaternary turbidites in the Congo Fan (Baudin et al., 2010).

Overall, the Markland appears to be a marginal source rock where penetrated in the wells, though possibly better in parts of Saglek Basin and in the latest (Danian) part of the interval. However, very few of the Markland shale samples analyzed for RockEval are from sediments older than Campanian. This is significant because there are no major oceanic anoxic events (OAE) recorded during Campanian to Danian time (Gradstein et al., 2004). The OAE 2 event in the Turonian is contemporaneous with the oldest Markland-age sediments in the basin. It is possible that because drilling has concentrated on basement highs, it has not encountered deeper water Turonian-age sediments where a marine source rock associated with OAE 2 could exist.

Overall, the vitrinite reflectance ratios within the Markland sequence are similar to those seen in the Bjarni sequence and when examining the values within individual wells no sharp decrease in reflectance occurred across the unconformity between the Bjarni sequence and the overlying Markland sequence. As with the Bjarni, the Markland strata buried to depths greater than 2500m

may have entered the oil window with significant oil production and expulsion predicted at depths of 3500-4000m in Hopedale Basin.

There are some indications of higher levels of maturation in the Saglek Basin. In Gilbert F-53, vitrinite reflectance ratios of 0.86, 0.91 and 0.95 were obtained from the samples at 3285m, 3425m, and 3525m respectively. These recorded ratios may be due to heating related to the development of a large igneous province and extensive volcanism in the northern part of the region during the Paleocene. Thus, in addition to slightly better source rock, the Markland sequence in the Saglek Basin may be more mature than in Hopedale, and therefore have more potential.

The chance of success maps for Markland source rock show low chances of success in the mid-shelf region of Hopedale Basin, where wells indicate relatively low TOC and limited maturity. It is slightly better in Saglek Basin where both maturity and TOC are greater in wells, and on the outer shelf and upper slope where maturity is likely (see Appendix B) if source rocks are present.

B. *Reservoir*

The Markland sequence is predominantly shale, with most wells in the Hopedale Basin having little or no sandy sediment within the interval. One exception is at the Freydis B-87 well where the sandy Freydis Member is a fine to coarse-grained poorly sorted and argillaceous sandstone and interpreted as a nearshore to deltaic deposit (McWhae et al., 1980). The Freydis Member sands are a potential reservoir with thick (>40 m) sand packages at the Freydis B-87 well and the Ogmund E-72 wells, however these two sand units are not connected. Thin (up to 10 m) basal sands are seen at North Bjarni F-06, overlying the Precambrian and the Bjarni sequence respectively. The sands in the uppermost reservoir section at North Bjarni F-06 were identified as Santonian aged (Upper Cretaceous) and contain upper to middle bathyal fauna, suggesting that they are sands reworked from pre-existing Bjarni sands. They are slightly less radioactive than the underlying sands, possibly due to a loss of feldspar content through reworking. While technically lying above the unconformity, these thin sands are mapped as part of the Bjarni succession because they cannot be differentiated seismically from the underlying sands.

In the Saglek Basin, Freydis sands are found in Skolp E-07 and Gilbert F-53. These two wells have much thicker Markland sections as compared to Hopedale Basin; in excess of 1500m in the case of Skolp E-07. At Gilbert F-53, sandstone, siltstone and mudstone interbeds dominate the lower part of the section but the sand intervals represent less than 10% of the Markland sequence. Williams (2007) described the paleoenvironment of the Markland sequence at the Gilbert F-53 well as inner neritic at the base becoming outer neritic upward. The Markland sequence at Skolp E-07 is quite different from anything seen elsewhere on the Labrador Shelf, containing four sand-dominated intervals, comprising about 400m of coarse clastics. Finely interbedded siltstone and mudstone separate the four sandy intervals. D'Eon-Miller and Associates (1987) described parts of the lower Markland succession at Skolp E-07 as terrestrial. Wedge-shaped stratal patterns on seismic lines passing through the Skolp half-graben indicate the faults bounding the half-graben were syn-depositional during Markland deposition. The mapped sands at Skolp E-07 do not extend beyond the Skolp half-graben. Sand near the base of Rut H-11 may also belong to the Markland sequence. The interval below 4040m was assigned to the Markland by the C-NLOPB, but the age is poorly constrained. Fensome (2015) assigned the

interval above 4093m a Thanetian age, but was not able to determine an age in the underlying sediments.

Full-diameter core analysis data for two sandstone intervals (7 m and 9 m) are available from Gilbert F-53. These sands have good reservoir characteristics, except where it is shaley, with typical porosities of 15-22% and permeabilities of 5-50mD (Figure C-7). Thus, it appears that other sands within the Markland interval (i.e. mapped Freydis sands) should be a fair to good reservoir where present.

The Chance of Success map for the Freydis reservoir reflects its limited areal extent. The probability of reservoir success was greatest where known occurrences could be mapped from wells. Elsewhere, the chance of success is interpreted as lower, though possible where basal transgressive sands or locally developed sands may occur.

C. Seal

The Markland sequence is a thick, mudstone dominated unit that is widespread across the shelf, providing an effective seal for both the underlying units and some of the sands within it. Markland mudstones or interbedded sands, muds and silts overlay and seal the Freydis sands at Freydis B-87 and Skolp E-07 (Figure A-3). At Ogmund E-72, the Freydis sands fill the entire Markland interval (Figure A-3). The shales in the overlying Kenamu sequence are therefore the seal for the Markland play at Ogmund E-72.

D. Trap

As in the Bjarni sequence, the Markland plays have mainly structural traps. In addition to syn-depositional faults found in some Markland depocenters (Figure 4), later faulting on the Labrador margin involved Markland strata, providing possibility for more structural traps in areas of the shelf where there are no syn-rift depocenters as well as on the slope and in the deep water (Figure 4). Stratigraphic traps are likely to be found on the slope and in the deep water, if Markland-aged strata exist there. On the shelf, the Markland sequence is observed to pinch-out in the southern Hopedale Basin, providing potential stratigraphic traps. Figure C-8 is the TCCOS map for the Markland plays.

Cartwright Sequence

A. Source Rock

The Cartwright sequence shales are a potential source rock. With the exception of the coarse-grained sand and conglomerate successions at Roberval K-92 and Gudrid H-55, samples with greater than 2% TOC have been reported from every well. Data from the Cartwright sequence has typical TOC's of 2-3%. Even in predominantly sandy wells like Ogmund E-72, Roberval C-02 and Cartier D-70, there were moderately organic-rich samples within the succession. The thick shale successions at South Labrador N-79 and Rut H-11 were richer in organic matter content. The succession at Rut H-11 averages 3.3% TOC over an interval more than 1000m thick. At South Labrador N-79, the interval from 2560-2850m averages nearly 5% TOC.

Hydrogen indices are very low to low, typically less than 100. The highest hydrogen indices of around 130 are seen in the upper part of the formation at South Labrador N-79 and Rut H-11. This is indicative of predominantly terrestrial organics, consistent with the visual

description of abundant partially degraded herbaceous kerogen (Geochem Laboratories, 1977), despite the marine fauna present in the shales. This suggests that the high organic matter content reflects a large influx of rapidly buried organic matter from a fluvial source rather than an anoxic marine basin. This indicates that the Cartwright sequence should be a fair to good source rock for gas, but a poor one for oil at least on the mid-shelf.

Cartwright shales are likely present farther offshore beyond well control, including on the slope and in the deepwater areas beyond (Figure 8) but their potential as source rocks is unproven by well data. In some modern deltas like the Rhone, TOC decreases offshore with lower sedimentation rates. The conditions may have been more favorable for organic matter preservation in the Paleocene, however. The presence of deep-water foraminifera in the Cartwright sequence (D'Eon-Miller and Associates, 1987) suggests the margin may have been narrow and steep. Rivers carrying abundant organic matter are favorable for high primary productivity and the combination of high productivity and water depths exceeding the depth of wave-mixing can produce dysoxic to anoxic conditions.

Borrelli et al. (2014) inferred the first arrival of a deep water mass derived from the sinking of Labrador Sea surface waters in the middle Eocene. It is possible that this reflects a change in the connectivity between the two ocean basins as seafloor spreading slowed. However, the middle Eocene was a time of global cooling, especially at high latitudes (Inglis et al. 2015), and wind-driven mixing of the oceans increased globally (Cramer et al., 2009). It is therefore possible that the vigorous circulation driven by the sinking of cold, well-oxygenated surface waters seen in the modern Labrador Sea was not characteristic of the region prior to the middle Eocene. The Paleocene-Eocene boundary also coincides with an oceanic anoxic event (Rohl et al., 2000). While there is neither a clear spike in TOC's in the RockEval data nor a low-density, high radioactivity spike in the logs that might correspond to an organic-rich anoxic shale in the well logs, a source rock corresponding to the Paleocene-Eocene thermal maximum is possible further offshore. Bojesen-Kofoed et al. (1999) found oil seeps onshore in western Greenland that they attributed to a Paleocene source rock. Budkewitsch et al. (2013) detected several possible oil slicks offshore of northern Labrador using satellite radar.

Vitrinite reflectance ratios in the Cartwright shales rarely exceed 0.55 in the Hopedale Basin, indicating that the Cartwright sequence is immature in those wells. Exceptions are the slightly higher ratios (up to 0.73) seen in Snorri J-90 (BASIN, 2019), and up to 0.85 at South Labrador N-79. However, the burial depth is less than 3000 m in most of the wells, so mature Cartwright source rocks farther offshore, where it is more deeply buried, are possible. The Corte Real P-85 well reached a depth of 4395 m without encountering the base of the Eocene. Slightly deeper and more mature Cartwright strata are found in the Saglek Basin, with a maximum vitrinite reflectance of 1.06 at 4093m in Rut H-11 (Avery, 2005e). This is the highest Ro recorded on the margin, and higher than the thermal model would predict. It is noteworthy that Rut H-11 is the northernmost well on the Labrador Shelf and has Paleocene igneous rocks at its base. Volcanic activity may possibly have played a role in its advanced maturation. North of our study near Baffin Island, the Paleocene shales in Hekja O-71 were immature, but Jauer (2009) suggested that the gas may have been from a downdip Cartwright source rock. No other discovery on the margin has been attributed to a Cartwright source rock, although it is possible that the Snorri J-90 discovery is sourced from the Cartwright rather than the Bjarni.

Chance of success mapping for source rock within the Cartwright Sequence largely reflects the mapped depth of burial and inferred degree of maturity (see Appendix B). A sizable region of the outer shelf, upper slope and some depocenters on the continental rise appear to have been

buried sufficiently to allow thermal maturation (Figure 8). As noted above, although the lack of well control in these areas limit certainty, conditions appear to have been favorable for development of source rock in the deep water of this study area and accordingly they have been assigned good chances of success.

B. Reservoir

The Gudrid sands (Figure A-4) are a potentially important reservoir on the Labrador Margin. Gudrid sands host the 1975 Snorri J-90 significant discovery, which is estimated by the C-NLOPB to contain 3 billion m^3 of gas (.1 TCF, 2 MMBls NGLs). A much larger discovery (estimated at 85 billion m^3 or 2 TCF of gas, Jauer 2009) was found in equivalent sandstones near Baffin Island at Hekja O-71.

In south Labrador, the Cartwright Sequence consists of two widely distributed Gudrid intervals consisting of coarse-grained sand and conglomerate laterally separated by widespread fine- to medium-grained Gudrid sand. In the Cartier D-70 well, a mudstone separates the lower coarse-grained Gudrid sand from the upper fine- to medium-grained sand. This mudstone can be mapped but is very limited in lateral extent. At the Freydis B-87 well another laterally limited mudstone separates two intervals of coarse-grained sand and conglomerate. Stratal relations between the mapped sands do not give a clear indication of relative ages. In Central Labrador, the Cartwright Sequence is muddier than to the south, however a coarse-grained sand at Tyrk P-100 and a medium-grained sand with interbedded muds at Herjolf M-92 have been mapped as laterally equivalent, although separated by mudstone. At South Labrador N-79, an interval of thin, interbedded very-fine- to fine-grained sands and silts is also laterally equivalent to the sand intervals at Tyrk P-100 and Herjolf M-92. Seismic facies suggest this unit could be sandier north of South Labrador N-79. These sand bodies may represent lobes from different fluvial sources.

Few thick Gudrid sands are penetrated in the Saglek Basin on the Labrador Shelf, but thick sands are seen in the Hekja O-71 well, southeast of Baffin Island. Skolp E-07 contains a predominantly sandy interval from 960 to 987m of uncertain age (Williams, 2017), however it is mapped as a Gudrid sand because it is within the Cartwright Sequence as the overlying section is early Ypresian (early Eocene), and the underlying section is early Danian (early Paleocene).

Core analysis data for the Gudrid sands are very limited in Labrador. The only full-diameter core was taken from Snorri J-90 where no core analysis results were reported to the C-NLOPB. There are a few measurements from sidewall cores from the Gudrid H-55 and Freydis B-87 wells, but the bulk of the data plotted in Figure C-9 is from Hekja O-71. The data from Hekja O-71 indicate a strong log-linear permeability-porosity trend, but the few samples from the sidewall cores have rather low permeabilities for the porosities recorded. Given that the Hekja O-71 sands are derived from a different provenance, they may not be suitable for estimating permeability of the Gudrid sands in offshore Labrador.

Log analysis indicates that where the Gudrid sands are thick, porosity is very good, averaging 21-25%, and exceeding 30% locally. The sidewall cores are described as friable sandstones and unconsolidated sands. Porosity is typically lower (10-15%) toward the base of the section, due to dolomite cement (Balkwill et al., 1990). However, inspection of the sample logs indicate the lower part is often coarse grained (e.g. Roberval K-92; D'Eon-Miller and Associates, 1987), so it may be quite permeable. Thus, very high net:gross ratios and moderate to high porosities can be anticipated within the Gudrid sands.

The presence of Paleocene reservoir sands in deeper water is possible but unproven by well data. There is an unconformity at the top of the sequence, therefore erosion of the Gudrid sands and re-deposition into deeper water likely occurred at least locally. The most favorable areas for accumulation of such sands would be thick depocenters on the slope, especially seaward of well-developed Gudrid sands.

The highest chances of reservoir success for the Cartwright sequence exist in areas where good reservoir sands identified in the wells were tied to the seismic data and mapped. Moderate chances of success were assigned in thick slope depocenters downdip of mapped Gudrid sands. Lower chances of success were assigned to areas of the outer shelf and upper slope with thin Cartwright sequences, as these might represent bypass zones. The more distal deep water regions were also assigned a lower chance of success, with the expectation that during this time the coarser sands mapped on the shelf are less likely to reach the distal deep water regions.

C. Seal

The Gudrid Sand plays of the Cartwright sequence are sealed by fine-grained sediments of the Kenamu sequence. In the southern Hopedale Basin, a thick mudstone interval directly overlies the sand-dominated Cartwright Sequence. In the Saglek Basin, interbedded sands and muds separate the Cartwright sequence from the fine-grained upper Kenamu sequence therefore the Kenamu sequence is interpreted to be an effective seal.

D. Trap

The Gudrid sands of the Cartwright sequence are not restricted to the limits of the Cretaceous depocenters, however later faulting throughout the Labrador Margin created structural traps for the Cartwright plays in fault zones not associated with Cretaceous depocenters (Figures 4, 8). Stratigraphic traps occur where there are lateral grain-size and facies changes (Figure A-4). Figure C-10 is the TCCOS Map for the Gudrid Sands.

4. Kenamu Sequence

A. Source Rock

The Kenamu is characteristically organic rich, particularly in the lower (Ypresian-age) part. One thousand, two hundred seventy five samples from the Kenamu sequence in fifteen Labrador wells yield an average TOC of 2.96% (Table C-1). Densely sampled wells were sampled at regular intervals; therefore 3% TOC should be a fair approximation of the interval as a whole. Every well had an average of greater than 2% TOC except Skolp E-07 where the Kenamu is relatively thin and sandy, and Pothurst P-19 where the lower part of the Kenamu sequence was not penetrated. The distribution of organic matter content through the sequence is relatively uniform on the Labrador Margin, and tends to be higher in the lower section. Few samples had TOC's less than 2%. Most relatively organic-poor samples were from silty or sandy intervals near the top of the section. Samples with more than 5% TOC were very rare, but 4-4.8% was common in the lower part of the section.

As with the Cartwright, the hydrogen in the Kenamu were generally quite low (Table C-1), with very few samples exceeding 130. This is consistent with predominantly terrestrial organic materials, similar to the Cartwright sequence, and visual descriptions of the kerogen confirm this

interpretation (Geochem Laboratories, 1977). The hydrogen indices were slightly higher at wells that were farther offshore such as Pothurst P-19, Corte Real P-85, and Rut H-11. These three wells were the only ones where any samples exceeded 200. The high HI samples from Pothurst P-19 had relatively low TOC's (<2%, Petro-Canada, 1983), but three samples from Rut H-11 from 2890m, 2950m, and 2980m had 4-4.5% TOC and ~200 HI (Petro-Canada, 1984a). A sample from Corte Real P-85 had an exceptionally high TOC (8.79%) and an HI of 313 at 2840m (Petro-Canada, 1984b). These were the only indications of oil prone source rock potential found within the Kenamu sequence.

The Paleocene-Eocene thermal maximum occurred close to the boundary between the Kenamu and Cartwright sequences. Additionally, there were two carbon isotope excursions in the early Eocene that have been associated with oceanic anoxia, the Elmo and Azolla events (Lourens et al., 2005; Brinkhuis et al., 2006). None of these events resulted in a clear signature in the RockEval results or well logs, but a source rock related to oceanic anoxia farther offshore is possible. The unusually high TOC sample from Corte Real P-85 resembles an anoxic source rock however, carbon isotope analysis would be necessary to confirm this. The high TOC sample is close to the base of the Bartonian section (Nøhr-Hansen et al., 2016), and is later than any known global event. The high TOC could record deposition in an oxygen-minimum zone, developed in an area below the mixing depth underneath highly productive surface waters.

Table C-1. Kenamu Formation RockEval Summary by Well

	Thickness	Samples	TOC	HI	OI
Hopedale Basin					
Roberval C-02	507	9	2.23	93	49
Hopedale E-33	455	43	2.25	58	150
Ogmund E-72	336	10	3.35	56	138
North Bjarni F-06	691	18	3.06	88	63
North Leif I-05	1010	106	3.15	50	136
Roberval K-92	507	33	2.62	78	142
South Hopedale L-39	455	7	2.61	82	42
Herjolf M-92	726	70	3.05	60	134
South Labrador N-79	1015	101	3.02	70	125
Bjarni O-82	634	66	2.73	79	121
Corte Real P-85	>2193	127	3.15	96	60
Saglek Basin					
Karlsefni A-13	1337	8	2.57	72	102
Skolp E-07	80	7	1.47	42	179
Gilbert F-53	860	38	3.4	96	80
Rut H-11	656	43	3.57	113	46
Pothurst P-19	>808	100	1.84	82	110
Average (of wells)			2.83	77	112
Average (all samples)		1275	2.96	82	127

The Kenamu sequence is generally immature in the wellbores. Vitrinite reflectance ratios of 0.5 or greater were rare at depths less than 3000m. The only exceptions were Gilbert F-53, which reached 0.5 at 2065m and Herjolf M-92, which reached 0.5 as shallow as 1838m (Avery, 2005a and 2005b). The reason for the apparent greater maturity at those wells was unclear. The highest ratios reported were 0.62 in Corte Real P-85 and at Rut H-11, at 4400m depth and at 3835m respectively. In summary, while the Kenamu is a potential source rock, thermal modeling indicates that it is sufficiently mature to expel hydrocarbons in only a limited area of the margin (see Appendix B).

In the parts of the outer shelf and slope where the Kenamu sequence is buried sufficiently for thermal maturation, there is no well control to confirm the presence of source rock. However, the same arguments used to propose a relatively high probability of source rock in areas beyond well control for the Cartwright are equally valid for the Kenamu.

Thus, although the Kenamu is very favorable for source rock presence, the areas where the chance of success are high are quite limited. Chance of success mapping for the Kenamu sequence largely reflects the mapped depth of burial and inferred degree of maturity (see Appendix B). As noted above, although there is a lack of well control in these areas, conditions appear to have been favorable for source rock development and accordingly they are assigned positive chances of success. Elsewhere, though good source rock potential likely exists, thermal maturity is insufficient.

B. Reservoir

The Leif sands of the Kenamu sequence are described by McWhae et al (1980) as a fine-grained, quartzose sand with varying amounts of siltstone and mudstone, however the grain size analysis of Miller and D'Eon (1987), as published in Wielens and Williams (2009a, b, c), indicate coarse-grained Leif sands are present at several wells and at varying stratigraphic intervals. With the exception of Skolp E-07, where the base of the Kenamu is a medium- to coarse-grained sand, the Leif sands are found in the upper Kenamu Sequence. The thickest Leif sand is at Karlsefni A-13, the type-section for the Leif Member, where it is just over 200 m thick and ranges from fine- to medium-grained. Elsewhere, the Leif sands tend to be thin and sheet-like with a widespread distribution. The Leif sand at the type-section can be mapped for thousands of square kilometers, although it thins considerably away from Karlsefni A-13. At some wells up to three separate sand units are identified.

Relatively little is known about the Leif sands of the Kenamu sequence, because no full-diameter core material is available. Both petrophysical analysis and core analysis of four sidewall cores from Leif M-48 indicate that it has good reservoir potential. The analyzed samples varied in porosity from 28 to 32%, and recorded permeabilities of 65 to 250 mD. Descriptions of the analyzed samples for all four samples are described as fine-grained sand (Eastcan Exploration, 1973b). The moderate permeabilities recorded, despite very high porosities, are likely due to the fine grain size.

The increased sand supply in northern Labrador could be from a continental drainage system exiting Hudson Strait at that time or from sediments eroding off the Torngat Mountains in northeast Labrador. The lack of seismic coverage and provenance data for the Leif sand make it impossible to draw firm conclusions.

The highest chances of reservoir success exist in areas where good reservoir sands encountered in the wells are mapped. Moderate chances of success were assigned in thick slope depocenters downdip of the Leif sands. Lower chances of success were assigned to areas of the

outer shelf and upper slope where the Kenamu sequence is thin, as these might represent bypass zones. The more distal deep water regions were also assigned a lower chance of success, with the expectation that coarser-grained sandy sediments would likely be deposited before reaching distal deep water areas. The overall probability of reservoir in the Kenamu Sequence was judged to be poorer than the Cartwright, on the basis that the section on the shelf is more mud-dominated.

C. Seal

The Leif sand reservoirs found in the mid-Kenamu sequence are sealed by the overlying upper Kenamu shales. Additional seals for the Leif sands sequence of the Kenamu sequence come from fine-grained sediments of the Mokami sequence.

D. Trap

Late-stage faulting on the Labrador Margin involved much of the Kenamu sequence, therefore structural traps are highly likely for the Leif reservoirs found in those fault zones (Figures 4, 8). In the southern deep water, a gravity-driven fault domain (Figures 4, 8), consisting of both extensional and compressional fault zones, provides structural traps, particularly in the observed toe-thrusts. This deformation zone is expected to consist of a mix of mudstone and sandstone, and therefore lateral facies changes are potential stratigraphic traps. Stratigraphic traps are also possible on the shelf, where structural faulting is less likely. Figure C-11 is the TCCOS map for the Kenamu sequence.

5. Mokami Sequence

A. Source Rocks

RockEval results from the Mokami sequence indicate there are organic rich muds that could potentially be source rocks. However, the young age and shallow burial depth makes it unlikely that sufficient maturity to produce hydrocarbons on the Labrador Margin would have occurred. Therefore, no detailed analysis of the source rock characteristics was attempted. The play element chance of success in the Mokami sequence reservoirs is predicated on hydrocarbons migrating from deeper parts of the section.

B. Reservoir

The Mokami sequence is a predominantly shaly interval, similar to the Kenamu sequence, but becomes significantly sandier upwards. No Mokami sand cores have been analyzed for porosity and permeability. On logs, Mokami sands generally appear similar to the Leif Member of the Kenamu sequence. However, some coarser sands, minor gravel and coal are reported on sample logs of the Mokami, and there is biostratigraphic evidence for significant unconformities within the section in many wells (Nøhr-Hansen et al, 2016). Thus, in addition to the shallow marine sands similar to the Leif Member of the Kenamu sequence, there is a possibility of coastal and fluvial sands encountered in the Mokami sequence. As the strata are generally unconsolidated to poorly consolidated, porosity and permeability of sands within the Mokami sequence are likely to be good.

C. Seal

   The only possible seals known for Mokami reservoirs are overlying fine-grained sediments within the Mokami sequence, since the Saglek sequence consists of coarse-grained progradational sands that are overlain by glacial till in many places.

D. Trap

Some mass-transport deposits have been identified within the Mokami sequence. Gravity-driven faults within these deposits may be good structural traps. The Cenozoic gravity-driven fault domain in the southern deep water region (Figures 4, 8) identified as effective traps for the Kenamu sequence are also expected to be effective traps for the Mokami sequence. On the shelf, the lower Mokami sequence is faulted by the same late-stage extensional faults that are structural traps for the underlying sequences, however scouring is expected to be a hindrance to trapping and sealing near the Labrador Marginal Trough (Figures 4, 8). Figure C-12 is the TCCOS map for the Mokami sequence.
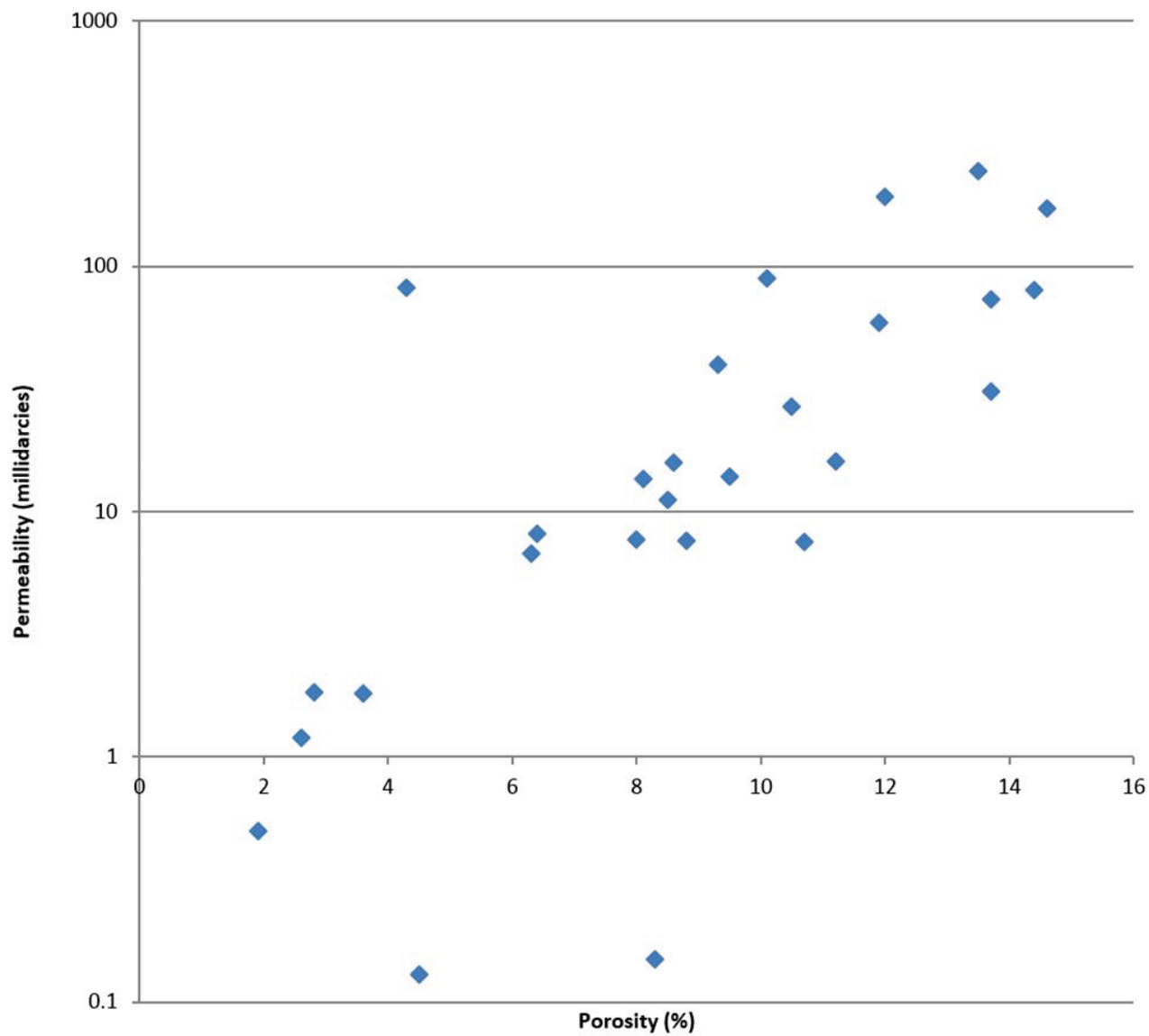
FIGURE C-1. Porosity-permeability cross-plot of Paleozoic dolomite, Gudrid H-55
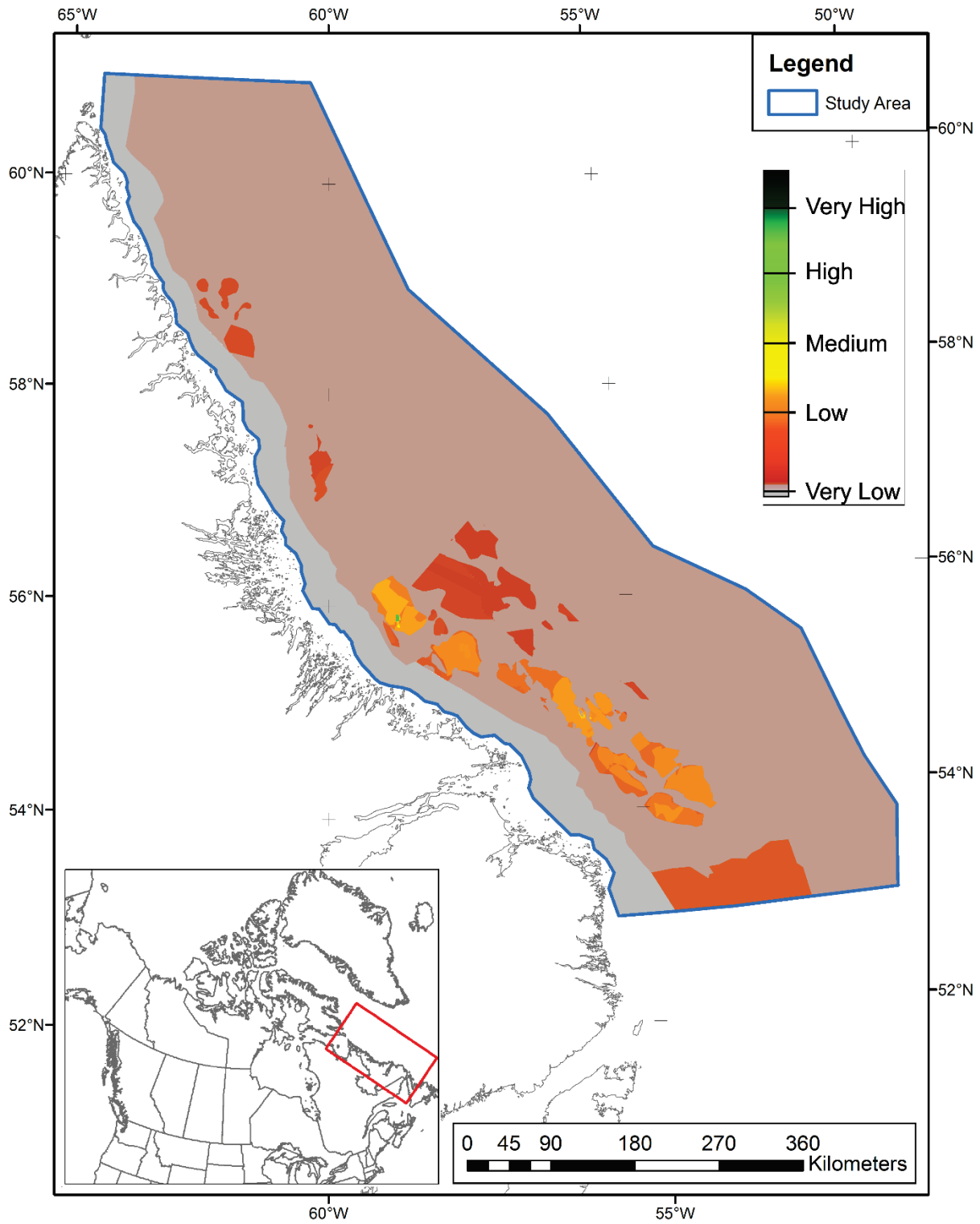
FIGURE C-2. Technical Combined Chance of Success Map (TCCOS) for Paleozoic Plays
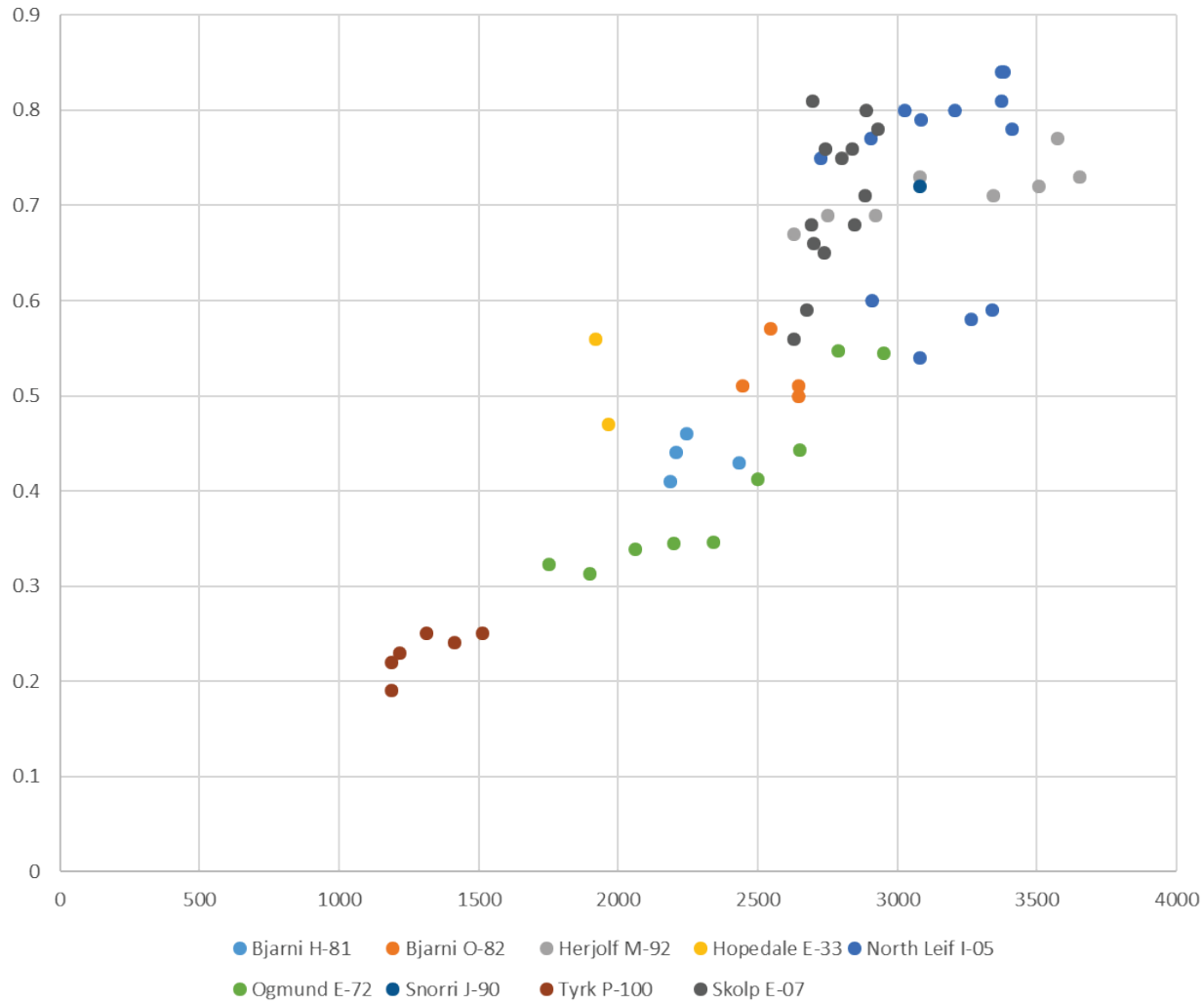
FIGURE C-3. Depth below current mean sea level vs vitrinite reflectance ratio (Ro). Note that depth below sea level was used to avoid being influenced by bathymetric relief.
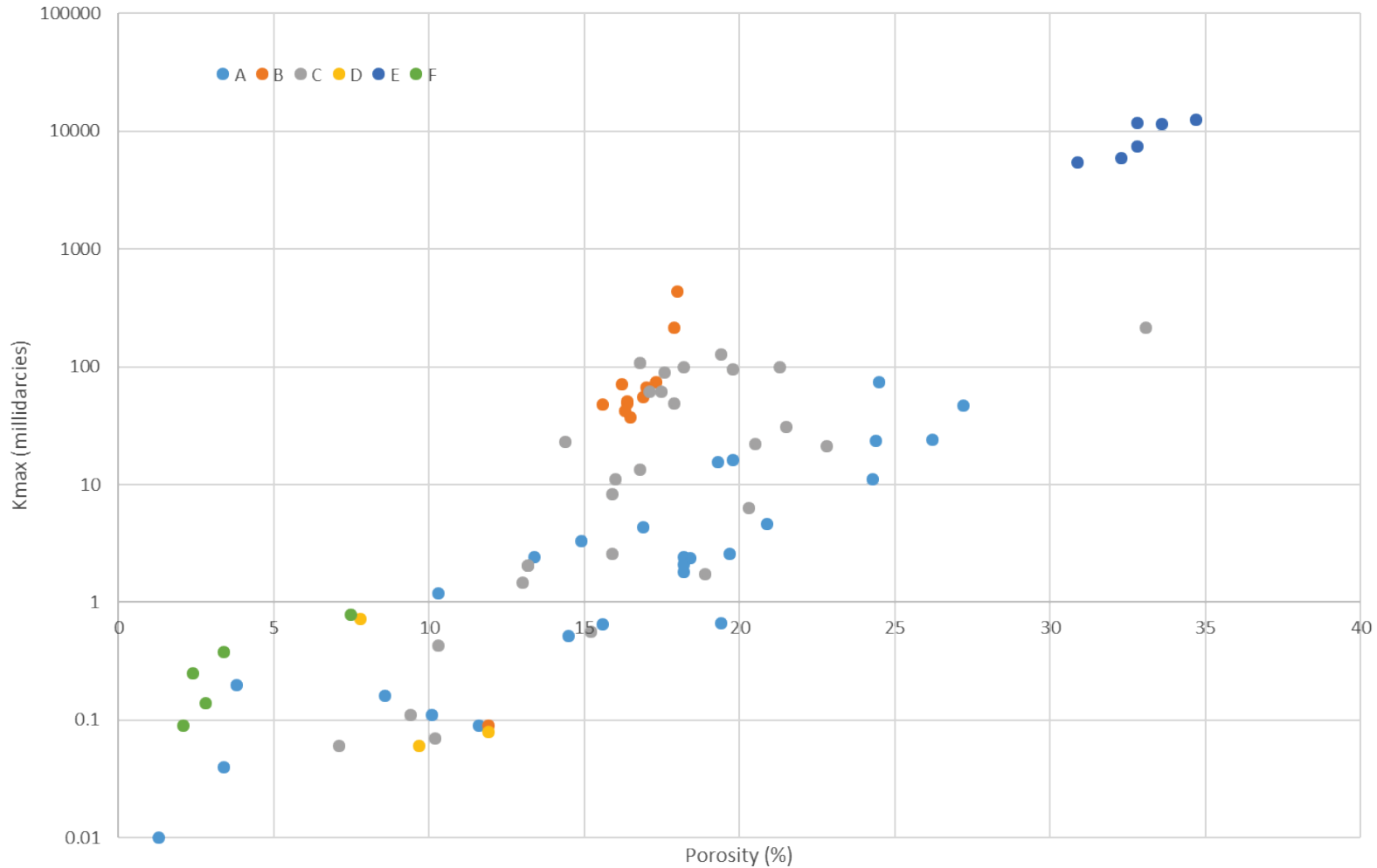
Figure C-4. Permeabilty- Porosity Crossplot of data from cores from 4 wells within the Bjarni Formation. Data from Core Laboratories (1979), Petro-Canada (1980b, 1981b, 1981c). Color coded by sample descriptions.
A – Sandstones described as argillaceous, carbonaceous or having shale breaks. B – Clean sandstones with coarse sand or pebbles. C – Clean, very fine to medium sandstones. D – Iron-oxide cemented sandstones. E – Unconsolidated Sands. F – Calcite-cemented conglomerates.
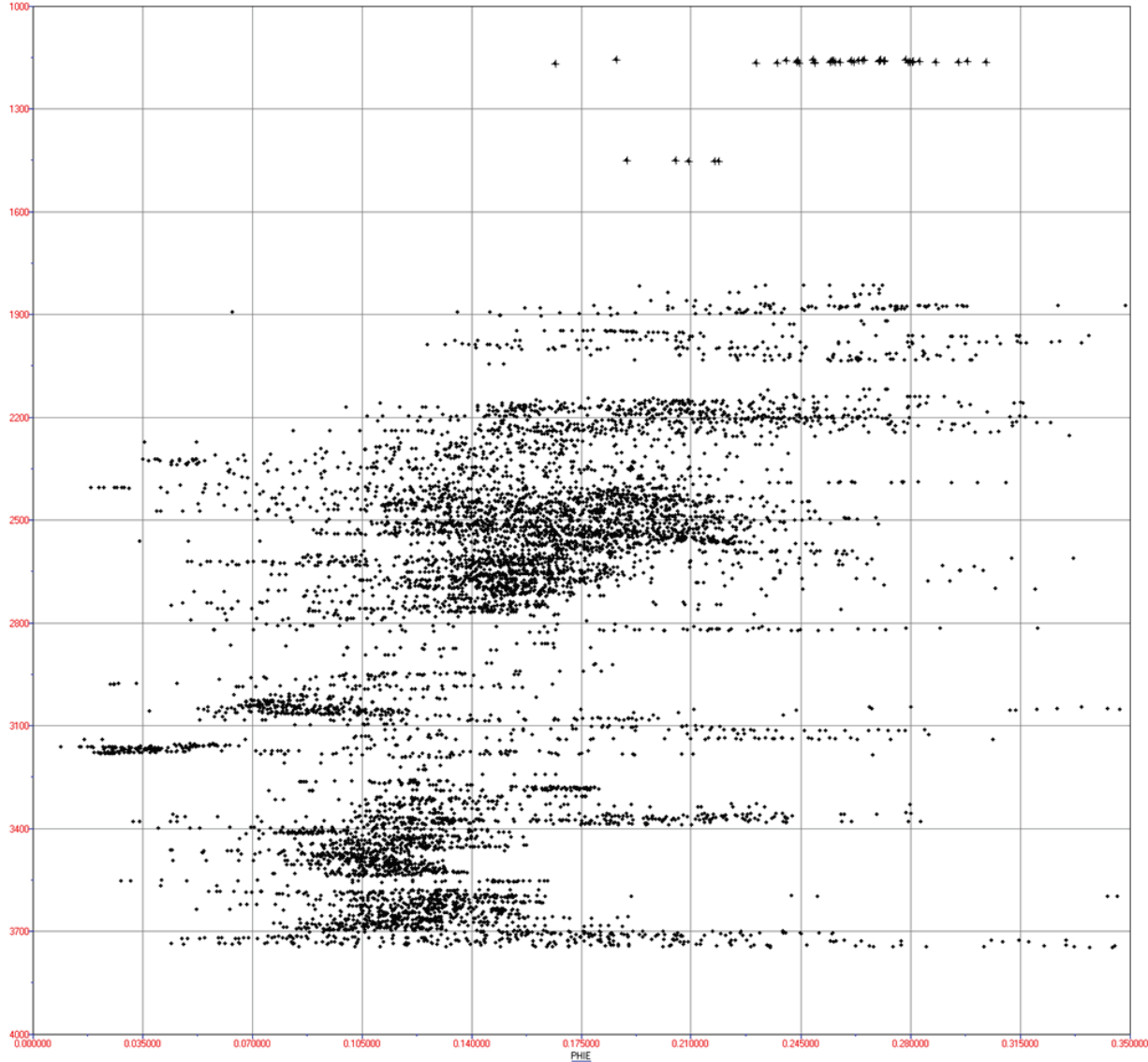
FIGURE C-5. Effective porosity vs depth for clean sandstones (Vsh < 0.25) in Bjarni Fm based on petrophysics of all Hopedale Basin wells. Sands with higher shale content were excluded to limit impact of facies and isolate degree of cementation with depth.

73
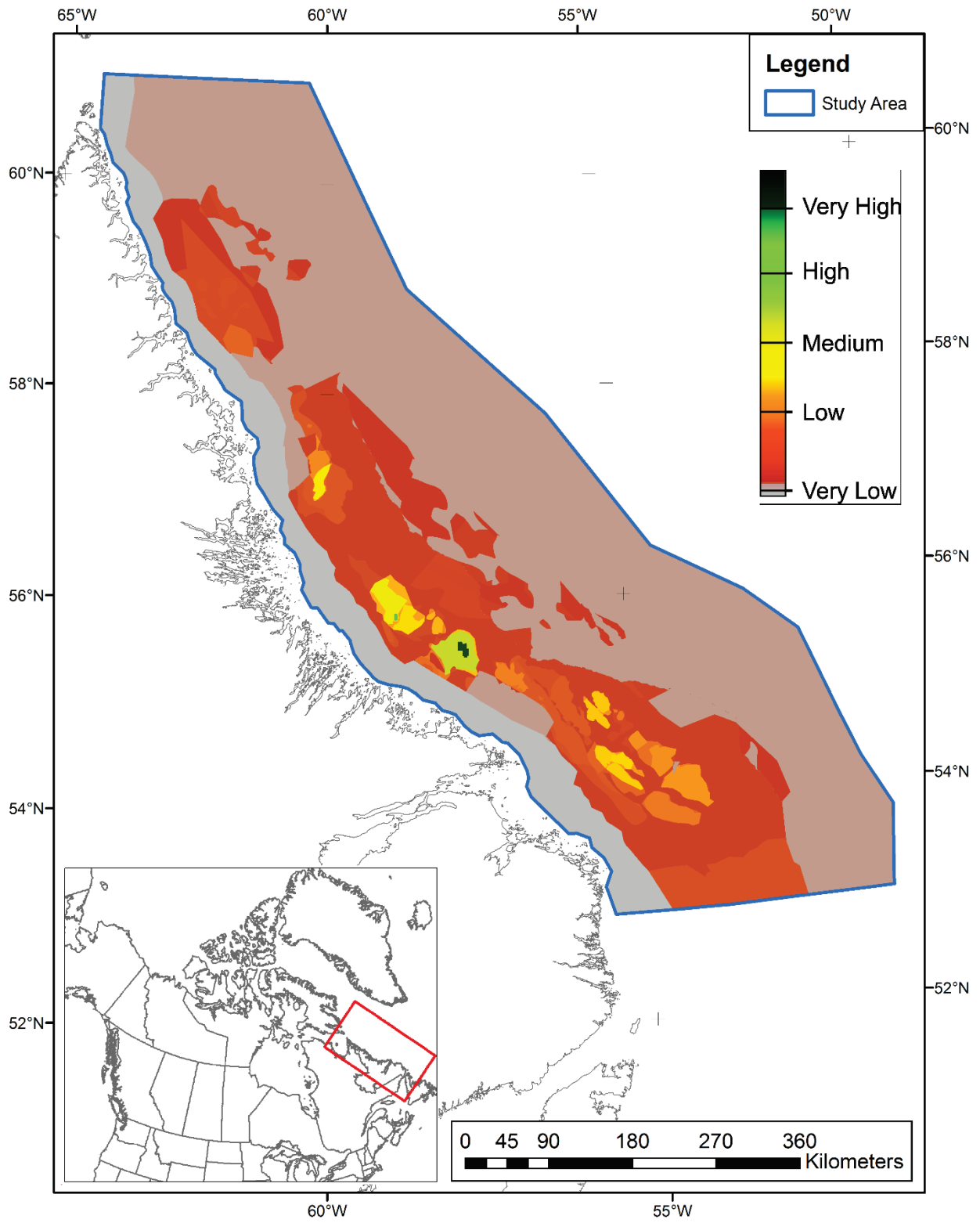
FIGURE C-6. Technical Combined Chance of Success (TCCOS) for Bjarni sequence plays.
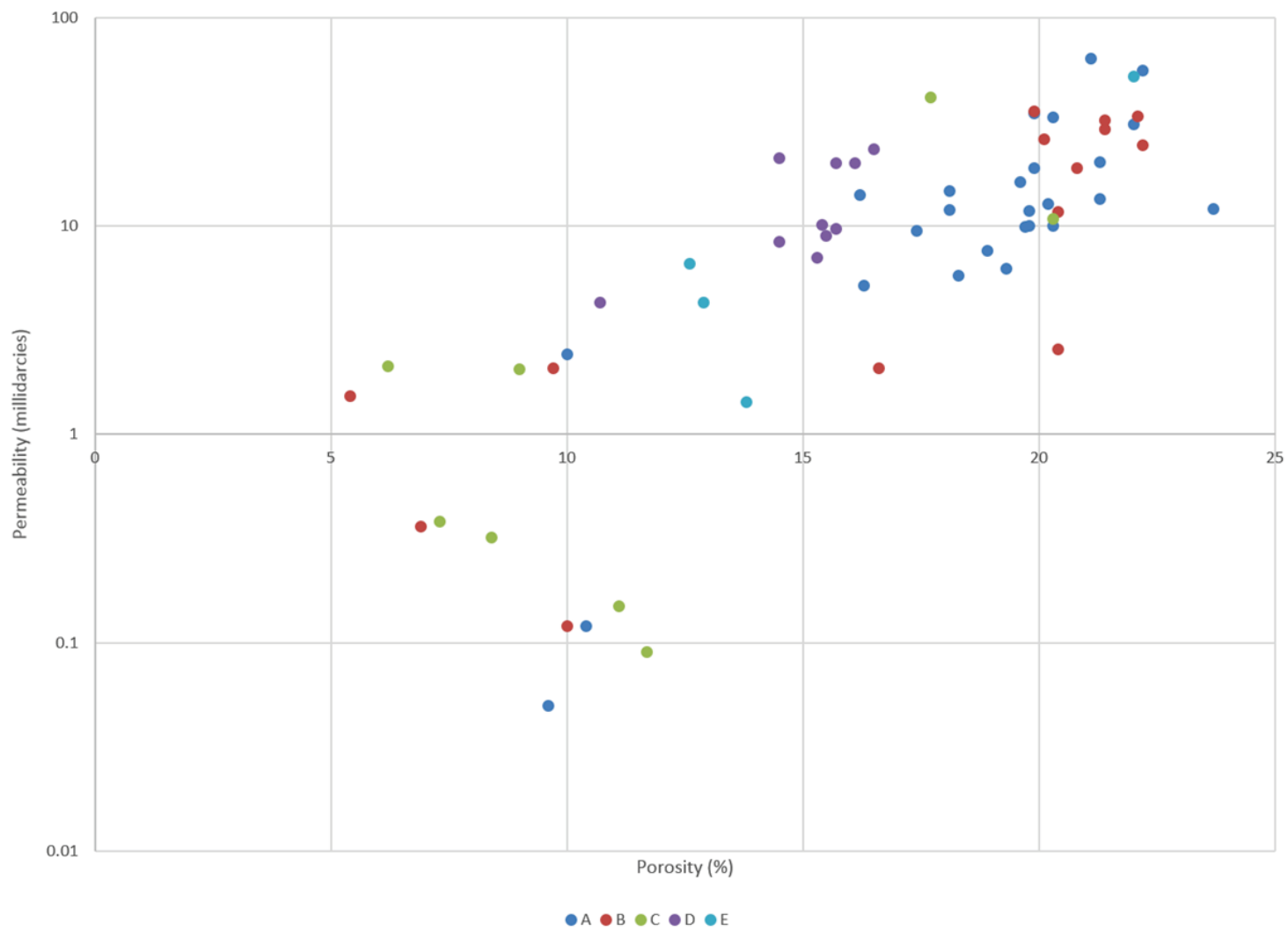
Figure C-7. Porosity permeability crossplot, Freydis Member from Gilbert F-53, with lithology descriptions A - iron-cemented sandstones containing coarse sand or pebbles. B - iron-cemented sandstones, very fine to medium grained. C - muddy sandstones. D - Other sandstones containing coarse sand or pebbles. E - Other sandstones, very fine to medium grained.
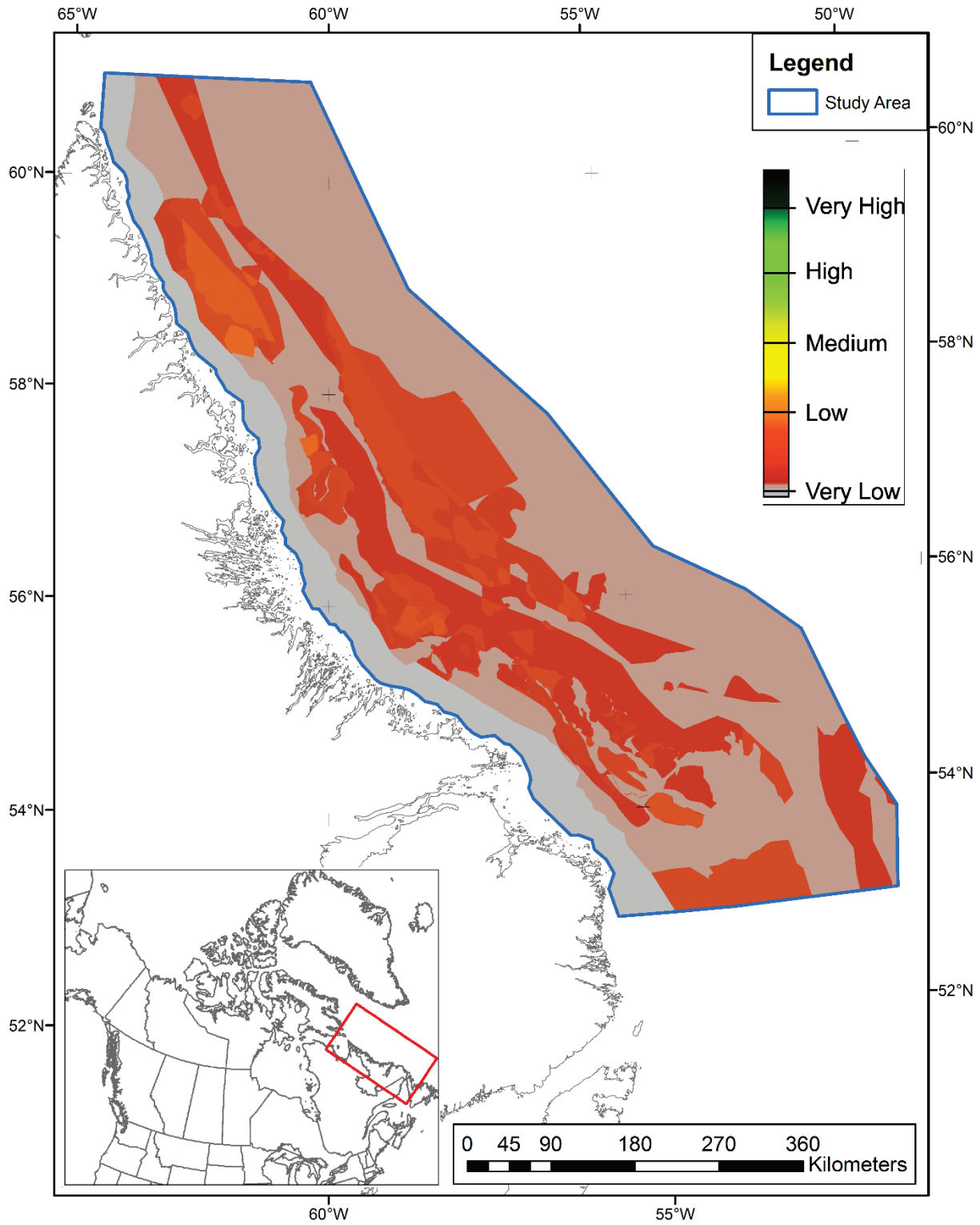
Figure C-8. Technical Combined Chance of Success (TCCOS) Map for the Markland plays
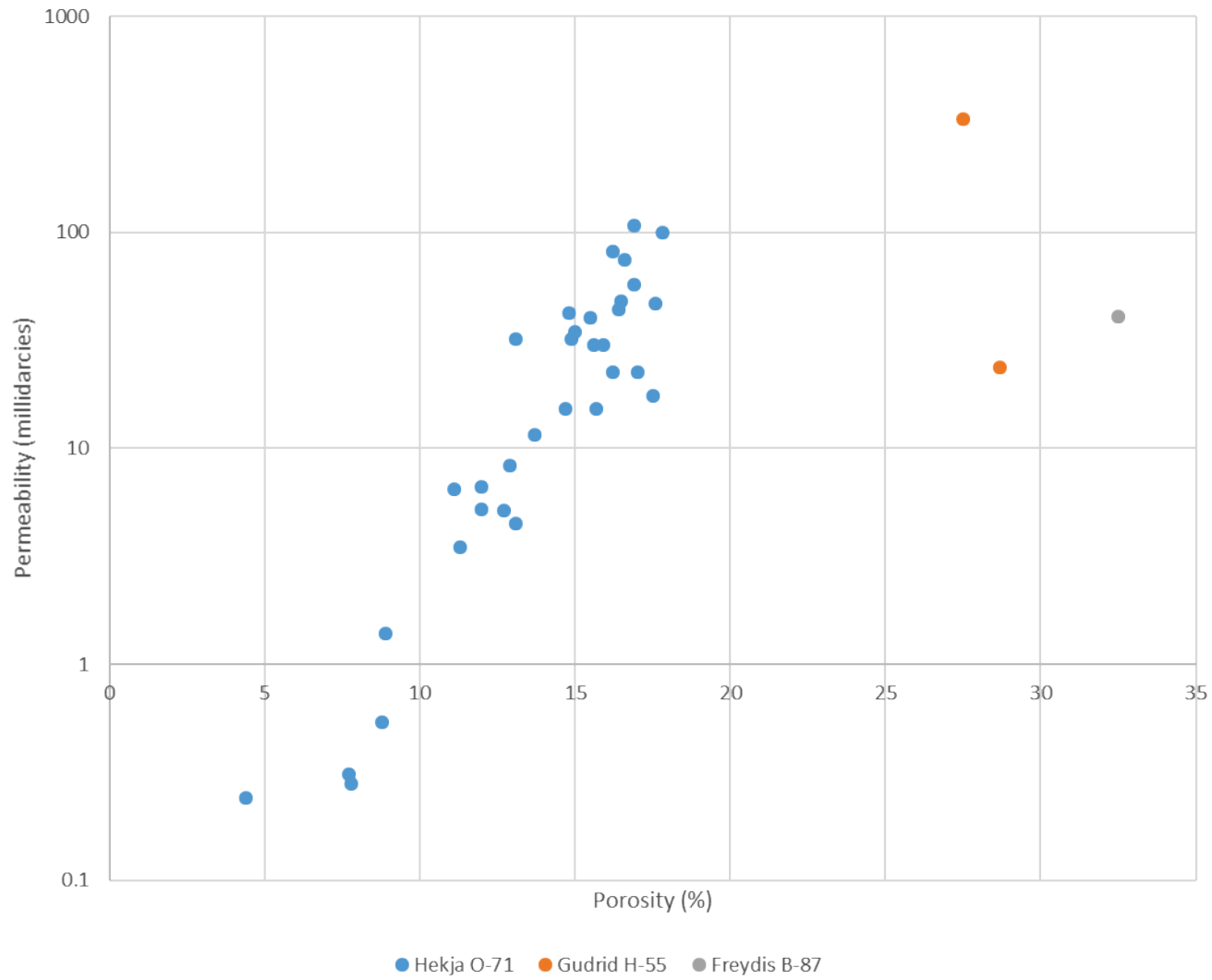
Figure C-9. Gudrid Formation Porosity and Permeability. Dot color indicates the well sampled.
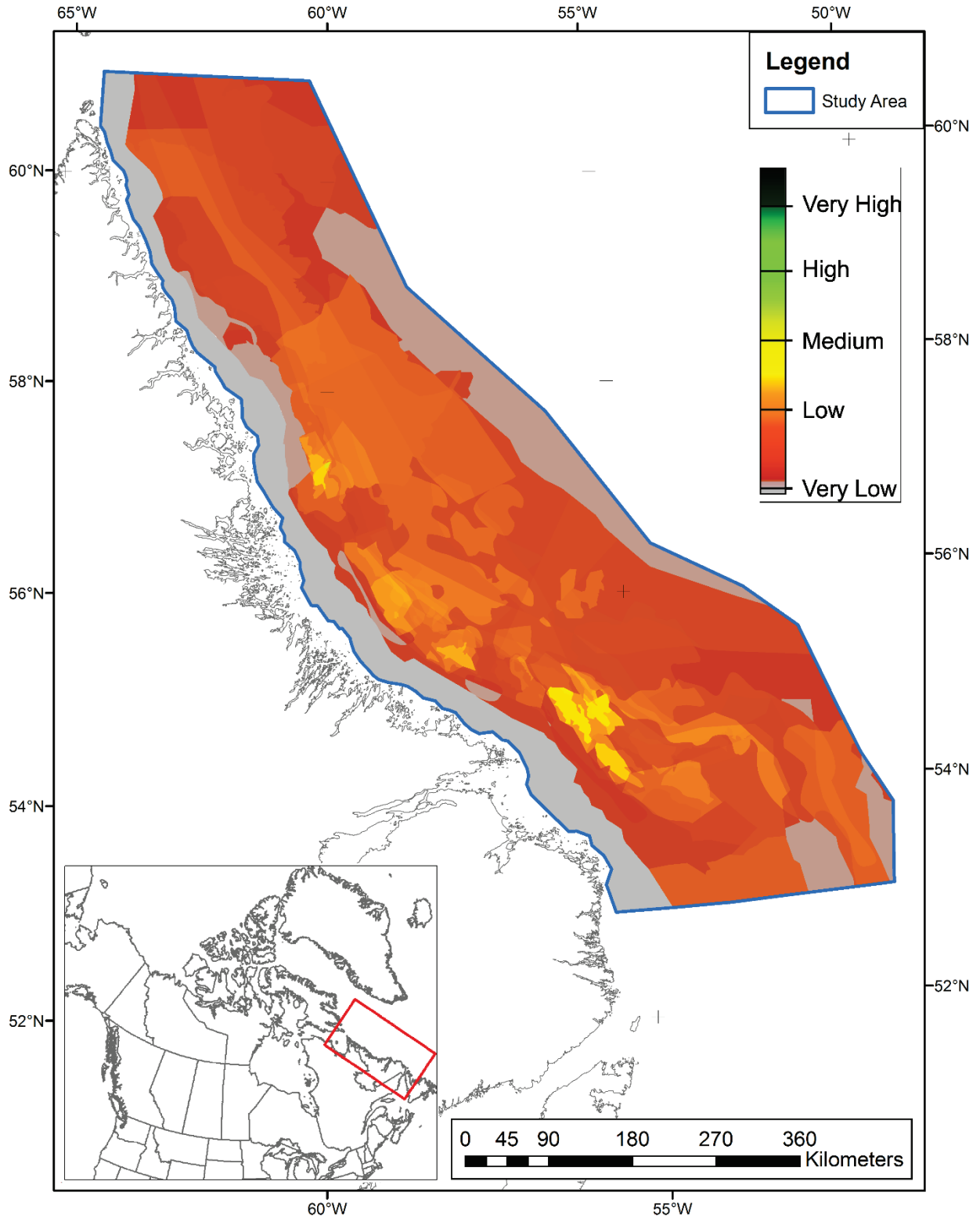
Figure C-10. Technical Combined Chance of Success (TCCOS) map for the Cartwright sequence.
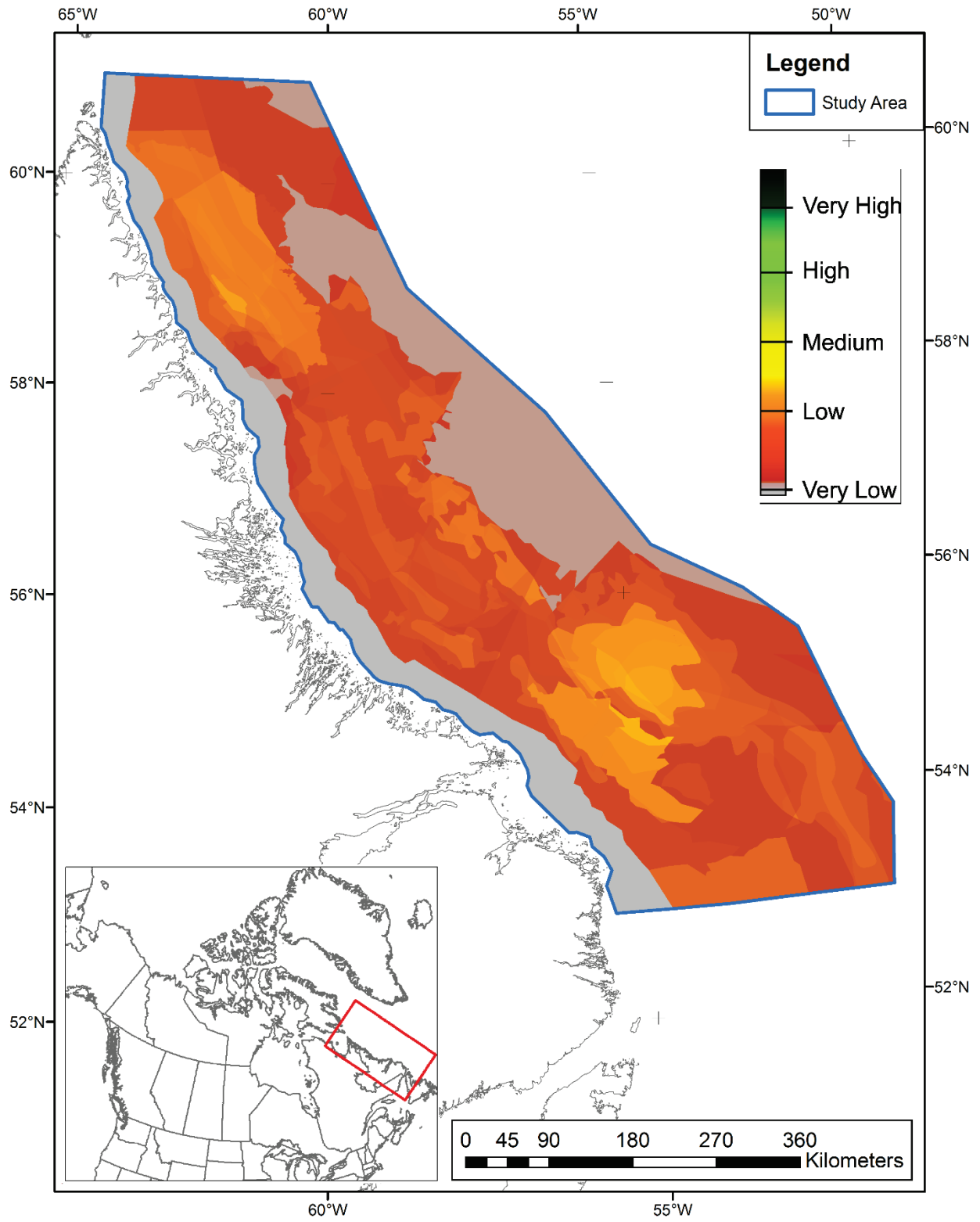
Figure C-11. Technical Combined Chance of Success (TCCOS) map for the Kenamu Sequence.
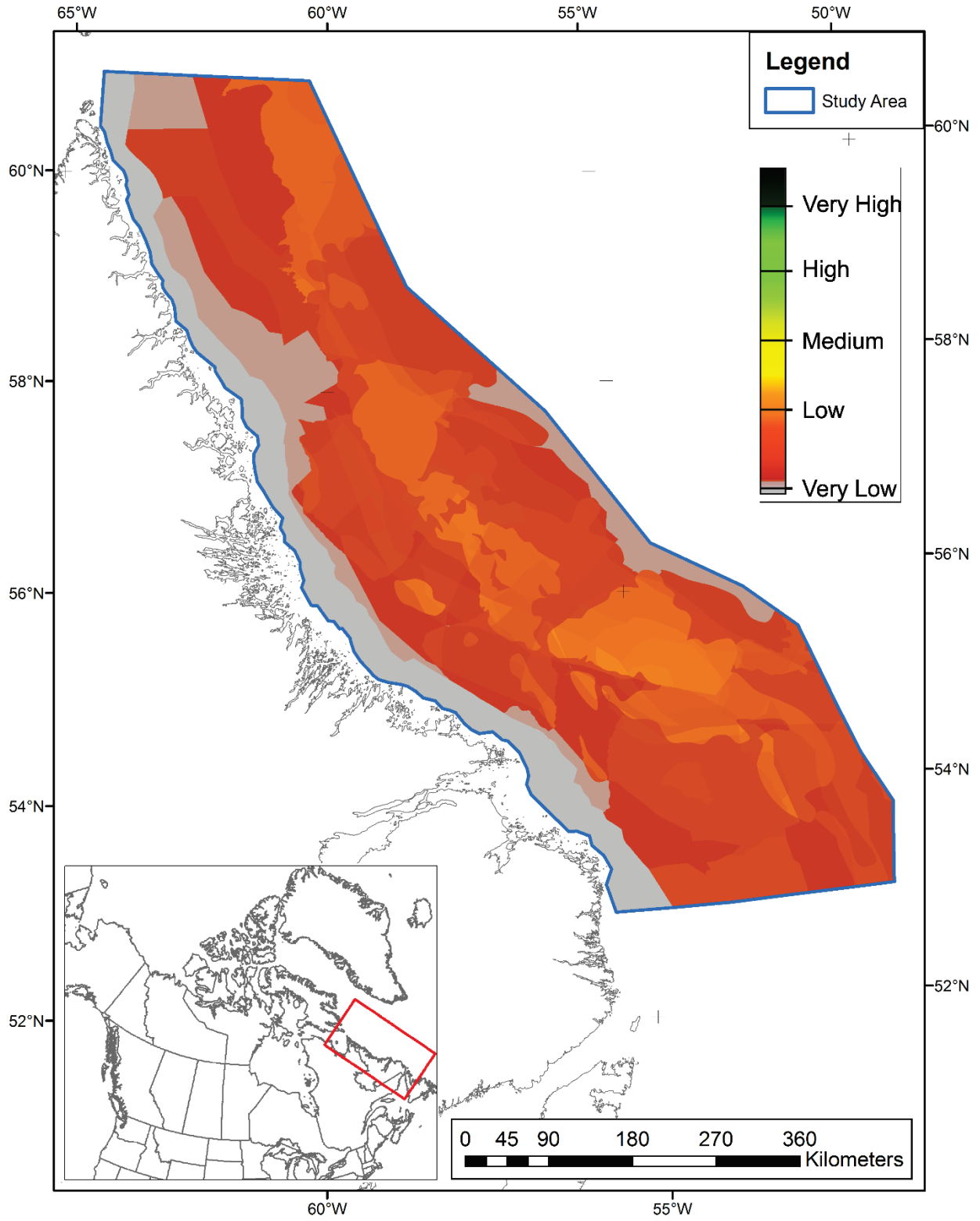
Figure C-12. Technical Combined Chance of Success (TCCOS) map for the Mokami Sequence.

APPENDIX D. UNCONVENTIONAL HYDROCARBON POTENTIAL

Conventional hydrocarbons were the primary focus of this study. Canada does not currently exploit unconventional resources such as gas hydrates, shale gas or coalbed methane in offshore areas. However, gas hydrates have been the focus of considerable GSC research and collaborations with international scientists. The following is a brief summary of the potential for these petroleum resource types within the study area.

1. **Gas Hydrates**

Gas hydrates are solid compounds in which gaseous hydrocarbons, most commonly methane, are bound with water in a crystalline compound called a clathrate. These deposits are thought to represent a large hydrocarbon resource globally (Kvenvolden, 1993; Milkov, 2004). Their potential importance in Labrador was first postulated by Taylor et al. (1979). Gases trapped in clathrates can be methane from biogenic sources or a mixture of hydrocarbons from thermogenic sources. Organic-rich mudrocks that could be sources for these gases are abundant on the Labrador Margin, and as some of these mudrocks are known to have reached thermal maturity (Appendix B), both thermogenic and biogenic gas can be expected on the Labrador margin.

Majorowicz and Osadetz (2003) analyzed the extent of gas hydrate in the Labrador Sea, using a function of gas composition, temperature and depth from Sloan (1998). They predicted methane hydrates would be stable over much of the Labrador slope and in the deeper troughs on the Labrador Shelf (Figure 5), including within the wellbores of Hopedale E-33, South Hopedale L-39, South Labrador N-79, and Corte Real P-85. The calculated zones shown in Figure 5 assume Type I hydrates which are entirely methane, and stable at shallower depths than Type II hydrates, which contain significant amounts of ethane and heavier hydrocarbons. Majorowicz and Osadetz (2003) found evidence of gas hydrates in the Saglek and Mokami formations in well logs, but noted that they were deeper than predicted for Type I hydrates. They suggested that might be an indication of a thermogenic contribution to the gas.

In addition to direct detection by drilling, methane hydrates can be identified from bottom simulating reflectors (BSR) on seismic surveys (Shipley et al., 1979; Hyndman and Spence, 1992). Mosher (2011) found BSR that he attributed to gas hydrates in two locations offshore Labrador (Figure 5). The first was on the continental slope seaward of Makkovik Bank between 620 and 2555m water depths, at an average of 443m below the seafloor. The second was in Hamilton Spur at water depths of 1075 – 2100m at an average depth of 335m below the seafloor. Mosher (2011) estimated the combined volume of these two areas at 25-75 billion m^3, assuming the hydrates extended to the seafloor and had a hydrocarbon saturation of 2-6%. Additionally, Stead et al. (2017) identified areas displaying BSR shown in Figure 5.

In summary, there is evidence from well logs, seismic data, and modeling work that a significant gas hydrate resource may exist on the Labrador margin. Riedel et al. (2009) found that hydrates were preferentially found in coarse-grained sediments; the Saglek Formation in the study area would be a suitable host. Additional work such as drilling with core sampling would be needed to delineate the size and extent of the resource before it could be exploited.

2. **Shale Gas and Oil**

Hamblin (2006) assessed the potential for shale gas plays throughout Canada's major onshore sedimentary basins. Offshore areas were not considered in that publication, presumably because they were viewed as uneconomic, but some of the sequences in offshore Labrador have similar characteristics to onshore shale plays. Hamblin (2006) postulated that thick, organic rich mudstones with type III kerogens that have not fully matured and expelled their hydrocarbons might be particularly favorable for shale gas. The Bjarni, Cartwright and Kenamu sequences all share these characteristics over significant parts of the study area. The Markland sequence tends to be poorer in organic matter than the other sequences, but may be richer in the deeper parts of Cretaceous depocenters that have not been drilled.

A comprehensive assessment of the potential for shale gas in the study area is beyond the scope of this study. Evaluating shale gas reserves is complex as gas may be present as free gas in pores and fractures, in solution in fluids, and adsorbed onto organic matter or clay minerals (Hamblin, 2006). Furthermore, there is insufficient information on factors controlling shale reservoir performance, such as mineralogy and matrix permeability. An outline of the region where at least one of the potential source rock sequences has entered the oil window (based on the thermal modeling in Appendix B) is shown in Figure 5 to approximate the potential area where shale plays might exist.

3. **Coalbed Methane**

Dawson (1995) surveyed the potential coalbed methane plays in Canada, but did not address offshore areas. The only sequence with significant amounts of coal in the study area is the Bjarni. In some wells, such as Snorri J-90, the lower part of the Bjarni contains a large number of thin coal seams. The Bjarni could be comparable to the productive Pottsville Formation of the Black Warrior Basin in the southeastern United States where individual coal beds are less than 2m thick, but the total coal thickness is typically 9-15m (Ellard et al., 1992).

Permeability is a critical factor controlling the productivity of coalbed methane reservoirs (Schraufnegel, 1993). Zuber (1998) found that permeability decreased with increasing overburden pressure, and indicated that at greater depths than 1500m, permeability was likely too low to support production. Given that the burial depths of the Bjarni sequence exceed this over most of the study area, coalbed methane is not likely to be a significant resource on the Labrador margin.

APPENDIX E. POTENTIAL MINERAL RESOURCES

The province of Newfoundland and Labrador is rich in a variety of economic minerals, with a forecasted Gross Value of Mineral Shipment of $3,973,714 in 2019 (Government of Newfoundland, 2019). Major mine operations in Labrador include the Iron Ore Company of Canada (iron), Tata Steel and Minerals Canada (iron), and Vale (nickel-copper-cobalt), which operate producing mines. Iron production is concentrated in western Labrador; ore is transported by rail to Sept-Iles, QC where it is shipped to market.

In the Labrador Sea the icebreaking bulk carrier *Umiak I* transports concentrated ore from the Voisey's Bay nickel-copper-cobalt mine to the Long Harbour Nickel Processing Plant in Long Harbour, Newfoundland (Vale, 2017). To load ore the *Umiak I* must navigate an island filled, 90 km channel to Edward's Cove (FedNav, 2019). Figure 6 shows mines and mineral occurrences in Labrador; coastal Labrador has mapped occurrences of nickel, copper, cobalt, and uranium. Although the majority of these shows are undeveloped, there remains potential for discovery and development of economic mineral deposits.

As the geology of onshore Labrador is drastically different from the offshore geology of the study area trends and mineral occurrences mapped on land cannot be extrapolated into bedrock of the marine environment. However, it is possible that the Archean and Proterozoic rocks of the Labrador Marginal Trough contain similar mineral deposits to those onshore.

Figure 6 highlights a potential uranium resource within sands of the Bjarni Formation. Umpleby (1979) noted that in some areas sands of the Bjarni Formation have higher radioactivity than overlying Cretaceous shales. This may be due to high concentrations of K-feldspars, but there has not been comprehensive mineralogical analysis to confirm this, nor are spectral gamma ray curves available. Alternatively, there could be significant uranium deposits. In the Toutunhe Formation in China, it has been shown that formation water migration through volcanic tuff can oxidize uranium, which migrates into the permeable Toutunhe sandstone (Wang et al., 2013). The reduction and concentration of uranium in the Toutunhe sandstone occurs when the uranium enriched waters contact hydrocarbons within the sandstone and the uranium is deposited as UO_2 (Wang et al., 2013; Hou et al., 2014). The Bjarni Formation has some of the same characteristics: a potential uranium source in volcanic rocks or underlying continental crust, and is known to contain hydrocarbons. There is no hard evidence of significant uranium deposits in the Bjarni Formation, but the elevated radioactivity coupled with the general conditions of Bjarni deposition (near to sources of uranium, available hydrocarbon for uranium reduction) suggests there may be regions of uranium enrichment within the study area.

APPENDIX F. REVIEWED DOCUMENTS

Avery, M.P., 1976a. Vitrinite reflectance measurements of Gudrid H-55. Geological Survey of Canada - Atlantic Internal report EPGS-DOM-22-76MPA, 3 p.

Avery, M.P., 1976b. Vitrinite reflectance measurements of Karlsefni A-13. Geological Survey of Canada - Atlantic Internal report EPGS-DOM-54-76MPA, 4 p.

Avery, M.P., 1987. Vitrinite Reflectance (Ro) of dispersed organics from Cartier D-70. Geological Survey of Canada – Atlantic Internal report EPGS-DOM-05-87MPA, 12 p.

Avery, M.P., 2005a. Vitrinite reflectance data for Gilbert F-53. Geological Survey of Canada Open File Report 4979, 17 p.

Avery, M.P., 2005b. Vitrinite reflectance data for Herjolf M-92. Geological Survey of Canada Open File Report 4981, 18 p.

Avery, M.P., 2005c. Vitrinite reflectance data for Petro-Canada et al. North Leif I-05. Geological Survey of Canada Open File 4978, 15 p.

Avery, M.P., 2005d. Vitrinite reflectance data for Petro Canada et al. Pothurst P-19. Geological Survey of Canada Open File 5059, 13 p.

Avery, M.P., 2005e. Vitrinite reflectance data for Petro-Canada et al Rut H-11. Geological Survey of Canada Open File 4980, 13 p.

Avery, M.P., 2008. Vitrinite reflectance data for Hopedale E-33. Geological Survey of Canada Open File Report 5969, 11 p.

Avery, M.P., 2009. Vitrinite reflectance data for Total Eastcan et al Roberval K-92. Geological Survey of Canada Open File 6052, 13 p.

Avery, M.P. and Hacquebard, P.A., 1976. Vitrinite Reflectance Measurements of Bjarni H-81. Geological Survey of Canada – Atlantic Internal Report EPGS-DOM-01-76MPA, 4 p.

Avery, M.P. and Hacquebard, P.A., 1980. Vitrinite reflectance measurements of coals and dispersed organic matter in Eastcan et al. Skolp E-07. Geological Survey of Canada – Atlantic Internal Report No. EPGS-DOM.1-80PAH, 3 p.

Balkwill, H.R., McMillan, N.J., MacLean, B., Williams, G.L., and Srivastava, S.P., 1990. Geology of the Labrador Shelf, Baffin Bay, and Davis Strait, *in* Geology of the Continental Margin of Eastern Canada, Keen, M.J., and Williams, G.J. (ed.), p. 293-348.

Barss, M.S. 1977. Organic matter type and thermal alteration index – Karlsefni H-13. Geological Survey of Canada – Atlantic Internal report EPGS-DOM-03-77MSB, 4 p.

Barss, M.S., 1978. Organic matter type and thermal alteration index – Herjolf M-92. Geological Survey of Canada - Atlantic Internal Report EPGS-DOM-03-78MSB, 5 p.

Barss, M.S. Bujak, J.P., and Williams, G.L., 1979. Palynological zonation and correlation of sixty-seven wells, eastern Canada: Geological Survey of Canada Paper, p. 78-24.

BASIN, 2019. BASIN Database: Natural Resources Canada. http://basin.gdr.nrcan.gc.ca/index_e.php [accessed February 2019]

Baudin, F., Disnar, J.-R., Martinez, P., and Dennielou, B., 2010. Distribution of the organic matter in the channel-levees systems of the Congo mud-rich deep-sea fan (West Africa). Implication for deep offshore petroleum source rocks and global carbon cycle: Marine and Petroleum Geology, v. 27, p. 995-1010.

Bell, J.S. (ed.), 1989. Labrador Sea. Geological Survey of Canada, East Coast Basin Atlas Series, 112 p., https://doi.org/10.4095/127152.

Bell, J.S., and Howie, R.D., 1990. Paleozoic Geology, in Geology of the Continental Margin of Eastern Canada, M.J. Keen and G.L. Williams (ed.), Geological Survey of Canada, Geology of Canada No. 2, p. 141-165.

Bojesen-Koefoed, J.A., 2002. Petroleum geochemistry: selected wells from the eastern Canada offshore area: Geological Survey of Denmark and Greenland Data Report 2002/114. 58 p.

Bojesen-Koefoed, J.A., Christiansen, F.G., Nytoft, H.P., and Pedersen, A.K., 1999. Oil seepage onshore West Greenland: evidence of multiples source rocks and oil mixing, in Fleet, A.J., Boldy, S.A.R., (ed.), Petroleum Geology of Northwest Europe: Proceedings of the 5th conference, p. 305-314: London Geological Society.

Borrelli, C., Cramer, B.S., and Katz, M., 2014. Bipolar Atlantic deepwater circulation in the middle-late Eocene: Effects of Southern Ocean gateway openings: Paleoceanography, v. 29, p. 308-327.

BP, 1978. Well History – Abandonment Report BP Columbia et al Indian Harbor M-52. Report submitted to C-NLOPB. 328 p.

BP Research Center, 1977. The biostratigraphy of well Indian Harbour M-52 below 7750 ft. (BP Canada-Columbia-Chevron) Offshore Labrador, Canada, Report submitted to C-NLOPB, 13 p.

Brinkhuis, Schouten, S., Collinson, M.E., Slujis, A., Sinninghe Damste, J.S., Dickens, G., et al., 2006. Episodic fresh waters in the Eocene Arctic Ocean: Nature, v. 441, p. 606-609.

Budkewitsch, P., Pavlic, G., Oakey, G., Jauer, C., and Decker, V., 2013. Reconaissance mapping of suspect oil seep occurrences in Baffin Bay and Davis Strait using satellite radar: preliminary results: Geological Society of Canada Open File 7068.

Bujak-Davies Group, 1987. Biostratigraphy and Maturation of 17 Labrador and Baffin Bay Wells; Geological Survey of Canada Open File 1936, 54p.

Bujak-Davies Group, 1989. Biostratigraphy and Maturation of Gilbert F-53 and Gjoa G-37. Geological Survey of Canada Open File Report 1931, 65 p.

C-NLOPB, 2016a. Land Issuance—Active Call for Bids.
   https://www.cnlopb.ca/exploration/issuance/#bids-active. Accessed May, 2019.

C-NLOPB, 2016b. Land Rights Issuance Process.
   https://www.cnlopb.ca/exploration/issuanceprocess/. Accessed May, 2019.

C-NLOPB, 2019. Schedule of Wells: Newfoundland and Labrador Offshore Area. Accessed
   February, 2019.

Canterra, 1983. Final Well Report Canterra et al South Hopedale L-39. Report submitted to
C-NLOPB, 96 p.

Chalmers, J.A., 1991. New evidence on the structure of the Labrador Sea/Greenland continental
   margin: Journal of the Geological Society, London, v. 148, p. 899-908.

Chalmers, J.A., 1997. The continental margin off southern Greenland: along-strike transition from an
   amagmatic to a volcanic margin: Journal of the Geological Society, v. 154, p. 443-463.

Chalmers, J.A., 2000. Offshore evidence for Neogene uplift in central west Greenland: Global and
   Planetary Change, v. 24, p. 311-318.

Chevron, 1978. Well History Report - Chevron et al Hopedale E-33, Report submitted to
   C-NLOPB, 29p.

Chevron, 1980. Well History Report Chevron et al South Labrador N-79, Report submitted to
   C-NLOPB, 65p.

Chian, D., Louden, K.E., Reid, I., 1995. Crustal structure of the Labrador Sea conjugate margins and
   implications for the formation of nonvolcanic continental margins, Journal of Geophysical
   Research, v. 100, p. 24239-24253.

Connelly, J.N. and Ryan, B., 1996. Late Archean evolution of the Nain Province, Nain, Labrador:
   imprint of a collision: Canadian Journal of Earth Sciences, v. 33, p. 1325-1342.

Core Laboratories Canada Ltd., 1977. Fluid analyses for Eastcan Exploration Ltd. Eastcan et al Herjolf
   M-92. Report submitted to C-NLOPB, 12 p.

Core Laboratories Canada Ltd., 1979. Roberval K-92 Full Diameter Core Analysis. Report submitted
   to C-NLOPB, 4p.

Cramer, B.S., Toggweiler, J.R., Wright, J.D., Katz, M.E., and Miller, K.G., 2009. Ocean overturning
   since the Late Cretaceous: Inferences from a new benthic foraminiferal isotope compilation:
   Paleoceanography, https://doi.org/10.1029/2008PA001683.

Culshaw, N., Brown, T., Reynolds, P.H. and Ketchum, J.W., 2000. Kanairiktok shear zone: the
   boundary between the Paleoproterozoic Makkovik Province and the Archean Nain Province,
   Labrador, Canada. Canadian Journal of Earth Science, 37, p. 1245–1257,
   https://doi.org/10.1139/e00-035.

Dafoe, L.T., Williams, G.L., and Dickie, K., 2015. Deltaic and fully marine settings interpreted from conventional core, offshore Labrador, Canada: Geoconvention 2015 abstracts, p. 1-3.

D'Eon-Miller and Associates, 1987. Labrador Shelf – Paleoenvironments, Geological Survey of Canada, Open File Report 1722, 186 p.

Dam, G., Nøhr-Hansen, H., Pedersen, G.K., and Sonderholm, M., 2000. Sedimentary and structural evidence of a new early Campanian rift phase in central Nuussuaq, West Greenland: Cretaceous Research, v. 21, p. 127-154.

Dawson, F.M., 1995. Coalbed methane: A comparison between Canada and the United States: Geological Survey of Canada Bulletin 489, 68 p.

Dehler, S.A., and Keen, C.E., 1993. Effects of rifting and subsidence on thermal evolution of sediments in Canada's east coast basins: Canadian Journal of Earth Sciences, v. 30, p. 1782-1798.

Delescluse, M., Funck, T., Dehler, S.A., Louden, K.E., and Watremez, L., 2015. The oceanic crustal structure at the extinct, slow to ultraslow Labrador Sea spreading center: Journal of Geophysical Research, v. 120, p. 5249-5272.

Dickie, K., Keen, C.E., Williams, G. and Dehler, S.A. 2011. Tectonostratigraphic evolution of the Labrador Margin, Atlantic Canada. Marine and Petroleum Geology, 28, p. 1663–1675, https://doi.org/10.1016/j.marpetgeo.2011.05.009.

Dietrich, J., Lavoie, D., Hannigan, P., Pinet, N., Castonguay, S., Giles, P., and Hamblin, A., 2011. Geologic setting and resource potential of conventional petroleum plays in Paleozoic basins in eastern Canada, Bulletin of Canadian Petroleum Geology, v.59, p. 54-84.

Duk-Rodkin, A., and Hughes, O.L., 1994. Tertiary-Quaternary drainage of the pre-glacial Mackenzie Basin: Quaternary International, v. 22, p. 221-241.

Eastcan et al, 1973a. Well History Report Eastcan et al Bjarni H-81. Report submitted to C-NLOPB, 45 p.

Eastcan Exploration, 1973b. Well History Report Eastcan et al Leif M-48. Report submitted to C-NLOPB, 57p.

Eastcan Exploration, 1975a. Well History Report Eastcan et al Gudrid H-55. Report submitted to C-NLOPB, 45 p.

Eastcan Exploration, 1975b. Study of fluids collected from the Gudrid and Bjarni Wells. Report submitted to C-NLOPB, 11 p.

Eastcan Exploration, 1976a. Well History Report Eastcan et al Cartier D-70. Report submitted to C-NLOPB, 48 p.

Eastcan Exploration, 1976b. Well History Report Eastcan et al Freydis B-87. Report submitted to C-NLOPB, 44 p.

Eastcan Exploration, 1977a. Well history report Eastcan et al Karlsefni A-13. Report submitted to C-NLOPB, 56p.

Eastcan Exploration, 1977b. Well History Report Eastcan et al Snorri J-90. Report submitted to C-NLOPB, 44p.

Ellard, J.S., Roark, R.P., Ayers Jr., W.B., 1992. Geologic controls on coalbed methane production: an example from the Pottsville Formation (Pennsylvanian Age), Black Warrior Basin, Alabama, USA *in* Beamish, B.B., Gamson, P.D., (eds.), Symposium on Coalbed Methane Research and Development in Australia: James Cook University, Townsville, Australia, v. 1, p. 45-61.

Fednav. 2019. The World's Strongest: Umiak I - http://www.fednav.com/fr/worlds-strongest-umiak-i [accessed March, 2019].

Fensome, R.A., 2015. Palynological analysis of two Labrador Shelf wells: Rut H-11 and Karlsefni A-13. Geological Survey of Canada Open File Report 7738. 20 p.

Fowler, M.G., Obermajer, M., Jiang, C., 2019. Organic geochemical data from Northern Canada. Rock-Eval/TOC data for twelve wells from the Labrador Shelf, Eastern Canada, offshore Newfoundland and Labrador; Geological Survey of Canada, Open File 8570, 12 p.

Funck, T., Hansen, A.K., Reid, I.D. and Louden, K.E. 2008. The crustal structure of the southern Nain and Makkovik provinces of Labrador derived from refraction seismic data. Canadian Journal of Earth Sciences, 45, p. 465–481, https://doi.org/10.1139/E08-007.

Funck, T., Jackson, H.R., Louden, K.E. and Klingelhöfer, F. 2007. Seismic study of the transform-rifted margin in Davis Strait between Baffin Island (Canada) and Greenland: What happens when a plume meets a transform. Journal of Geophysical Research: Solid Earth, 112, p. 1–22, https://doi.org/10.1029/2006JB004308.

Funck, T., Louden, K.E. and Reid, I.D. 2001. Crustal structure of the Grenville Province in southeastern Labrador from refraction seismic data: evidence for a high-velocity lower crustal wedge. Canadian Journal of Earth Sciences, 38, p. 1463–1478, https://doi.org/10.1139/cjes-38-10-1463.

Geochem Laboratories, 1977. Hydrocarbon source facies analysis Total Eastcan Herjolf M-92 well offshore Labrador, Report submitted to C-NLOPB, 131p.

Geochem Laboratories (Canada) Ltd., 1978a. Hydrocarbon source facies analysis Total Eastcan et al Cartier D-70 well Labrador continental shelf. Report submitted to C-NLOPB, 53 p.

Geochem Laboratories, 1978b. Hydrocarbon source facies analysis B.P. Columbia Chevron Indian Harbour M-52 well, Labrador continental shelf. Report submitted to C-NLOPB, 58 p.

Geochem Laboratories, 1978c. Hydrocarbon source facies analysis Total Eastcan et al Karlsefni H-13 well Labrador continental shelf. Report submitted to C-NLOPB, 75 p.

Geochem Laboratories, 1978d. Hydrocarbon Source Facies Analysis Total Eastcan et al Leif M-48 well Labrador continental shelf. Report submitted to C-NLOPB, 58 p.

Government of Newfoundland and Labrador, 2019. Gross Value of Mineral Shipments By Commodity: Department of Natural Resources. https://www.geosurv.gov.nl.ca/minesen/mineral_shipments/ [accessed February 2019]

Gower, C., Schärer, U. and Heaman, L.M. 1992. The Labradorian orogeny in the Grenville Province, eastern Labrador, Canada. Canadian Journal of Earth Sciences, v. 29, p. 1944–1957, https://doi.org/10.1139/e92-152.

Gradstein, F.M., and Williams, G.L., 1976. Biostratigraphy of the Labrador Shelf; Geological Survey of Canada Open File 349, 39 p.

Gradstein, F.M., Ogg, J.G., and Smith, A.G., 2004. A Geologic Time Scale 2004: Cambridge University Press, 1 p.

Grant, A.C., 1972. The continental margin off Labrador and eastern Newfoundland – morphology and geology, Canadian Journal of Earth Sciences, v. 9, p. 1394-1430.

Hall, J., Louden, K.E., Funck, T., and Deemer, S., 2002. Geophysical characteristics of the continental crust along the Lithoprobe Eastern Canadian Shield Onshore-Offshore Transect (ECSOOT): a review: Canadian Journal of Earth Sciences, v. 39, p. 569-587.

Hamblin, 2006. The "shale gas" concept in Canada: a preliminary inventory of possibilities: Geological Survey of Canada Open File 5384, 103 p.

Hamdani, Y., and Marechal, J.-C., 1993. Paleo heat flow of eastern Canada's passive margins: Tectonophysics, v. 225, p. 107-121.

Haq, B.U., and Al-Qahtani, A.M., 2005. Phanerozoic cycles of sea-level change on the Arabian platform. GeoArabia , v. 10, p. 127-160.

Hillier, S., 1994. Pore-lining chlorites in siliciclastic reservoir sandstone: electron microprobe, SEM and XRD data, and implications for their origin. Clay Minerals, v. 29, p. 665-679.

Hou, B., Michaelsen, B., Li, Z., Keeling, J., and Fabris, A., 2014. Paleovalley-related uranium: Exploration criteria and case studies from Australia and China: Episodes, v. 37, p. 150-171.

Hyndman, R.D., and Spence, G.D., 1992. A seismic study of methane hydrate marine bottom simulating reflectors: Journal of Geophysical Research, v. 97, p. 6683-6698.

Inglis, G.N., Farnsworth, A., Lunt, D., Foster, G.L, Hollis, C.J., Pagani, M., Jardine, P.E., Pearson, P.N., Markwick, P., Raynman, L., Galsworthy, A.M.J., and Pancost, R.D., 2015. Descent towards the icehouse: Eocene sea surface cooling, inferred from GDGT distributions: Paleoceanography, v. 30, p. 1000-1020.

INRS-Petrole, 1983. Adsorbed gases study of the Skolp E-07, Herjolf M-92 and Indian Harbour M-52 wells in the Labrador Shelf. Report to Eastcan et al., 16 p.

Japsen, P., Bonow, J.M., Green, P.F., Chalmers, J.A., and Lidmar-Bergstrom, K., 2006. Elevated, passive continental margins: Long-term highs or Neogene uplifts? New evidence from West Greenland: Earth and Planetary Science Letters, v. 248, p. 330-339.

Jauer, C.D., 2009. Hekja O-71, a major stranded gas discovery offshore Baffin Island with seismic examples of probable gas vents: Geological Survey of Canada, Open File 6432. 1 sheet.

Jauer, C.D., and Budkewitsch, P., 2010. Old marine seismic and new satellite radar data: Petroleum exploration of north west Labrador Sea, Canada Marine and Petroleum Geology, v. 27, p. 1379-1394, doi:101016/j.marpetgeo.2010.03.003

Jauer, C.D., Oakey, G.N., Williams, G., Wielens, J.B.W.H., and Haggart, J.W., 2014. Saglek Basin in the Labrador Sea, east coast Canada: stratigraphy, structure and petroleum systems: Bulletin of Canadian Petroleum Geology, v. 62, p. 232-260.

Jenkins, W.A.M., 1984. Ordovician rocks in the Eastcan et al. Freydis B-87 and other wells in offshore Atlantic Canada: Canadian Journal of Earth Sciences, v. 21, p. 864-868.

Josenhans, H.W., Zevenhuizen, J., and Klassen, R.A., 1986. The Quaternary geology of the Labrador Shelf, v. 23, p. 1190-1213.

Keen, C.E., Dickie, K. and Dehler, S.A. 2012. The volcanic margins of the northern Labrador Sea: Insights to the rifting process. Tectonics, v. 31, p. 1–13, https://doi.org/10.1029/2011TC002985.

Keen, C.E., Dickie, K. and Dafoe, L.T. 2018a. Structural characteristics of the ocean-continent transition along the rifted continental margin, offshore central Labrador. Marine and Petroleum Geology, v. 89, p. 443–463, https://doi.org/10.1016/j.marpetgeo.2017.10.012.

Keen, C.E., Dickie, K. and Dafoe, L.T. 2018b. Structural evolution of the rifted margin off northern Labrador: the role of hyperextension and magmatism. Tectonics, v. 37, p. 1955–1972, https://doi.org/10.1029/2017TC004924.

Keen, C.E., and Piper, D.J.W., 1990. Geological and historical perspective, Geology, *in* Geology of the Continental Margin of Eastern Canada, M.J. Keen and G.L. Williams (ed.), Geological Survey of Canada, Geology of Canada No. 2, p. 5-30.

Keen, M. and Williams, G. (ed.), 1990. Geology of the Continental Margin of Eastern Canada. Geological Survey of Canada, 855 p.

Kvenvolden, K.A., 1993. A primer on gas hydrates, *in* The Future of Energy Gases, USGS Professional Paper 1570, p. 279-291.

Lister, C.J., King, H.M., Atkinson, E.A., Kung, L.E., and Nairn, R., 2018. A probability-based method to generate qualitative petroleum potential maps: adapted for and illustrated using ArcGIS. Geological Survey of Canada, Open File 8404, 50 p.

Lourens, L.L., Slujis, A., Kroon, D., Zachos, J.C., Thomas, E., Rohl, U., Bowles, J., and Raffi, I., 2005. Astronomical pacing of late Palaeocene to early Eocene global warming events: Nature, v. 435, p. 1083-1087.

Majorowicz, J.A., and Osadetz, K.G., 2003. Natural gas hydrate stability in the East Coast offshore-Canada: Natural Resources Research, v. 12, p. 93-104.

Majorowicz, J.A., Osadetz, K. and Safanda, J., 2011. Methane gas hydrate stability models on continental shelves in response to glacio-eustatic sea level variations: Examples from Canadian oceanic margins: Energies, v. 6, p. 5775-5806.

McMillan, N.J., 1973. Shelves of Labrador Sea and Baffin Bay, Canada, *in* The Future Petroleum Provinces of Canada—Their Geology and Potential; Canadian Society of Petroleum Geologists, p. 473-517.

McWhae, J.R.H., Elie, R., Laughton, K.C., and Gunther, P.R., 1980. Stratigraphy and petroleum prospects of the Labrador Shelf; Bulletin of Canadian Petroleum Geology, v. 28, p. 460-488.

Margold, M., Stokes, C.R., Clark, C.D. and Kleman, J. 2015. Ice streams in the Laurentide Ice Sheet: a new mapping inventory. Journal of Maps, 11, p.380–395. https://doi.org/10.1080/17445647.2014.912036.

Milkov, A.V., 2004. Global estimates of hydrate-bound gas in marine sediments: How much is really out there?: Earth Science Reviews, v. 66, p. 183-197.

Miller, K.G., Komminz, M.a., Browning, J.V., Wright, J.D., Mountain, G.S., Katz, M.E., Sugarman, P.J., Cramer, B.S., Christie-Blick, N., and Pekar, S.F., 2018. The Phanerozoic record of global sea-level change: Science, v. 310, p. 1293-1298.

Miserocchi, S., Langone, L., and Tesi, T., 2007. Content and isotopic composition of organic carbon within a flood layer in the Po River prodelta (Adriatic Sea): Continental Shelf research, v. 27, p. 338-358.

Moir, P.N. 1989. Lithostratigraphy I Labrador Sea Review and type Sections. In: Bell, J. S. (ed.) East Coast Basin Atlas Series: Labrador Sea. Geological Survey of Canada, p. 26–27.

Moir, P.N., Bell, J.S., Cridland, R., Hunter, D., Pethyrycz, B., Sullivan, G., Kyle, P., Balkwill, H.R., Lavine, G., and Avery, M.P., 1989. Geochemistry Labrador Sea, geothermal gradients and depths to gas generation, *in* East Coast Basin Atlas Series, Labrador Sea, Atlantic Geoscience Center, Geological Survey of Canada, p. 86-87.

Mosher, D.C., 2011. A margin-wide BSR gas hydrate assessment: Canada's Atlantic Margin: Marine and Petroleum Geology, v. 28, p. 1540-1553.

Myers, R.A., and Piper, D.J.W., 1988. Seismic stratigraphy of late Cenozoic sediments in the northern Labrador Sea: a history of bottom circulation and glaciation: Canadian Journal of Earth Sciences, v. 25, p. 2059-2074.

Nantais, P.T., 1984. Regional hydrocarbon potential of the Labrador Shelf. Geological Survey of Canada Open File 1197, 50 p.

Nøhr-Hansen, H., Williams, G.L., and Fensome, R.A., 2016. Biostratigraphic correlation of the western and eastern margins of the Labrador-Baffin Seaway and implications for the regional geology: Geological Survey of Denmark and Greenland Bulletin 37, 74 p.

Oakey, G.N. and Chalmers, J.A. 2012. A new model for the Paleogene motion of Greenland relative to North America: Plate reconstructions of the Davis Strait and Nares Strait regions between Canada and Greenland. Journal of Geophysical Research: Solid Earth, 117, p. 1–28, https://doi.org/10.1029/2011JB008942.

Okwese, A.C., Pe-Piper, G., Piper, D.J.W., 2012. Controls on regional variability in marine pore-water diagenesis below the seafloor in Upper Jurassic-Lower Cretaceous prodeltaic sandstone and shales, Scotian Basin, Eastern Canada: Marine and Petroleum Geology, v. 29, p. 175-191.

Otis Engineering, 1981. Petro Canada Exploration North Bjarni F-06 Labrador Shelf P.T. #1-4. Report submitted to C-NLOPB, 116 p.

Parnell, J., Bowden, S., and Mark, D., 2018. Petroleum generation and migration in the Cambro-Ordovician Laurentian margin succession of NW Scotland: Journal of the Geological Society, v. 175, p. 33-43.

Pe-Piper, G., Piper, D.J.W. and Triantafyllidis, S. 2013. Detrital monazite geochronology, Upper Jurassic-Lower Cretaceous of the Scotian Basin: significance for tracking first-cycle sources. Geological Society, London, Special Publications, v. 386, p. 293–311. https://doi.org/10.1144/SP386.13.

Pepper, A.S., and Corvi, P.J., 1995. Simple kinetic models of petroleum formation 1. Oil and gas generation from kerogen: Marine and Petroleum Geology, v. 12, p. 291-319.

Petersen, H.I., 2006. The petroleum generation potential and effective oil window of humic coals related to coal composition and age: International Journal of Coal Geology, v. 67, p. 221-248.

Petro-Canada, 1980a. Biostratigraphy of the Petro-Canada et al. Gilbert F-53 well, Report submitted to C-NLOPB, 11 p.

Petro-Canada, 1980b. Well History report Petro-Canada et al. Ogmund E-72. Report submitted to C-NLOPB, 258 p.

Petro-Canada, 1980c. Well history report Petro-Canada et al. Roberval C-02. Report submitted to C-NLOPB, 161 p.

Petro-Canada, 1980d. Geochemical Evaluation Petro-Canada et al. Roberval C-02. Report submitted to C-NLOPB, 122 p.

Petro-Canada, 1981a. Well history report, Petro-Canada et al. Bjarni O-82, Report submitted to C-NLOPB, 101p.

Petro-Canada, 1981b. Well history report, Petro-Canada et al. North Bjarni F-06. Report submitted to C-NLOPB, 114 p.

Petro-Canada, 1981c. Well history report, Petro-Canada et al. North Leif I-05. Report submitted to C-NLOPB, 222 p.

Petro-Canada, 1981d. Geochemical Evaluation Petro-Caanda et al. Ogmund E-72. Report submitted to C-NLOPB, 74 p.

Petro-Canada, 1981e. Petrography of the Freydis and Bjarni Sandstones in the Petro-Canada et al. Ogmund E-72 well. Report submitted to C-NLOPB, 43 p.

Petro-Canada, 1982a. Geochemical Evaluation Petro-Canada et al. North Leif I-05. Report submitted to C-NLOPB, 92 p.

Petro-Canada, 1982b. Well History Report Petro-Canada et al. Pothurst P-19. Report submitted to C-NLOPB, 91 p.

Petro-Canada, 1983a. Well History Report Petro-Canada et al. Corte-Real P-85. Report submitted to C-NLOPB, 116 p.

Petro-Canada, 1983b. Final Geochemistry Report Petro-Canada et al. Pothurst P-19. Report submitted to C-NLOPB, 82 p.

Petro-Canada, 1983c. Well History Report Petro-Canada et al. Rut H-11. Report submitted to C-NLOPB, 82 p.

Petro-Canada, 1984a. Final Geochemistry Report Petro Canada et al. Rut H-11. Report submitted to C-NLOPB, 100 p.

Petro-Canada, 1984b. Final Geochemistry Report Petro-Canada et al. Corte Real P-85. Report submitted to C-NLOPB, 92 p.

Piper, D.J.W., Mudie, P., Fader, G., Josenhans, H.W., MacLean, B. and Vilks, G. 1990. Quaternary Geology. In: Keen, M. and Williams, G. (ed.) Geology of the Continental Margin of Eastern Canada, p. 475–607.

Powell, 1979. Geochemical Studies Labrador Shelf. Geological Survey of Canada Atlantic internal report, 40 p.

Rashid, M.A., 1975. Geochemical characteristics of organic matter of Gudrid H-55. Atlantic Geoscience Centre: Organic Geochem Investigations of Offshore Oil Wells Report No. 6, 18 p.

Rashid, M.A., 1976. Geochemical analysis of Hydrocarbons present in Freydis B-87. Atlantic Geoscience Centre: Geochemical Investigations of Offshore Oil Wells Report No. 11, 21 p.

Rashid, M.A., and Leonard, J.D., 1975. Organic geochemical investigations of the East coast offshore exploratory wells – Report No. 5 Geochemical charactreristics of organic matter of sedimentary sequences penetrated by Eastcan et al Leif M-48. Atlantic Geoscience Centre Internal report, 22 p.

Rashid, M.A., Purcell, L.P., and Hardy, I.A., 1980. Source rock potential for oil and gas of the east Newfoundland and Labrador Shelf areas, *in* Facts and Principles of World Oil Occurrence, Miall, A.D. (ed.), Canadian Society of Petroleum Geologists Memoir 6, p. 589-608.

Reiter, M., and Jessop, A.M., 1985. Estimates of terrestrial heat flow in offshore eastern Canada: Canadian Journal of Earth Sciences, v. 22, p. 1503-1517.

Reston, T.J., 2007. The formation of non-volcanic rifted margins by the progressive extension of the lithosphere: the example of the West Iberian margin, *in* Karner, G.D., Manatschal, G., and Pinheiro, L.M. (ed.), Imaging, Mapping and Modelling Continental Lithosphere Extension and Breakup: Geological Society of London Special Publications 282, p. 77-110.

Reston, T.J., 2009, The structure, evolution and symmetry of the magma-poor rifted margin of the North and Central Atlantic: A synthesis: Tectonophysics, v. 468, p. 6-27.

Riedel, M., Collett, T., Malone, M., and IODP Expedition 311 Scientists, 2009. Gas hydrate drilling transect across northern Cascadia margin—IODP Expedition 311: the Geological Society of London Special Publications v. 319, p. 11-19.

Riley Geoscience, 2014. Cretaceous-Tertiary Stratigraphy of the Labrador Shelf – Wells: Hare Bay E-21, Herjolf M-92, North Bjarni F-06, Ogmund E-72, Pothurst, P-19, Roberval K-92 and Snorri J-90. Report prepared for Nalcor Energy, 56 p.

Riley Geoscience, 2016. Cretaceous-Tertiary Stratigraphy of the Labrador Shelf – Wells: Freydis B-87, Hopedale E-33, Karlsefni A-13, North Leif I-05 and South Hopedale L-39. Report prepared for Nalcor Energy, 31 p.

Robertson Research, 1974. Report on a petroleum geochemical study of the Eastcan Gudrid H-55 well, Labrador Sea offshore Canada. Report submitted to C-NLOPB, 50 p.

Robertson Research, 1975. A maturation study of parts of a core from 6348 to 6369 feet in the Eastcan Freydis B-87 well, drilled offshore Eastern Canada, 5 p.

Robertson Research, 1980. The Micropalaeontology, Palynology and Stratigraphy of the Total Eastcan Gilbert F-53 well. Report submitted to the C-NLOPB, 9 p.

Robertson Research, 1982. Geochemical evaluation of the Chevron et al Hopedale E-033 well offshore Newfoundland. Report submitted to C-NLOPB, 36 p.

Robertson Research, 1983. Preliminary Geochemical Evaluation Report of the Canterra et al South Hopedale L-39 well offshore Newfoundland. Report submitted to C-NLOPB, 38 p.

Robertson Research, 1984. The micropaleontology, palynology and stratigraphy of the South Hopedale L-39 well, Labrador Shelf, offshore eastern Canada, Report submitted to C-NLOPB, 30 p.

Roest, W.R., and Srivastava, S.P., 1989. Sea-floor spreading in the Labrador Sea: a new reconstruction: Geology, v. 17, p. 1000-1003.

Rohl, U., Bralower, T.J., Norris, G., and Wefer, G., 2000. A new chronology for the late Paleocene thermal maximum and its environmental implications: Geology, v. 28, p. 927-930.

Schlanger, S.O., Arthur, M.A., Jenkyns, H.C., and Scholle, P.A., 1987. The Cenomanian-Turonian Oceanic Anoxic Event, I. Stratigraphy and distribution of organic carbon-rich beds and the marine $\delta_{13}C$ excursion: Geological Society Special Publication 26, p. 371-399.

Schwartz, S.S., 2008. Diagenesis and porosity development of Paleozoic carbonate and early to mid Cretaceous siliciclastic reservoir intervals, Hopedale Basin, Labrador Shelf. MSc. Thesis, Memorial University of Newfoundland, 149 p.

Sheppard, M., and Hawkins, 1980. Petroleum resource potential of offshore Newfoundland and Labrador; Government of Newfoundland and Labrador, Special Report PD-80-2, 8 p.

Shipley, T.H., Houston, M.H., Buffler, R.T., Shaub, F.J., McMillen, K.J., Ladd, J.W., and Worzel, J.L., 1979. Seismic reflection evidence for the widespread occurrence of possible gas-hydrate horizons on continental slopes and rises: American Association of Petroleum Geologists Bulletin, v. 63, p. 2204-2213.

Sinninghe, D.J.S., and Koster, J., 1998. A euxinic southern North Atlantic Ocean during the Cenomanian/Turonian oceanic anoxic event: Earth and Planetary Science Letters, v. 158, p. 165-173.

Sinninghe, D.J.S., Kuypers, M.M.M., Pancost, R.D., and Schouten, S., 2008. The carbon isotopic response of algae (cyano)bacteria, archaea and higher plants to the late Cenomanian perturbation of the global carbon cycle: Insights from biomarkers in black shales from the Cape Verde Basin (DSDP Site 367): Organic Chemistry, v. 39, p. 1703-1718.

Sloan, E.D., 1998. Clathrate hydrates of natural gases: Marcel-Dekker, New York, 705 p.

Srivastava, S.P., 1978. Evolution of the Labrador Sea, and its bearing on the early evolution of the North Atlantic; Royal Astronomic Society Geophysical Journal, no. 52, p. 313-357.

Srivastava, S.P., 1985. Evolution of the Labrador Sea and its implications to the motion of Greenland along Nares Strait; Tectonophysics, v. 114, p. 29-53.

Srivastava, S.P., and Roest, W.R., 1999. Extent of oceanic crust in the Labrador Sea: Marine and Petroleum Geology, v. 16, p. 65-84.

St.-Onge, M.R., Van Gool, J.A.M., Garde, A.A., and Scott, D.J., 2009. Correlation of Archean and Palaeoproterozoic units between northeastern Canada and western Greenland: constraining the pre-collisonal upper plate accretionary history of the Trans-Hudson orogeny: Geological Society of London Special Publications 318, p. 193-235.

Stead, C.L., Carter, J.C., Norris, D.N., and Cameron, D.C., 2017. BSR distribution from newly acquired 2D seismic and the potential link to thermogenic petroleum systems, offshore Newfoundland and Labrador, Canada: 79th EAGE Conference and Exhibition: June 12-17, Paris, France, Th C2 10 [abstract].

Taylor, A., Weitmiller, R., and Judge, A., 1979. Two risks to drilling and production off the east coast of Canada—earthquakes and gas hydrates, *in* Denver, W., (ed.), Proc. Vol. Symp. Research on the Labrador Coastal and Offshore Region: Memorial University, Newfoundland, p. 91-105.

Tenneco Oil & Minerals, 1972. Well history report Tenneco et al. Leif E-38. Report submitted to C-NLOPB, 98 p.

Thrane, K, 2014. Provcenance study of Paleocene and Cretaceous clastic sedimentary rocks from the Davis Strait and the Labrador Sea, based on U-Pb dating of detrital zircons: Bulletin of Canadian Petroleum Geology, v. 62, p. 330-396.

Tissot, B.P., and Welte, D.H., 1984. Petroleum formation and occurrence. Springer-Verlag, 699 p.

Total Eastcan Exploration, 1977. Well history report Eastcan et al. Herjolf M-92. Report submitted to C-NLOPB, 96 p.

Total Eastcan Exploration, 1978a. Well History Report total Eastcan et al. – Roberval, K92. Report submitted to C-NLOPB, 72 p.

Total Eastcan Exploration, 1978b. Well History Report: Total Eastcan et al. – Skolp E-07, unpublished report, 166 p.

Total Eastcan Exploration, 1979. Well History Report Total Eastcan et al. Tyrk P-100, Report submitted to C-NLOPB, 126 p.

Total C.F.P., 1979a. Geochemical study of Roberval K-92, Report submitted to C-NLOPB, 30 p.

Total C.F.P., 1979b. Geochemical study of Skolp E-07. Report submitted to C-NLOPB, 34 p.

Total-C.F.P., 1980a. Geochemical study of Bjarni O-82 (Total Eastcan). Report submitted to C-NLOPB, 10 p.

Total-C.F.P., 1980b. Geochemical study of Tyrk P-100 (Labrador), Report submitted to C-NLOPB, 26 p.

Total Laboratories, 1980c. Bisostratigraphical Study of the Roberval K-92 Eastcan well. Report submitted to C-NLOPB, 10 p.

Total Leonard, 1976. Snorri J-90 Analysis of Well Test Data. Report submitted to C-NLOPB, 24 p.

Umpleby, D.C., 1979. Geology of the Labrador Shelf; Geological Survey of Canada Paper 79-13, 34 p.

Vale, 2017. Long Harbour: Vale. http://www.vale.com/canada/EN/aboutvale/communities/long-harbour/Pages/default.aspx

Wang, D.., and Hesse, R., 1996. Continental slope sedimentation adjacent to an ice-margin. II. Glaciomarine depositional facies on Labrador Slope and glacial cycles: Marine Geology, v. 135, p. 65-96.

Wang, L., Mao, Z.Q., Sun, Z.C., Luo, X.P., and Song, Y., 2013. Genesis analysis of high gamma ray (GR) sandstone reservoir: Taking Toutonhe formation of Junggar basin, northwest china as an example: Applied Mechanics and Materials, v. 394, p. 585-590.

Wardle, R.J., Gower, C., Ryan, B., Nunn, G., James, D. and Kerr, A. 1997. Geological Map of Labrador; 1:1 million scale. Government of Newfoundland and Labrador, Department of Mines and Energy, Geological Survey Map 97-07.

Welford, J.K, and Hall, J., 2013. Lithospheric structure of the Labrador Sea from constrained 3-D gravity inversion: Geophysical Journal International, v. 195, p. 767-784.

White, R., and McKenzie, D., 1989. Magmatism at rift zones: the generation of volcanic continental margins and flood basalts: Journal of Geophysical Research, v. 94, p. 7685-7729.

Wielens, H.J.B. and Williams, G. 2009a. Stratigraphic cross section Gjoa-Snorri Saglek - Hopedale Basin, in the Labrador Sea on the east coast of Canada, from North to South. Geological Survey of Canada Open File 5903, 1 p.

Wielens, H.J.B. and Williams, G. 2009b. Stratigraphic cross section South Hopedale-Tyrk, Hopedale basin, in the Labrador Sea, on the east coast of Canada, from North to South. Geological Survey of Canada Open File 5904, 1 p.

Wielens, H.J.B.. and Williams, G. 2009c. Stratigraphic cross-section Gudrid-Freydis, Hopedale Basin South, in the Labrador Sea, on the east coast of Canada, from North to South. Geological Survey of Canada Open File 5905, 1 p.

Williams, G.L., 1976. Kerogen Type and Thermal Alteration Index Report. Geological Society of Canada – Atlantic Internal Report EPGS-DOM-50-76GLW, 4 p.

Williams, G.L., 2007. Palynological analysis of Gilbert F-53 – 525 – 3550m. Geological Survey of Canada Open File Report 5450, 22 p.

Williams, G.L., 2015. Palynological analysis of conventional cores from 13 Labrador Shelf wells. Geological Survey of Canada Atlantic Internal report MRG-PAL-03-2015-GLW, 36 p.

Williams, G.L., 2017a. Palynological analyses of the two Labrador Shelf wells, Petro-Canada et al. Corte Real P-85 and Petro-Canada et al. Pothurst, P-19, offshore Newfoundland and Labrador. Geological Survey of Canada, Open File 8182, 50 p.

Williams, G.L. 2017b. Palynological analyses of the two Labrador Shelf wells, Petro-Canada et al. Roberval C-02 and Total Eastcan et al. Roberval K-92, offshore Newfoundland and Labrador. Geological Survey of Canada, Open File 8183, 63 p.

Williams, G.L., Ascoli, P., Barss, M.S., Bujak, J.P., Davies, E.H., Fensome, R.A., and Williamson, M.A. 1990. Biostratigraphy and related studies, *in* Geology of the Continental Margin of Eastern Canada, Keen, M.J., and Williams, G.J., (ed.), p. 87-140.

Williams, S.H., Burden, E.T., and Mukhopadhyay, 1998. P.K., Thermal maturity and burial history of Paleozoic rocks in western Newfoundland: Canadian Journal of Earth Sciences, v. 35, p. 1307-1322.

Wright, R., Atkinson, I. and Carter, J., 2016. Labrador deepwater exploration: Insights into its prospectivity from broadband seismic, AVO analysis and seabed coring: Arctic Technology Conference, St. John's NL, OTC 27376 [abstract].

Zachos, James, Pagani, M., Sloan, L., Thomas, e., Billups, K., 2001. Trends, rhythms and aberrations in global climate 65 Ma to present. Science, v. 292, p. 686-693.

Zagorevski, A., Van Staal, C.R., and McNicoll, V.J., 2007. Distinct Taconic, Salinic, and Acadian deformation along the Iapetus suture zone, Newfoundland Appalachians: Canadian Journal of Earth Sciences, v. 44, p. 1567-1585.

Zhang, S., Creaser, R.A., and Pell, J., 2014. Discovery of organic-rich black shale xenolith from kimberlite on the Hall Peninsula, Nunavut and its implication for petroleum potential in Cumberland Sound: Bulletin of Canadian Petroleum Geology, v. 62, p. 125-131.

Zuber, M.D., 1998. Production characteristics and reservoir analysis of coalbed methane reservoirs: International Journal of Coal Geology, v. 38, p. 27-45.

APPENDIX G GLOSSARY OF TERMS

(* from or modified from Schlumberger Limited's The Oilfield Glossary,
http://www.glossary.oilfield.slb.com)

Anticline: An arch-shaped fold in which the oldest rocks form the core of the fold and progressively younger rocks are found outward.

Anticlinorium: A series of parallel anticlinal folds on which minor folds are superimposed on a large scale anticline.

Archean: Geological Eon from approximately 4 billion to 2.5 billion years ago.

Argillaceous – Describes rocks or sediments containing silt or clay sized particles.

Arkosic: Describes sands or sandstones that are relatively rich in feldspar.

Authigenic: Minerals formed in place by chemical alteration of the sedimentary rock after deposition.

*Basement: Older igneous or metamorphic rocks of the crust beneath the sedimentary section that are generally not considered to host hydrocarbon resources.

*Bathyal: Refers to the environment between the depths of 200m and 2000m.

*Biostratigraphy: The application of plant and animal fossils to date and correlate strata, providing information about the age and depositional environment of the rocks hosting the fossils.

Carbonaceous: Containing carbon, typically used to describe sediments with fine coal fragments, *not* carbonate minerals.

*Carbonate: A class of sedimentary rock whose chief mineral constituents (95% or more) are calcite and aragonite (both CaCo3) and dolomite [CaMg(CO3)2]. Limestone and chalk are carbonate rocks.

Carboniferous: Geological period from 359 to 299 million years ago.

Cenozoic: Geological Era approximately 66 million years ago to present.

*Clastic: Sediment consisting of broken fragments derived from pre-existing rocks and transported elsewhere and redeposited before forming another rock. Examples of common clastic sedimentary rocks include siliciclastic rocks such as conglomerate, sandstone, siltstone and shale. Carbonate rocks can also be broken and reworked to form clastic sedimentary rocks.

Condensate – A low density, liquid hydrocarbon that condenses from natural gas when it cools to surface temperatures.

*Continental Shelf: Relatively shallow region of the seafloor extending from the shoreline to a depth of approximately 200m where the continental slope begins. The shelf is typically relatively flat with a gentle seaward slope.

Continental Slope: Region between the continental shelf and deep ocean basins with a relatively steep basinward slope.

Cretaceous: Geologic period from approximately 145 million to 66 million years ago.

***Detrital:** Refers to particles of rock derived from mechanical breakdown of pre-existing rocks by weathering and erosion.

Devonian: Geologic period from approximately 419 to 359 million years ago.

Diachronous: Geologic surface or deposit which varies in age significantly.

Dipmeter: Wireline log used to interpret the orientation of surfaces in rocks.

***Dolostone:** A rock composed chiefly of the mineral dolomite.

***Fluvial:** Refers to deposition in a river or running water.

***Formation**: A body of rock that is sufficiently distinctive and continuous, and can be mapped.

***Gamma Ray Log:** Wireline log used to measure the radioactivity of rocks, commonly used to recognize clay-rich intervals.

***Half-graben:** A geologic structural low bounded by a normal fault along one side.

***Hydrate:** An unusual occurrence of hydrocarbon in which molecules of natural gas, typically methane, are trapped in ice molecules. More generally, hydrates are compounds in which gas molecules are trapped within a crystal structure. Hydrates form in cold climates, such as permafrost zones and in deep water. To date, economic liberation of hydrocarbon gases from hydrates has not occurred, but hydrates contain quantities of hydrocarbons that could be of great economic significance. Hydrates can affect seismic data by creating a reflection or multiple.

***Hydrogen Index:** Parameter determined from pyrolysis analysis that is a measure of the amount of liquid hydrocarbon generated by thermal cracking of organic material.

***Kerogen –** Naturally occurring solid, insoluble organic matter found in source rocks. Kerogens can be described as Type I (mainly derived from algal material), Type II (mixed terrestrial and marine source material), or Type III (woody terrestrial source material).

***Litharenite** – a sandstone with relatively abundant lithic material (grains that are neither feldspar nor quartz).

***Lithostratigraphy:** The study and correlation of strata on the basis of the mineral content, grain size, texture and color of the rocks, or on the nature of log responses.

***Magma:** molten rock below the earth's surface. May cool at depth forming igneous rock or extrude onto the surface as lava.

*Maturation: The process of a source rock becoming capable of generating oil or gas when exposed to appropriate pressures and temperatures.

*Mega-sequence: A large group of relatively conformable strata, normally from the same era, that represents cycles of deposition and is bounded by unconformities or correlative conformities.

Mesozoic: Geological Era approximately 145 to 252 million years ago.

*Migration: The movement of hydrocarbons from their source into reservoir rocks.

*Mineral: A crystalline substance that is naturally occurring, inorganic, and has a unique or limited range of chemical compositions. Minerals are homogeneous, having a definite atomic structure. Rocks are composed of minerals, except for rare exceptions like coal, which is a rock but not a mineral because of its organic origin. Minerals are distinguished from one another by careful observation or measurement of physical properties such as density, crystal form, cleavage (tendency to break along specific surfaces because of atomic structure), fracture (appearance of broken surfaces), hardness, lustre and colour. Magnetism, taste and smell are useful ways to identify only a few minerals.

Multichannel seismic: Refers to a seismic survey in which the data was acquired with multiple detectors at different locations for sensing returning seismic waves generated by each source point.

*Neritic: Describing the environment and conditions between low tide and the continental shelf, typically 200m water depth.

Ordovician: Geological period from approximately 485 to 444 million years ago.

Paleozoic: Geological Era from approximately 252 to 541 million years ago.

Palynomorph: Organic-walled structures of microscopic size (typically 5 to 500 microns). Includes pollen grains, spores, and dinoflagellate cysts.

Pleistocene: Geological Epoch from approximately 2.5 million to 10 thousand years ago.

Pliocene: Geological Epoch from approximately 5.3 million to 2.5 million years ago.

*Passive Margin – Margin of a continent that does not coincide with the boundary of a lithospheric plate and where collision is not occurring. Characterized by rifted, rotated blocks of thick sediment.

*Petroleum System: Geologic components and processes necessary to generate and store hydrocarbons, including a mature source rock, migration pathway, reservoir rock, trap and seal. Appropriate relative timing of formation of these elements and the processes of generation, migration and accumulation are necessary for hydrocarbons to accumulate and be preserved.

*Petrophysical: Refers to wireline logs that measure physical properties of rocks (e.g. radioactivity, resistivity) and to algorithms to quantitatively estimate properties such as porosity and water saturation from those logs.

Phanerozoic: Geological eon from approximately 541 million years ago to present.

*Play: A family of prospects and/or discovered pools that share a common history of hydrocarbon generation, migration, reservoir development, and trap configuration; forms a natural geological population limited to a specific area.

*Pool: A subsurface oil accumulation. An oil field can consist of one or more oil pools or distinct reservoirs within a single large trap. The term "*pool*" can create the erroneous impression that oil fields are immense caverns filled with oil, instead of rock filled with small oil-filled pores.

*Progradation: Accumulation of sequences by deposition in which beds are deposited successively basinward. Thus, the position of the shoreline migrates into the basin during episodes of progradation.

Proterozoic: Geologic eon encompassing ages of 2500 – 541 million years ago. This eon represents the youngest portion of the Precambrian and is sub-divided into three geologic eras: Paleoproterozoic (oldest), Mesoproterozoic and Neoproterozoic (youngest).

*Pyrolysis: A type of geochemical analysis in which the sample is gradually heated to assess the abundance of organic material, its thermal maturity, and the types of hydrocarbons it might generate or have generated.

*Reservoir: A subsurface body of rock having sufficient porosity and permeability to store and transmit fluids. Sedimentary rocks are the most common reservoir rocks as they have more porosity than most igneous and metamorphic rocks and form under temperature conditions at which hydrocarbons can be preserved. A reservoir is a critical component of a complete petroleum system.

Rifting: Process of stretching and thinning of the continental crust, eventually forming a rift basin.

RockEval: Machine used to run pyrolysis experiments on samples for characterization of source rock.

*Seal: A relatively impermeable rock, commonly shale, anhydrite or salt that forms a barrier or cap above and around reservoir rock such that fluids cannot migrate beyond the reservoir. A seal is a critical component of a complete petroleum system.

*Sedimentary Basin: Depression in the earth's crust within which sediments have accumulated.

*Sequence: A group of relatively conformable strata that represents a cycle of deposition and is bounded by unconformities or correlative conformities.

Serpentinized Mantle Peridotite: Rock rich in the mineral serpentine interpreted as forming through hydration from sea water of a mantle rock rich in the mineral olivine.

*Siliciclastic: Sediment composed of predominantly silicate minerals that were broken from pre-existing rocks, transported and redeposited.

*Source rock: A rock rich in organic matter which, if heated sufficiently, will generate oil or gas. Typical source rocks, usually shales or limestones, contain about 1% organic matter and at least 0.5% total organic carbon (TOC), although a rich source rock might have as much as 10% organic matter.

*Stratigraphy: The study and correlation of strata (layered rocks) based on lithology, fossil content, or age.

Syn-rift: Refers to sediments that were deposited during a rifting event.

*Synthetic Seismogram: The result of a model predicting the seismic response of the earth, commonly called a synthetic. A direct one-dimensional model of acoustic energy travelling through the layers of the earth. The synthetic seismogram is generated by convolving the reflectivity derived from digitized acoustic and density logs with the wavelet derived from seismic energy. By comparing the predicted response of marker beds on the synthetic seismogram to the reflections on the seismic data, the correlation of the seismic to the wells can be improved.

*Texturally immature: Refers to sediments that are poorly sorted (contain grains of a wide range of sizes) or contain angular grains as opposed to rounded ones.

Thermal alteration index: A measure of the thermal maturity of organic matter determined from the color change in palynomorphs due to heating.

Thermal sag: Regional scale subsidence resulting from cooling of the crust.

*Transgression: The migration of the shoreline out of a basin and onto land, resulting in sediments characteristic of deeper water overlying sediments characteristic of shallow water.

*Trap: A configuration of rocks suitable for containing hydrocarbons and sealed by a relatively impermeable formation through which hydrocarbons will not migrate. Traps are described as structural traps (in deformed strata such as folds and faults) or stratigraphic traps (in areas where rock types change, such as unconformities, pinch-outs and reefs). A trap is an essential component of a petroleum system.

Turbidite: Sedimentary deposit formed by turbidity current. A turbidity current is a turbulent water mass that moves downslope because of its high density (due to sediment concentration) relative to the surrounding water.

Unconformity: Geological surface separating younger rocks from significantly older rocks.

*Unconventional resource: An umbrella term for oil and natural gas that is produced by means that do not meet the criteria for conventional production. What has qualified as unconventional at any particular time is a complex function of resource characteristics, the available exploration and production technologies, the economic environment, and the scale, frequency and duration of production from the resource. Perceptions of these factors inevitably change over time and often differ among users of the term. At present, the term is used in reference to oil and gas resources whose porosity, permeability, fluid trapping mechanism, or other characteristics differ from conventional sandstone and carbonate reservoirs. Coalbed methane, gas hydrates, shale gas, fractured reservoirs, and tight gas sands are considered unconventional resources.

*Vitrinite reflectance: A measure of the thermal maturity of organic matter. The reflectivity of at least 30 grains of the organic material vitrinite measured in units of percentage reflectance.

Vug – A cavity, void or large pore in a rock, especially one created by dissolution of carbonate rock.

*Wavelet – A one-dimensional pulse, usually the basic response from a single reflector. Its key attributes are its amplitude, frequency, and phase.